Engineering Library

APR 20 1936

UNITED STATES DEPARTMENT OF COMMERCE

Journal of Research

of the

National Bureau of Standards

Vol. 16, No. 3 March 1936

CONTENTS

RP	TITLE AND AUTHOR	Page
868.	Ionosphere studies during partial solar eclipse of February 3, 1935. By Samuel S. Kirby, Theodore R. Gilliland, and Elbert B. Judson, ...(Price 5c)	213
869.	Reversal temperature and population of excited states in the cesium discharge. Fred L. Mohler....(Price 5c)	227
870.	Absorption of X-rays by lead glasses and lead-barium glasses. George Singer....(Price 5c)	233
871.	Distillation and separation of arsenic, antimony, and tin. John A. Scherrer....(Price 5c)	253
872.	Note on the effect of a cover glass in reflectance measurements. Deane B. Judd and Kasson S. Gibson....(Price 5c)	261
873.	Some tests of steel columns incased in concrete. Ambrose H. Stang, Herbert L. Whittemore, and Douglas E. Parsons....(Price 10c)	265

The articles listed above may be purchased separately (see paper II) at the prices indicated in the table of contents

A monthly periodical of pure and applied science published by our National Government

Journal of Research

of the

National Bureau of Standards

The January 1936 issue of the Journal of Research of the National Bureau of Standards began the sixteenth semiannual volume of this periodical. Fundamental researches in progress in the Bureau's laboratories are reported in this JOURNAL. If you are interested in new developments in science and technology, you should receive the JOURNAL. If you are not already a subscriber you are invited to send in your subscription.

Technical News Bulletin

This is a monthly publication containing short articles reporting progress of work in the Bureau laboratories, abstracts of papers which appear in the Journal of Research, accounts of scientific and technical meetings in which the Bureau has taken part, a list of all publications by members of the staff, and other items within the Bureau's fields. The BULLETIN is designed primarily to give a general and timely review of the activities of the Bureau in brief form. It is a prompt and reliable source of official information. If you have not already subscribed for the BULLETIN, you are invited to do so.

ANNUAL SUBSCRIPTION	Prices	
	United States, Canada, Cuba, Mexico, Newfoundland, Republic of Panama	Other countries
Journal of Research of the National Bureau of Standards:		
12 monthly issues (2 volumes), paper covers	$2.50	$3.25
Bound volume (½ year, 1 volume), blue buckram . . .	3.00	3.50
Technical News Bulletin, 12 monthly issues	.50	.70

Research Papers, reprinted individual articles appearing in the Journal of Research, are available from the Superintendent of Documents shortly after appearance of the monthly issue of the JOURNAL.

Address orders only to
Superintendent of Documents, U. S. Government Printing Office,
Washington, D. C.

UNITED STATES DEPARTMENT OF COMMERCE
DANIEL C. ROPER, Secretary
NATIONAL BUREAU OF STANDARDS
LYMAN J. BRIGGS, Director

✦

Journal of Research

of the

National Bureau of Standards

✦

Volume 16, Number 3

March 1936

UNITED STATES
GOVERNMENT PRINTING OFFICE
WASHINGTON : 1936

For sale by the Superintendent of Documents, Washington, D. C. - - - - Price 25 cents
$2.50 per year on subscription

The prices of the separate Research Papers appearing in this JOURNAL are given on the front cover page. If 100 or more copies of any separate are ordered, a discount of 25 percent is allowed. Those who desire copies of separate Research Papers should send their orders and remittances without delay to the Superintendent of Documents, U. S. Government Printing Office, Washington, D. C. This will aid him to determine the number of copies to be printed for sale. Research Papers are not printed from electrotypes, and usually no more reprints can be had when the first and only printing is exhausted.

U. S. DEPARTMENT OF COMMERCE NATIONAL BUREAU OF STANDARDS

RESEARCH PAPER RP868

Part of Journal of Research of the National Bureau of Standards, Volume 16, March 1936

IONOSPHERE STUDIES DURING PARTIAL SOLAR ECLIPSE OF FEBRUARY 3, 1935

By Samuel S. Kirby, Theodore R. Gilliland, and Elbert B. Judson

ABSTRACT

Virtual height and critical-frequency measurements of the several regions of the ionosphere were made during the day of the solar eclipse of February 3, 1935, and during several days before and after the eclipse day. The eclipse was found to produce a decrease of the critical frequency of each region. The decrease of critical frequency was approximately in time phase with the eclipse, thus indicating an ionizing agency (probably ultraviolet light), originating in the sun and propagated at approximately the velocity of light. The decrease of equivalent electron density in each region during the eclipse was compared with the decrease in the exposed area of the sun's disk, and found to indicate that the ionization of the normal E region was diminished when the ionizing agency was decreased, by recombination of + and − charges, while the ionization of the F_2 region and a high stratum of the E was diminished by a process of attachment of electrons to neutral particles.

CONTENTS

		Page
I.	Introduction	213
II.	Experimental data	214
III.	Discussion of data	217
IV.	Conclusions	224
V.	References	224

I. INTRODUCTION

Previous to the solar eclipse of August 31, 1932, no quantitative determinations of the ionization densities of the several regions of the ionosphere had been made at the time of an eclipse. Measurements made by the National Bureau of Standards [1] [1] and other North American observers [2, 3] during this eclipse indicated that the main source of ionization of the E and F_1 regions was ultraviolet light. Similar effects for the F_2 region were not definitely found. Rose [4] reported a 30-percent decrease in ionization density but was not sure that he had followed the F_2 critical frequency all of the time. The National Bureau of Standards found a small decrease of ionization density during this eclipse, but the effect found was of approximately the same magnitude as variations found on some of the control days. The observations of Kenrick and Pickard [5] and Mimno and Wang [6] seem to apply to the F_1 region instead of the F_2.

The 1932 eclipse was total through the Province of Ontario, Canada, and Northeastern United States, where it could easily be observed.

[1] The figures given in brackets throughout the text correspond to the numbered references at the end of this paper.

At Washington, D. C., about 90 percent of the area of the sun's disk was obscured. The eclipse occurred during early and midafternoon. The season, hour of day, and percentage of totality seemed to be favorable for definite results. Such results were obtained for the E and F_1 regions but not for the F_2.

The partial solar eclipse of February 3, 1935, offered an opportunity for further study of the effects of eclipses on the ionosphere. The hour of day (late forenoon) seemed favorable, but the season and percentage of totality (35 percent of area of sun obscured) did not seem favorable for good results.

The effect of a winter eclipse on the F_2 region was of especial interest. It had been observed for several years by the National Bureau of Standards [7, 8] at Washington and the Bell Telephone Laboratories [9] at Deal, N. J., that the ionization density of the F_2 region was not a simple function of the intensity of solar radiation. The ionization densities reached maxima at about sunset in summer and shortly after noon in winter, the winter day values being higher than the summer day values [10]. The ionization density followed nearly in phase with the intensity of received solar radiation during the winter day. Therefore there was a possibility that the effect of an eclipse in the F_2 region would be more clearly indicated in the winter than in the summer.

The technique and equipment available for the observations in 1935 were considerably better than those available in 1932. The multifrequency automatic recorder [11] was available to measure the virtual heights and critical frequencies for the band 2,500 to 4,400 kc/s with a continuous frequency variation. This frequency band was swept through 10 times per hour on the eclipse day and also the 2 days before and the 2 days after. Each sweep through this band required 4.75 minutes. The records obtained gave the critical frequencies for the E and F_1 regions and during the eclipse three points for the F_2 region. The virtual heights and critical frequencies for the frequency band from 4,500 kc/s up to the F_2 critical frequencies were determined by manually operated equipment with which the frequency was varied in steps, usually 200 kc/s. Some manual observations were also made at frequencies below 2,500 kc/s. The general method of observation was to increase the frequency of the pulse transmitter from low values to high and measure the virtual heights until the critical frequency was exceeded. This general procedure has been followed at the National Bureau of Standards since August 1930 [12], the technique improving with experience and improvements of equipment. The ionization densities were computed from critical frequencies by equation 1 given later.

II. EXPERIMENTAL DATA

The data include critical-frequency and virtual-height measurements of the several ionized regions of the ionosphere, made by the methods just described. Figure 1 shows the photographic records obtained on the frequency band 2,500 to 4,400 kc/s. Scales for virtual heights and frequencies are indicated in the lower left-hand corner of figure 1. Critical frequencies are indicated by a more or less sharp rise of virtual height or a point of inflection. The critical

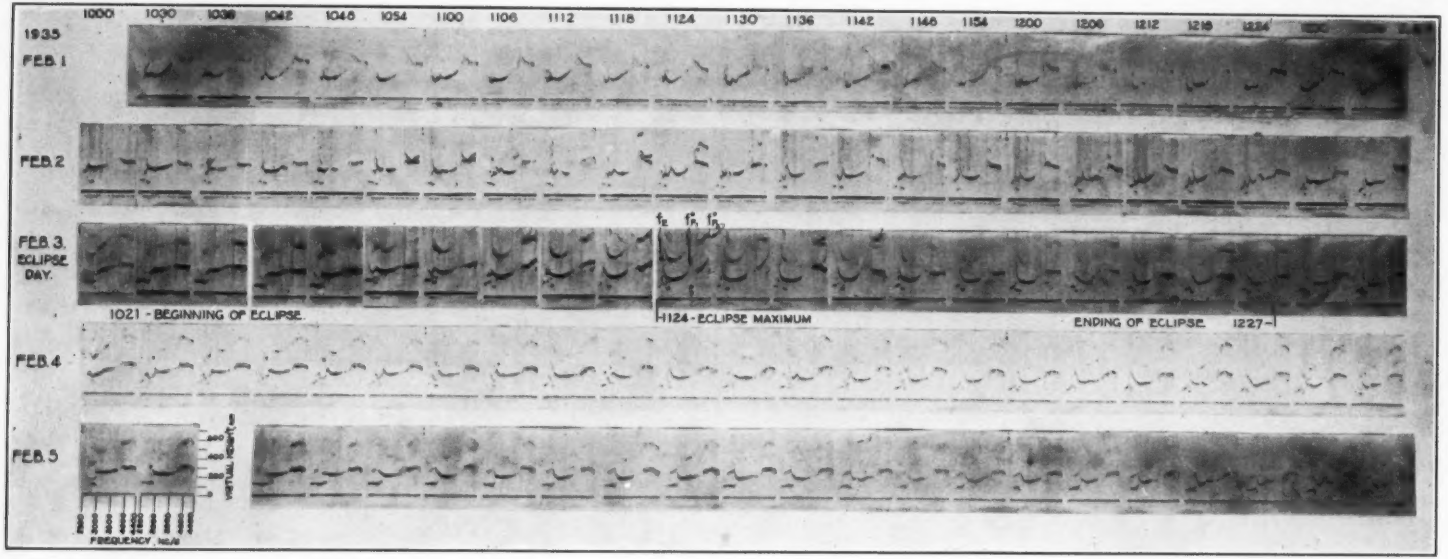

FIGURE 1.—*Automatic multifrequency records of ionosphere heights and critical frequencies for day of eclipse and 2 days before and 2 days after eclipse.*

frequency [2] of a given ionized region is the lowest frequency which will penetrate that region. The f_E and f^0_{F1} are indicated on these records. In addition to the manual measurements, three points of f^0_{F2} were obtained with the automatic recorder near the maximum of the eclipse.

The E region was complex throughout this series of measurements. It appeared to be stratified. Two or three critical frequencies appeared much of the time. The values of these critical frequencies varied independently, and frequently one critical frequency would disappear or a new one appear between sweeps of six-minutes separation. The two criticals appearing on February 3, between 1020 and 1112 EST, (fig. 4), are examples of this complexity. It was often impossible to follow a particular E critical frequency through a series of records taken during successive six-minute periods. Some experimenters [9] have distinguished the several stratifications below the F_1 region by separate names. With the conditions existing during the period of these experiments it did not appear that this could be done consistently. For the reasons given above the multiple E critical frequencies have been averaged for the four control days.

The critical frequencies of the F_1 region were single but not sharply defined. The poor definition is characteristic of winter f_{F1}. No double refraction was observed.

Three of the photographic records taken during the eclipse indicate f^0_{F2}. On the first of these, the record beginning at 1124 EST, f^0_{F2} is indicated at the end of the record 4,400 kc/s. On the record beginning at 1130 EST, f^0_{F2} is indicated clearly at 4,330 kc/s. The time at which this critical frequency was recorded was approximately 1134.5 EST. On the record beginning at 1136 EST f^0_{F2} was again indicated at 4,400 kc/s. These three records indicate the time of minimum f^0_{F2} positively to within 6 minutes and by interpolation probably to the nearest minute.

In figure 2 the data are shown for f_E and f^0_{F1} for February 1, 2, 4, and 5 obtained from the records of figure 1. No attempt was made in this figure to distinguish critical frequencies for any individual day.

In figure 3 are shown the data for f^0_{F2} for the eclipse day and several days before and after the eclipse. The data for each day are shown by a separate graph in this figure. It will be noted that there was considerable variation of critical frequency from day to day. This makes it somewhat difficult to compare the results of any given day on which a special phenomenon such as an eclipse occurs with the average of several normal days, because it is not known for certain what the results would have been on the given day had not the special phenomenon occurred. The Cheltenham Magnetic Observatory of the United States Coast and Geodetic Survey reported moderate magnetic disturbances for February 1 and 2. The magnetograms indicate that the disturbance of February 2 was much less severe than that on Feb. 1. The F_2 critical frequencies were much lower on these two days than on the other control days. Some other data obtained at the National Bureau of Standards indicate that this correspondence between magnetic disturbances and low f_{F2} frequently exists.

[1] f_E=critical frequency for the E region; f^0_{F1}=critical frequency for the F_1 region, ordinary ray; f^x_{F1}=critical frequency for the F_1 region, extraordinary ray; f^0_{F2}=critical frequency for the F_2 region, ordinary ray; f^x_{F2}=critical frequency for the F_2 region, extraordinary ray.

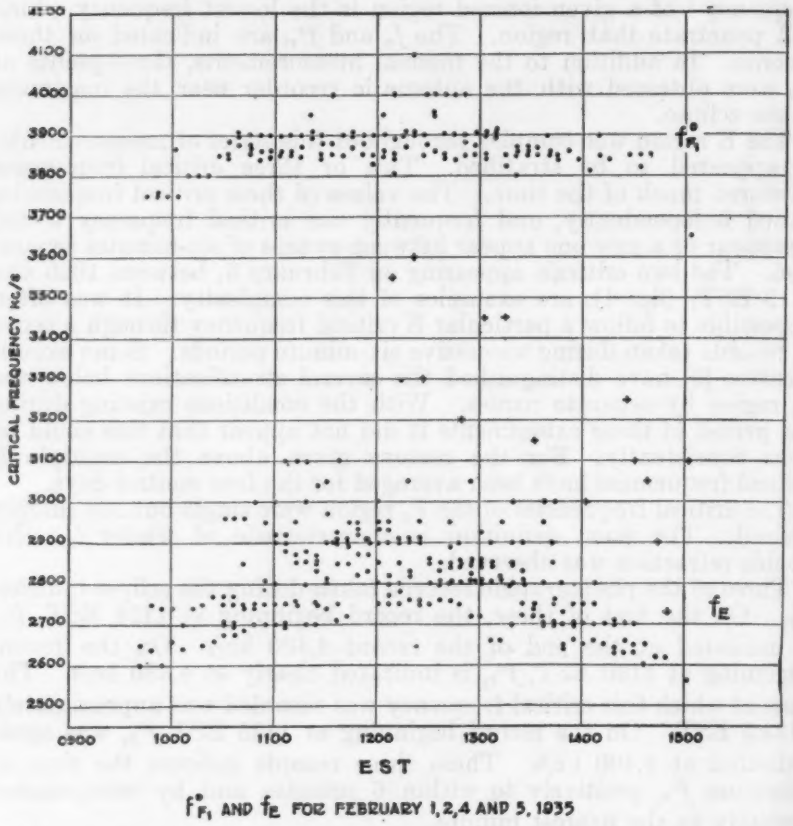

FIGURE 2.—*Critical frequency data for control days for* E *and* F_1 *regions.*

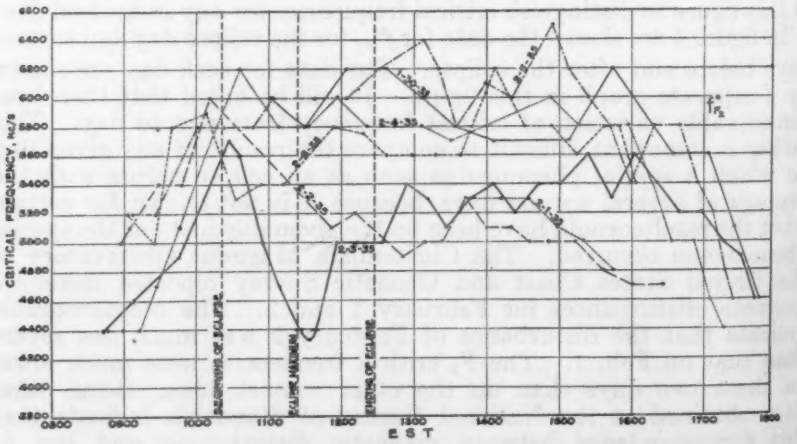

FIGURE 3.—*Critical frequency data for eclipse day and control days for* F_2 *region.*

Figures 1, 2, and 3 present the experimental data obtained in this investigation.

III. DISCUSSION OF DATA

Since there was a complexity of critical frequencies in the E region, and the critical values for a given region could not be traced through with certainty, an average was made of all the points obtained except a few widely scattered points indicated by + in figure 2.

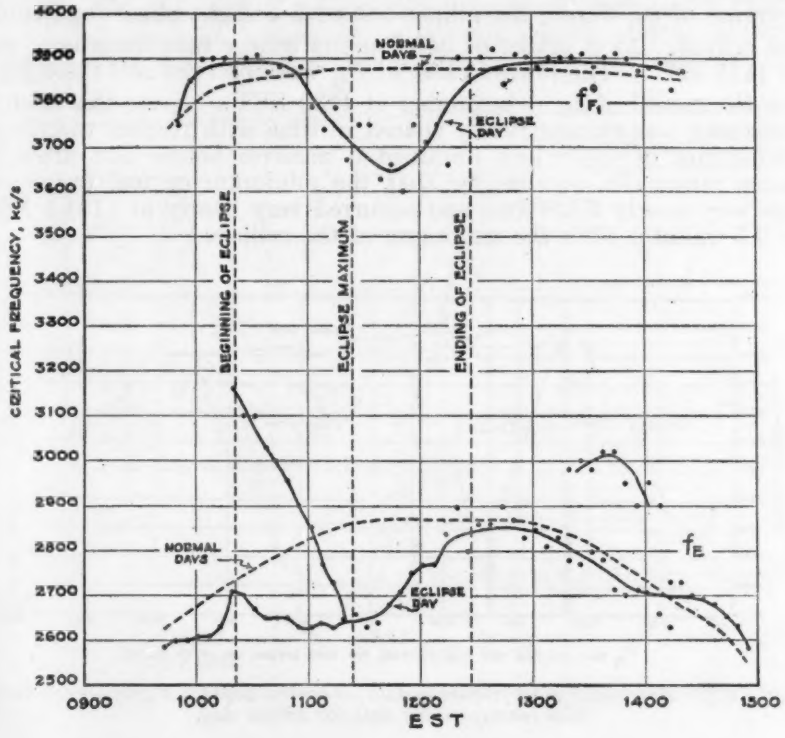

FIGURE 4.—*Averaged critical frequency data for control days for* E *and* F_1 *regions compared with corresponding data for eclipse day.*

These points were not used in the average simply because they were so widely scattered that they did not seem to belong to the E region. This average, and the individual critical frequencies obtained on the eclipse day, are shown in the lower part of figure 4. The branch beginning with a critical frequency of 3,160 kc/s at about 1020 EST and ending about 1120 EST by combining with the more normal appearing f_2 graph is of special interest although its significance is not clear. The critical frequencies forming this branch can be seen clearly in figure 1. Except for this branch the f_2 was less complex on

the eclipse day than on the control days. This figure indicates a decrease of f_s during the eclipse.

The upper part of figure 4 shows $f^{\circ}_{F_1}$ for the eclipse day and the average for the control days. This figure indicates a decrease of $f^{\circ}_{F_1}$ during the eclipse.

The $f^{\circ}_{F_2}$ for the eclipse day and the average for the control days is shown in figure 5. All of the data for the control days shown in figure 3 were used for the average. This figure shows a pronounced decrease of $f^{\circ}_{F_2}$ during the eclipse but with a slight phase lag behind the eclipse. At a height of 250 km the eclipse maximum occurred at 1125 EST. The lowest value of $f^{\circ}_{F_2}$ was observed at 1134.5 EST (on the record of fig. 1 beginning at 1130 EST). Since this critical frequency was symmetrically spaced in time with respect to critical frequencies of 4,400 kc/s obtained 6 minutes before and after, it seems reasonable to consider that the minimum critical frequency was very nearly 4,330 kc/s and occurred very nearly at 1134.5 EST or 9.5 minutes after the maximum of the eclipse.

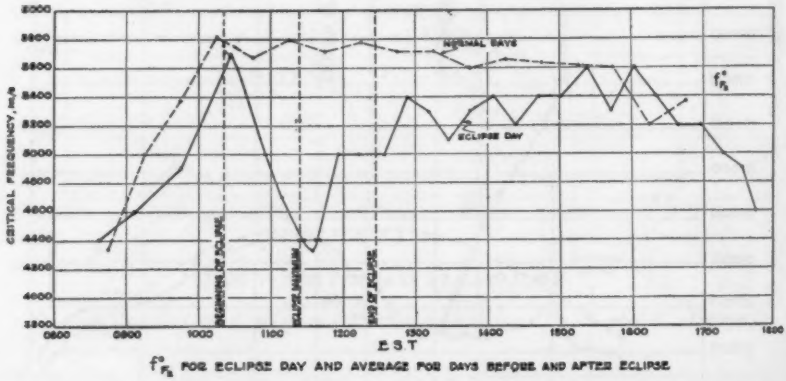

$f^{\circ}_{F_2}$ FOR ECLIPSE DAY AND AVERAGE FOR DAYS BEFORE AND AFTER ECLIPSE

FIGURE 5.—*Averaged critical frequency data for control days for* F_2 *region compared with corresponding data for eclipse day.*

Immediately before the eclipse, $f^{\circ}_{F_2}$ was nearly normal, while after the eclipse maximum it rose rapidly at first but later ceased to rise rapidly but reached normal between 1500 to 1600 EST. This effect might conceivably have been caused by the eclipse, but it is more likely that the normal value of $f^{\circ}_{F_2}$ was low during the eclipse day as on February 1 and 2. During the night following the eclipse $f^{x}_{F_2}$ remained below 2,500 kc/s from the hour 2030 EST to sunrise. This represents an exceptionally long sustained low value of ionization density of the F_2 region, but it has been recorded on other nights. It is not likely that this effect was caused by the eclipse. The ionization density during the night preceding the eclipse was also very low.

In the following paragraphs, let N_1 equal the ion density on the normal or control days, N_2 the ion density on the eclipse day, and f°_1 and f°_2 the critical frequencies of the ordinary ray on the control days and eclipse day, respectively. The ratios $\frac{N_2}{N_1}$ and $\left(\frac{N_2}{N_1}\right)^2$ will be com-

pared with the percentage of the sun's disk which was exposed on the eclipse day.

From familiar theory we may write the following equation expressing the relation between critical frequency and equivalent electron density:

$$N=1.24\ (f^{o})^{2}\cdot 10^{-2}, \tag{1}$$

where N=equivalent electrons per cm^3 for a given region, and f^{o}= the critical frequency in kc/s for the ordinary ray for the same region. For heavy ions equation 1 would have the same form but a greater numerical constant. Equation 1 is well known and is obtained directly from the fundamental theory of Eccles [13] and Larmor [14].

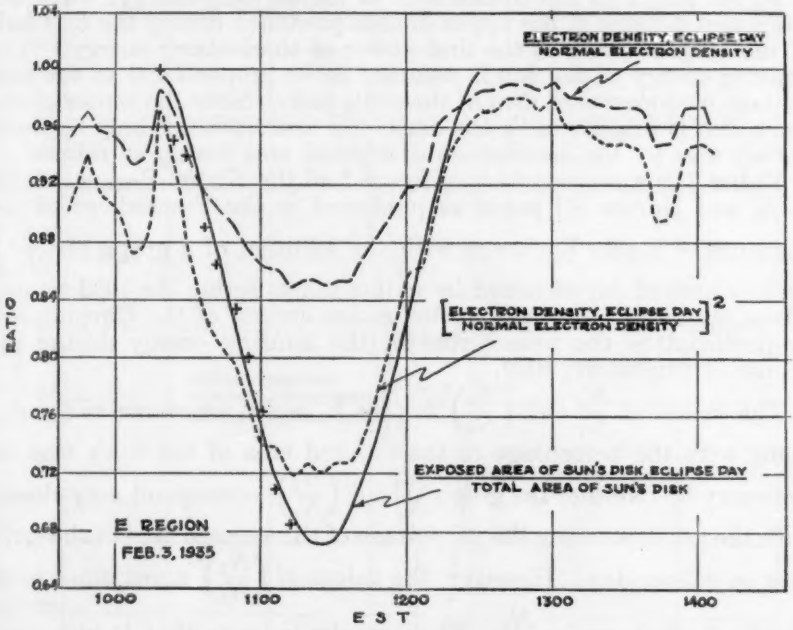

FIGURE 6.—*Comparison of normal electron density of* E *region during 1935 eclipse, with exposed area of sun's disk*

The + marks = $\frac{\text{electron density eclipse day}}{\text{normal electron density}}$ for upper branch of E region shown in figure 4.

From equation 1 we obtain

$$\frac{N_2}{N_1}=\left(\frac{f^{o}_2}{f^{o}_1}\right)^{2}. \tag{2}$$

The values of $\frac{N_2}{N_1}$ and $\left(\frac{N_2}{N_1}\right)^{2}$ for the E region are shown in figure 6. The values of f^{o}_1 and f^{o}_2 were taken for each 6-minute period from figures 4 and 5, so that allowance has been made for the varying zenith angle of the sun. The ratios of the exposed area of the sun's disk on the eclipse day to the total area of the sun's disk are shown in

the same figure. It may be seen that the graph for $\left(\frac{N_2}{N_1}\right)^2$ for the main E region corresponds closely to the graph showing the percentage of the exposed area of the sun's disk. The + marks in this figure represent values of $\frac{N_2}{N_1}$ instead of $\left(\frac{N_2}{N_1}\right)^2$ for the upper branch of the E region shown in figure 4. These values follow closely the graph showing the percentage of exposed area of the sun's disk. The value measured just before the eclipse began was assumed to be normal and was used for N_1. From the results shown in figure 6 it would appear that there were two different laws of recombination for these two strata of the E region. The ionization density for the lower E region varied as the square root of the ionizing energy, while the ionization density of the upper branch produced during the first half of the eclipse varied as the first power of the ionizing energy. The ionizing energy of the sun is assumed to be proportional to the percentage of the exposed area of the sun's disk. Since the center of the sun's disk is brighter than the limbs this assumption is only approximately true for the distribution of exposed area during an eclipse.

Figure 7 is a reproduction of figure 3 of the Kirby, Berkner, Gilliland, and Norton [1] paper as published in the Proceedings of the Institute of Radio Engineers with the addition of a graph of $\left(\frac{N_2}{N_1}\right)^2$ against hour of day obtained from data taken during the 1932 eclipse. These results indicate that the ionization density of the E region was proportional to the square root of the ionizing energy during the eclipse of August 31, 1932.

The values of $\frac{N_2}{N_1}$ and $\left(\frac{N_2}{N_1}\right)^2$ for the F_1 region are shown in figure 8 along with the percentage of the exposed area of the sun's disk on February 3. Neither the graph $\frac{N_2}{N_1}$ nor $\left(\frac{N_2}{N_1}\right)^2$ correspond very closely with the graph showing the percentage of the exposed area of the sun's disk on eclipse day. However, the values of $\left(\frac{N_2}{N_1}\right)^2$ agree much more closely than those for $\frac{N_2}{N_1}$. These results indicate that it was more probable that the ion density of the F_1 region was proportional to the square root rather than the first power of the ionizing energy.

The values of $\frac{N_2}{N_1}$ and $\left(\frac{N_2}{N_1}\right)^2$ for the F_2 region are shown in figure 9 along with the percentage of the exposed area of the sun's disk on February 3. In this case the graph $\frac{N_2}{N_1}$ corresponds closely with the graph showing the percentage of the exposed area of the sun's disk. This indicates that in the F_2 region at the time of this eclipse the ionization density was proportional to the first power rather than the square root of the ionizing energy of the sun.

Pedersen [15] shows that if there are $N-$ and $N+$ ions per cm^3 the rate of recombination is proportional to N^2. Furthermore, if I pairs of such ions are produced per cm^3 each second by some

agency, such as ultraviolet light, and I is proportional to the ionizing energy of this agency, then

$$\frac{dN}{dt}=I-\alpha N^2, \tag{3}$$

where α is the coefficient of recombination.

However, if the ionization is effectively of one sign, such as negative electrons surrounded chiefly by neutral gas particles, the effect of the electrons can be effectively destroyed by attachment to these neutral

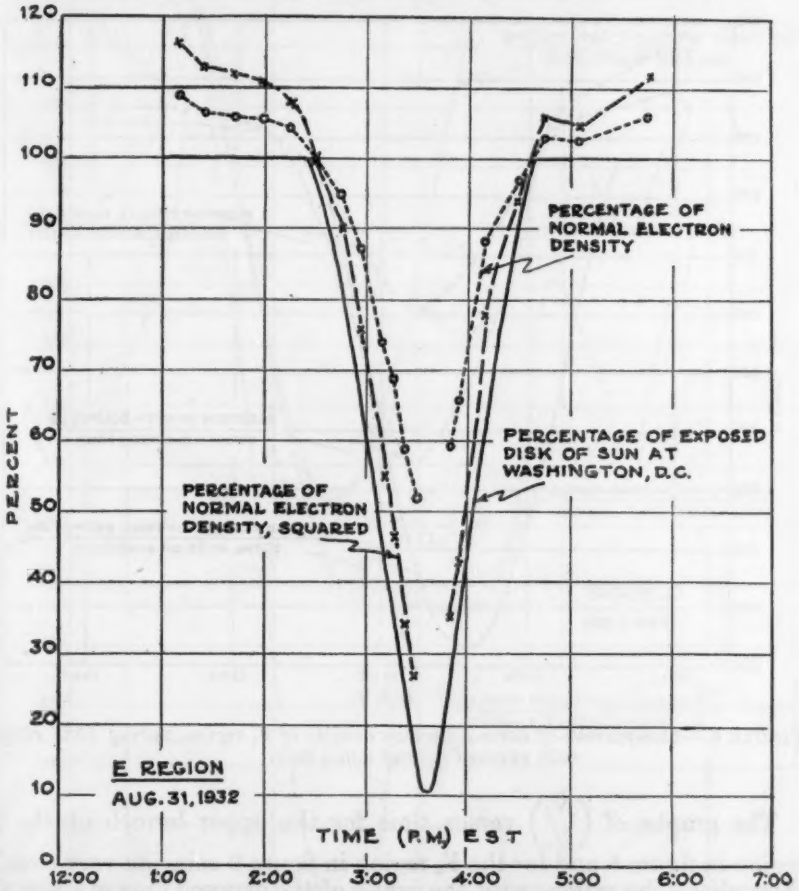

FIGURE 7.—*Comparison of normal electron density of* F_1 *region during 1932 eclipse, with exposed area of sun's disk.*

gas particles. The density and temperature of the gas will be assumed constant. Then the rate at which electrons are lost by attachment is proportional to N rather than N^2. An equation for this condition corresponding to equation 3 may be written as follows:

$$\frac{dN}{dt}=I-\beta N, \tag{4}$$

where β is the coefficient of attachment.

For both equations 3 and 4 $\frac{dN}{dt}=0$ at the lowest points of the graphs of N versus time. In figures 6 and 9 there were very small time

differences between the minimum of exposed area of the disk of the sun and the minimum ionization densities. Also the graphs of $\left(\frac{N_2}{N_1}\right)^2$ versus time for the normal E region in figures 6 and 7 coincide very closely throughout the eclipse with the graph of the ratio

$$\frac{\text{Exposed area of sun's disk on eclipse day}}{\text{Total area of sun's disk.}} \text{ versus time.}$$

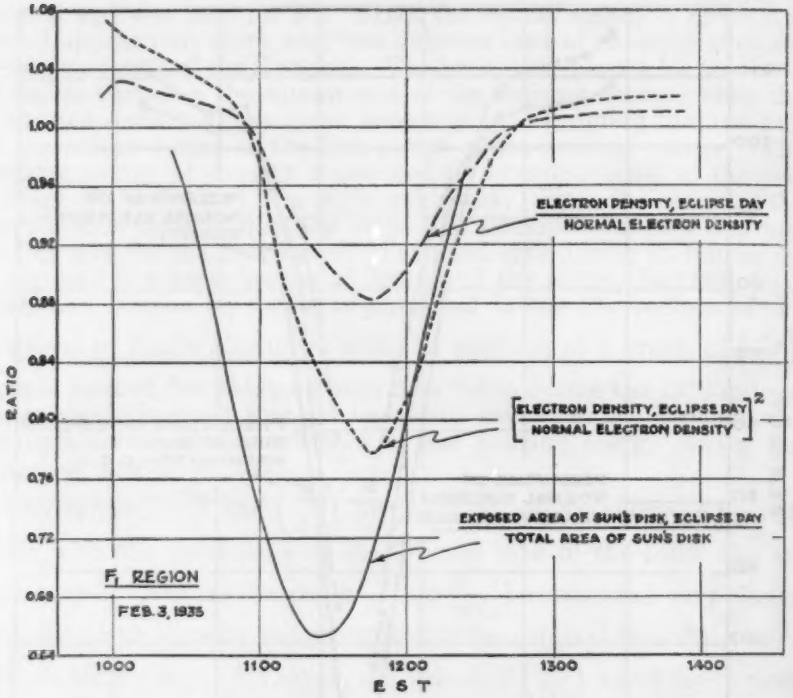

FIGURE 8.—*Comparison of normal electron density of* F_1 *region during 1935 eclipse with exposed area of sun's disk.*

The graphs of $\left(\frac{N_2}{N_1}\right)$ versus time for the upper branch of the E region in figure 6 and for the F_2 region in figure 9 coincide very closely throughout the eclipse with the graph of the exposed area of the sun's disk versus time. Therefore we may safely assume that $\frac{dN}{dt}$ was very small in comparison with either term in the right-hand members of equations 3 and 4 or for practical purposes $\frac{dN}{dt}=0$ at any point on the graphs mentioned in this paragraph for the conditions specified. This is equivalent to saying that equilibrium between ionization and recombination is reached quickly. Similar conclusions regarding the F_1 region at the time of this eclipse can hardly be drawn.

It now appears that figures 6 and 7 indicate that the ionization densities of the E region obeyed equation 3 and that N for these

regions was proportional to the square root of the ionizing energy. These results indicate the probability that the ionization of the normal E region at the times of these experiments was made up of + and − charges which recombined with one another when the ionizing energy

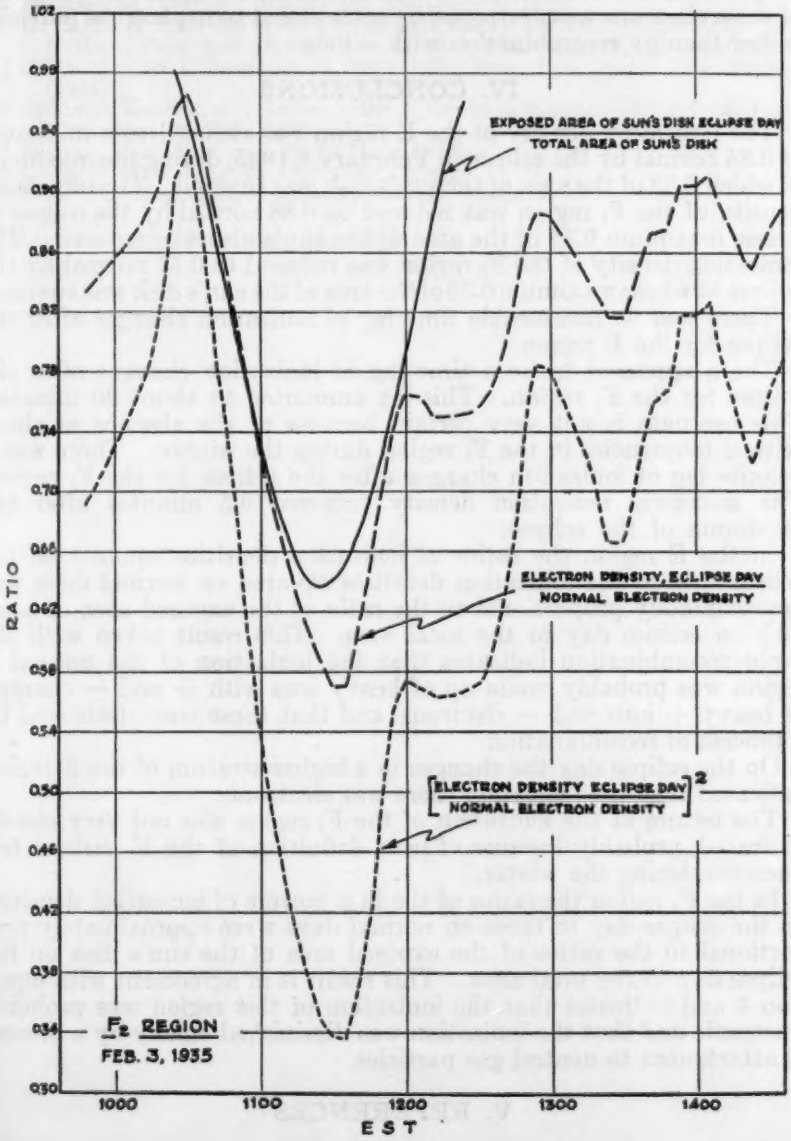

FIGURE 9.—*Comparison of normal electron density of F_2 region during 1935 eclipse with exposed area of sun's disk.*

was decreased. This condition could be satisfied with heavy + and − ions or with heavy+ ions and − electrons.

Also figures 6 and 9 indicate that the ionization densities of the region producing the upper branch of E region shown in figure 2, and

the F_2 region, were proportional to the ionizing energy. These results indicate the probability that the ionization of these two regions at the times of these experiments was made up of electrons. Magneto-ionic splitting is positive evidence that the F_2 region is electronic. The eclipse evidence checked this and in addition indicated that the effect of these electrons was destroyed by attachment to neutral gas particles rather than by recombination with +ions.

IV. CONCLUSIONS

The ionization density of the E region was reduced to a minimum of 0.85 normal by the eclipse of February 3, 1935, during the maximum of which 0.33 of the area of the sun's disk was covered. The ionization density of the F_1 region was reduced to 0.88 normal by the eclipse at whose maximum 0.35 of the area of the sun's disk was covered. The ionization density of the F_2 region was reduced to 0.57 normal by the eclipse at whose maximum 0.36 of the area of the sun's disk was covered.

There was no measurable time lag of ionization changes after the eclipse for the E region.

There appeared to be a time lag of ionization changes after the eclipse for the F_1 region. This lag amounted to about 20 minutes. This estimate is not very certain because of the absence of sharp critical frequencies in the F_1 region during the winter. There was a definite lag of ionization changes after the eclipse for the F_2 region. The minimum ionization density occurred 9.5 minutes after the maximum of the eclipse.

In the E region the ratios of ionization densities squared on the eclipse day to the ionization densities squared on normal days was approximately proportional to the ratio of the exposed area of sun's disk on eclipse day to the total area. This result taken with the rapid recombination indicates that the ionization of the normal E region was probably made up of heavy ions with + and − charges, or heavy + ions and − electrons, and that these were destroyed by a process of recombination.

On the eclipse day the changes in a higher stratum of the E region indicated that the ionization there was electronic.

The nature of the ionization of the F_1 region was not very clearly indicated, probably because of poor definition of the F_1 critical frequencies during the winter.

In the F_2 region the ratios of the first powers of ionization densities on the eclipse day to those on normal days were approximately proportional to the ratios of the exposed area of the sun's disk on the eclipse day to the total area. This result is in agreement with equation 4 and indicates that the ionization of this region was probably electronic and that the ionization was diminished chiefly by a process of attachment to neutral gas particles.

V. REFERENCES

The numbers in brackets correspond to the reference numbers throughout the text.

[1] Kirby, Berkner, Gilliland, and Norton. BS J. Research **11**, 289 (1933); Proc. Inst. Radio Eng. **22**, 247 (Feb. 1934).
[2] J. P. Schafer and W. M. Goodall. Science **76**, 444 (Nov. 11, 1932).
[3] John T. Henderson. Can. J. Research **8**, 1 (Jan. 1933).

[4] D. C. Rose. Can. J. Research **8,** 15 (Jan. 1933).
[5] Kenrick and Pickard. Proc. Inst. Radio Eng. **21,** 546 (April 1933).
[6] Mimno and Wang. Proc. Inst. Radio Eng. **21,** 529 (April 1933).
[7] Kirby, Berkner, and Stuart. Proc. Inst. Radio Eng. **21,** 757 (June 1933).
[8] Kirby, Berkner, and Stuart. BS J. Research **12,** 15 (1934); Proc. Inst. Radio Eng. **22,** 481 (1934).
[9] Schafer and Goodall. Nature **131,** 804 (June 3, 1933).
[10] Dr. E. O. Hulburt has given a reasonable theory for these phenomena. See Hulburt, Phys. Rev. **46,** 822 (Nov. 1, 1934), Terr. Mag. **40,** 193 (June 1935).
[11] Gilliland. BS J. Research **11,** 561 (1933); Proc. Inst. Radio Eng. **22,** 236 (1934).
[12] Gilliland, Kenrick, and Norton. BS J. Research **7,** 1083 (1931); Proc. Inst. Radio Eng. **20,** 286 (1932).
[13] Eccles. Proc. Roy. Soc. **87,** 79 (Aug. 1912).
[14] Larmor. Phil. Mag. **48,** 1025 (Dec. 1924).
[15] Pedersen. Propagation of Radio Waves. Chap. V.

WASHINGTON, December 16, 1935.

U. S. DEPARTMENT OF COMMERCE NATIONAL BUREAU OF STANDARDS

RESEARCH PAPER RP869

Part of Journal of Research of the National Bureau of Standards, Volume 16, March 1936

REVERSAL TEMPERATURE AND POPULATION OF EXCITED STATES IN THE CESIUM DISCHARGE

By Fred L. Mohler

ABSTRACT

Light from a tungsten strip lamp was projected through the positive column of a cesium discharge onto the slit of a spectrograph, and the lamp temperatures determined at which the cesium lines disappeared against the continuous background. Measurements were made on the lines 6S–6P to 6S–11P at different pressures and discharge currents. The reversal temperature decreases from the first to the third line and beyond the third there is no measurable difference. It increases with increasing current and with decreasing pressure. The number of atoms in an excited state is given by an equation of the form of the Boltzmann equation, with the reversal temperature replacing the equilibrium temperature. The number per cubic centimeter ranges in magnitude from 10^{12} for the first P state to 10^{6} for the highest states. In the range of conditions studied it was independent of pressure at constant current.

CONTENTS

	Page
I. Introduction	227
II. Experimental procedure	228
III. Results	229

I. INTRODUCTION

The number and distribution of atoms in excited states is an important factor in determining the intensity distribution of radiation in the spectrum of a discharge, and it must also influence the electrical characteristics of the discharge. Published measurements of the number of excited atoms deal for the most part with the first excited state. A notable exception is the studies of the anomalous dispersion in the neon discharge by Kopfermann and Ladenburg.[1] They found that the number of atoms in the first group of excited states (the Paschen 1*s* states) is about equal to the number in equilibrium at a temperature equal to the electron temperature. With the highest current attainable the group of 2*p* levels also approach this equilibrium value, but levels of higher energy are always far below it.

In a paper on collisions [2] of the first and second kind in the positive column of a cesium discharge I have included measurements of the number of atoms in the first and second P states (6^2P and 7^2P) using the method of reversal temperatures. This paper reports an extension of the measurements to higher lines of the principal series.

[1] Kopfermann and Ladenburg, Z. Phys. 48, 15, 26, 51, and 192 (1928); 65, 167 (1930); Naturwissenschaften 19, p. 513; 1931.
[2] Mohler, BS J. Research 9, 493 (1932) RP485.

The principle of the reversal-temperature measurement is as follows: If the image of an incandescent lamp is projected through a tube of gas or vapor onto the slit of a spectrograph, absorption lines of the gas will appear as dark lines. If the gas is electrically or thermally excited so as to be self-luminous the lines may appear either darker or brighter than the continuous background, and there is at least theoretically a lamp temperature at which the lines will disappear. (In practice this is often too high to attain with an incandescent lamp.) This is called the reversal temperature.

It can be shown [3] on the basis of elementary radiation theory that for a uniformly excited volume of gas the number of atoms per unit volume in an excited state N_2 of energy $E_{2,1}$ is related to the number in the lower state N_1 by the equation:

$$N_2 = N_1(g_2/g_1) \exp(-E_{2,1}/kT), \quad (1)$$

where the g's are the weights of the two states, and T is the reversal temperature. This equation is identical in form with the Boltzmann

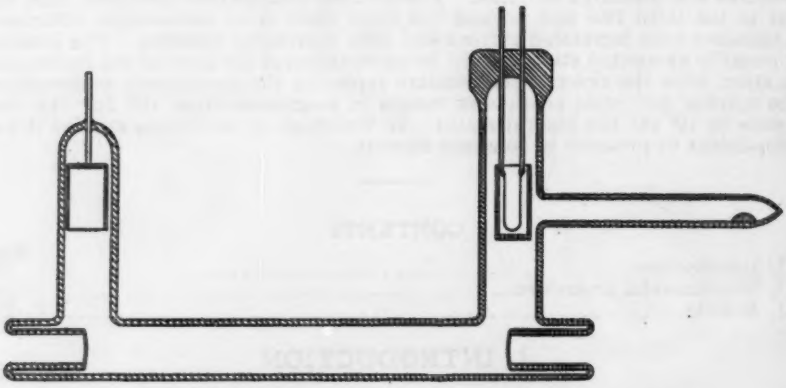

FIGURE 1.—*Discharge tube used to measure reversal temperature.*

equation, but it involves no assumption as to equilibrium and where there is not equilibrium different lines may give different values of T. T is quite independent of the strength of the absorption but the sensitivity of the method depends on the absorption.

II. EXPERIMENTAL PROCEDURE

Measurements were made with a columnar discharge in a tube of the shape shown in figure 1. The tube was 1.8 cm in diameter and the distance between the windows was 24 cm. The windows were in the discharge to avoid a reversing layer. Thin blown Pyrex windows were better than fused quartz, but discoloring of the windows by the alkali remained a source of error. The light from a gas-filled tungsten strip lamp passed along the axis of the tube. It was focused near the center of the tube and focused on the slit of the spectrograph by quartz fluorite achromats. A Hilger E1 quartz spectrograph was used.

[3] Hedwig Kohn, Phys. Z. 29, 49 (1928).

Corrections to be applied to the light intensity were measured by photographic densitometry. The brightness temperature of the image formed by the first lens within the discharge tube gives the true value of T. The tube was replaced by a quartz strip lamp to measure the ultraviolet intensity of the image. The tube was then put in place and the change in brightness measured. Half this change was taken to be the correction for one tube window. There is also a correction for the difference in emissivity of the tungsten in the ultraviolet as compared with the red, for the calibration of the quartz lamp was as usual in terms of red light. The sum of the corrections was a function of the wave length. Extreme values were

$$1/T \text{ (image)} - 1/T \text{ (lamp)} = .27 \times 10^{-4} \text{ at } 4555 \text{ A.}$$
$$1/T \text{ (image)} - 1/T \text{ (lamp)} = .30 \times 10^{-4} \text{ at } 3400 \text{ A.}$$

The procedure was to obtain a series of spectrograms with constant discharge conditions and with different currents in the strip lamp. Inspection showed which lamp current was closest to a match for each line and the calibrated temperature with the above correction gave the reversal temperature.

Good sensitivity and values of T within the range of the lamp could only be obtained in a limited range of discharge conditions. It required a number of trial exposures to find the useful range of lamp temperatures and exposure times. (Exposures ranged from 30 seconds to 30 minutes.) With the preliminary experience 8 or 10 exposures gave the reversal temperatures of all lines for one discharge condition. There is an uncertainty of at least 30° in picking the reversal temperature and there may be an equal or greater systematic error in the method used.

III. RESULTS

Table 1 summarizes the results and includes for comparison published values [4] of the reversal temperatures for the first doublet in the infrared and the electron temperature as obtained from probe

TABLE 1.—*Reversal temperatures for principal series lines of cesium*

Pressure	Current	Electron temperature	Reversal temperatures, in °K						
			8521 A 6S–6P	4555 A 6S–7P	3877 A 6S–8P	3612 A 6S–9P	3477 A 6S–10P	3398 A 6S–11P	Limiting value
μ	amp	°K							
350	2	2,520	2,260	2,160	2,115	2,115	2,140	----	2,115
350	1	2,320	2,090	2,020	1,985	1,970	1,970	----	1,970
350	.5	2,150	1,950	1,885	1,860	1,860	----	----	1,860
160	2	2,550	2,400	2,240	2,220	2,200	2,205	2,218	2,205
160	1	2,380	2,230	2,075	2,058	2,030	2,045	2,050	2,030
160	.5	2,120	2,140	1,985	1,938	----	----	----	1,938
76	2	2,640	2,450	2,340	2,290	2,280	2,270	2,270	2,270
76	1	2,530	2,340	2,160	2,110	2,080	2,080	2,070	2,080
76	.5	2,380	2,260	2,090	2,045	2,045	----	----	2,045

[4] Mohler, BS J. Research 9, 493 (1932) RP485.

measurements. Beyond the second line of the series the reversal temperatures are constant within experimental error. This regularity is important from a theoretical viewpoint and permits a fairly safe extrapolation to the series limit. The reversal temperature increases with increasing current and with decreasing pressure.

Table 2 expresses the results in terms of the number of excited atoms per cubic centimeter in each state $n^2P_{3/2}$ by use of equation 1. The negative exponent in the equation is always very large, ranging from 6.9 to 23.2, so the number of atoms in each state decreases rapidly with increasing energy even for constant values of T. A second regularity appears in table 2. The number of atoms in a given state at constant current is about the same for different pressures. A test of this relation over a wide range of pressures is desirable.

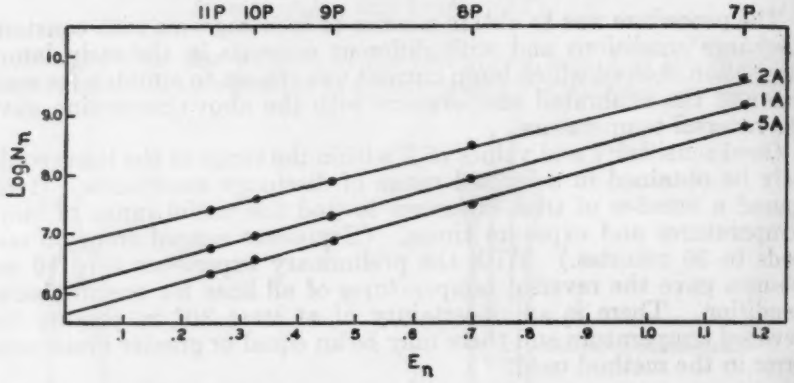

FIGURE 2.—*Plot of the log of the number of atoms in each excited state $nP_{3/2}$ versus the negative energy of the state.*

E_n is in electron volts measured from the ionized state as origin.

TABLE 2.—*Logarithms of the number of atoms in the states $n^2P_{3/2}$ per cubic centimeter*

Log N_s normal state	Current	Log N_6	Log N_7	Log N_8	Log N_9	Log N_{10}	Log N_{11}	Log N_∞
	amp							
15.73	2	12.80	9.71	8.47	7.90	7.59	7.39	6.81
17.73	1	12.54	9.28	7.96	7.31	6.96	6.77	6.13
17.73	.5	12.28	8.79	7.43	6.79	6.57	6.21	5.55
15.43	2	12.69	9.64	8.53	7.92	7.62	7.44	6.87
15.43	1	12.45	9.16	7.95	7.37	7.05	6.85	6.25
15.43	.5	12.32	8.85	7.47	6.86	6.51	6.31	5.67
15.10	2	12.42	9.58	8.41	7.84	7.54	7.36	6.81
15.10	1	12.29	9.08	7.82	7.14	6.82	6.62	6.02
15.10	.5	12.17	8.86	7.52	6.99	6.68	6.48	5.86
Energy of nP states (electron volts)		1.45	2.71	3.18	3.42	3.55	3.63	3.88

The results of table 2 are plotted in figure 2. The mean of log N_s for the three pressures is plotted as a function of the energy E_n. All results fall on three straight lines within experimental uncertainty, but theoretically the relation cannot be as simple as this. There is a real difference in temperature and therefore a real difference in slope

at the different pressures, but it is too small to see on the scale shown. If the populations are equal for 8P they will not be equal at the limit and vice versa.

The nearly constant value of T for higher series lines implies a nearly constant population of all states nP near the limit. This leads to an apparent paradox that is well recognized in the theory of distribution of energy in thermal equilibrium.[5] If there are an infinite number of states the number of excited atoms is infinite. Actually the lines beyond about $n=20$ are completely fused together by pressure broadening and random Stark effect of ions. It seems reasonable to assume that only about 20 discrete $^2P_{3/2}$ states exist and that for the 2 ampere discharge there are about 10^7 atoms in each state above $r=11$ and in order of magnitude 10^8 atoms in all P states above $n=11$. The number of atoms in the second state is then 10 times greater than in all higher P states, while the number in the first state is over 1,000 times that in the second state. The aggregate weight of every possible series term from $l=19$ to 0 is less than 1,000 times that of one $P_{3/2}$ term and, if it is assumed that all states are populated like the P states, there may be 10^{10} atoms in all the higher states. While these numbers are highly speculative it is worth while to see whether or not there are logical difficulties in extrapolating the experimental results and assuming that high energy states all have the same reversal temperature.

In spectroscopy it is commonly assumed that the initial states of a multiplet are populated in proportion to their statistical weight and experimental results confirm this for narrow multiplets.[6] It does not follow that the higher terms of a series which are of equal weight will be equally populated. The considerations of the preceding paragraph show that the series of terms must terminate either gradually or abruptly at some finite value. It has been found that in a limited range of conditions the population of P states tends to approach a constant value with increasing quantum number but this result cannot be generalized without further experiment. A paper on intensities of emission lines now in preparation gives some further evidence as to the range of validity of this relation.

WASHINGTON, January 7, 1936.

[5] Ruark and Urey, Atoms, Molecules and Quanta, p. 712 (McGraw-Hill Book Co., New York).
[6] See p. 697 of reference footnote 5.

U. S. Department of Commerce National Bureau of Standards

RESEARCH PAPER RP870

Part of Journal of Research of the National Bureau of Standards, Volume 16, March 1936

ABSORPTION OF X-RAYS BY LEAD GLASSES AND LEAD BARIUM GLASSES

By George Singer

ABSTRACT

The results of a study of the protective properties of a group of typical flint and barium-flint glasses are reported. In chemical composition, the protective glasses analyzed were found to resemble closely the denser optical flint and barium-flint glasses. The protection coefficients of the glasses were determined by an ionization method; of the various component elements it was found that only lead and barium contribute appreciably to the protective effectiveness of the glasses.

For flint glass empirical relations were established between the protection coefficient and the chemical composition, density, and refractivity; for barium-flint glass an empirical relation is given between the protection coefficient and the lead-oxide and barium-oxide components of the glass.

CONTENTS

		Page
I.	Introduction	233
II.	Methods of determining the protection coefficient of a material	234
III.	Experimental procedure	235
IV.	Description of glasses	237
V.	Protection coefficient and quality of radiation	239
VI.	Protection coefficient of glass for a narrow spectral band of radiation	241
	1. Flint glass	241
	2. Barium-flint glass	244
VII.	Empirical relations for protection coefficient of flint glass	246
	1. Protection coefficient and density	246
	2. Protection coefficient and refractive index	247
	3. Protection coefficient and chemical composition	247
VIII.	Empirical relations for barium-flint glass	249
	1. Effect of added barium oxide on protection coefficient	249
	2. Protection coefficient and chemical composition	250

I. INTRODUCTION

Gorton,[1] Dorsey,[2] and Kaye and Owen [3] have examined the X-ray protective properties of heavy flint glasses, and have correlated the protection coefficients [4] of these glasses with the glass density. How-

[1] W. S. Gorton, Am. J. Roentgenology 5, no. 10 (October 1918).
[2] N. Ernest Dorsey, Am. J. Roentgenology (March 1919).
[3] Kaye and Owen, Proc. Phys. Soc. London 35, 33D (1923).
[4] "Protection coefficient" has been defined by the American Advisory Committee on X-ray and Radium Protection as follows:
"The 'protection coefficient' of a protective material is the ratio of the thickness of lead to the thickness of material which absorbs a given X-ray beam to the same extent."
It is to be noted that the absorption coefficient of a material is a measure of its opacity to X-rays of a given quality as compared with that of metallic lead, and, therefore, depends not only upon the absorption properties of the material itself but upon those of lead as well. It is not a measure of the absolute opacity of the material.

ever, in recent years X-ray flint glasses have been largely supplanted by X-ray barium-flint glasses which, from the point of view of protection, are essentially different. Our tests of X-ray glasses have shown that the findings of the earlier studies (references 1, 2, and 3) are not directly applicable to the newer X-ray glasses without considerable extension and modification. This is principally because barium is of lower density and lower atomic number, and hence, has absorption properties differing from those of metallic lead. The object of the present study of X-ray glasses was:

1. To obtain the protection coefficient of flint and barium-flint glasses as a function of X-ray quality.
2. To correlate the protection coefficient with such readily determined physical properties of glass as density and refractive index.
3. To determine the relation between the protection coefficient of the glass and its chemical composition.

II. METHODS OF DETERMINING THE PROTECTION COEFFICIENT OF A MATERIAL

The relative X-ray opacities of materials are usually determined by either a photographic or an ionization method. Inasmuch as these two methods do not always give results which are in good agreement, and this fact is not usually appreciated, a brief discussion of them will be given.

The photographic method consists in simultaneously radiographing a glass sample and a lead echelon consisting of a prepared series of lead filters. This is usually done by placing the sample and echelon side by side directly upon the cassette containing the photographic film, and exposing them to radiation. It is desirable to reduce the distance between the radiographed material and photographic film to a minimum so as to avoid overlapping of the shadows cast and the inclusion of uncertain amounts of scattered radiation from both test sample and lead echelon. Successive exposures on the same or different films are also undesirable, for obvious reasons. That lead filter which gives directly or by interpolation the same photographic density as the sample is taken to be the lead equivalent of the sample. From this the protection coefficient is calculated.

The ionization method consists in comparing the current in a suitable X-ray ionization chamber obtained by using the sample as filter with the currents similarly obtained using a series of graduated lead filters. That thickness of lead which would give the same ionization current as the glass sample is then taken to be the lead equivalent of the sample.

Of these two methods, the photographic is more commonly used, since it requires a less elaborate experimental setup. Its chief advantage is that, unlike the ionization method, a constant source of X-rays is not essential, since the exposure of both the glass sample and the standard lead echelon are made simultaneously. With the ionization method the geometrical constants of the system used in making the measurements can be adjusted so as to minimize the effect of X-ray scattering from the glass and filters under test. By decreasing the solid angle subtended by the entrance diaphragm of the ionization chamber, and by sufficiently increasing the distance between the sample under test and the chamber, this scattering can be made

negligible. These adjustments are not possible with the photographic method; and consequently the protection coefficient so obtained usually differs from that obtained by the ionization method.

The result from the photographic method differs from that of the ionization method in that the former registers not only the transmitted radiation but in addition the secondary radiation from the material. Although it is true that from the point of view of protection, there is no need to distinguish between transmitted and scattered radiation from a protective material, it is desirable to separate the two factors, absorption and scattering. Unless this is done, a reproducible measure of the lead equivalent or protection coefficient of a material is more or less doubtful. Moreover, since the secondary radiation from glass has a different spectral composition than that of metallic lead, it is questionable whether two such different radiations can be satisfactorily compared by photographic means. Little is

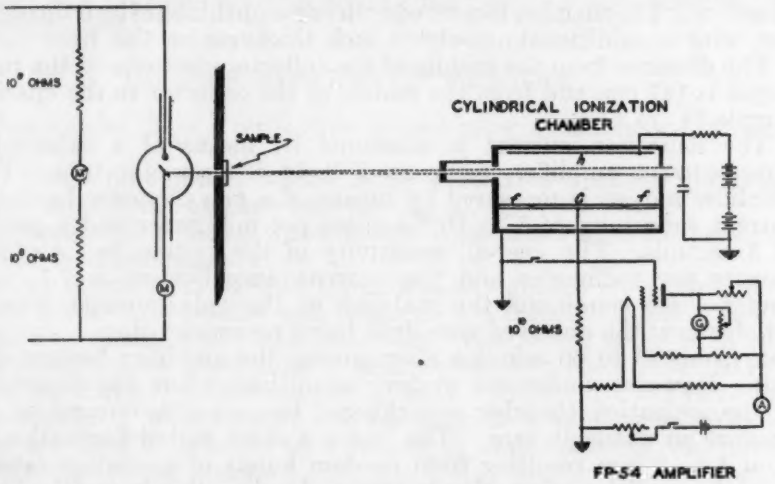

FIGURE 1.—*Diagram of the apparatus used in determining the lead equivalent of a protective material.*

known concerning the variation in photographic sensitivity with X-ray quality, and in the absence of definite information on this point, it is unsafe to assume that the sensitivity of the emulsion used is not a function of wave length.[5]

III. EXPERIMENTAL PROCEDURE

The ionization method and experimental arrangement sketched in figure 1 were used here. For measuring the relative absorption properties of materials the cylindrical ionization chamber is better suited than is the parallel-plate ionization chamber commonly used in dosage standardization. The X-ray intensities which must be measured in opacity tests are necessarily very low; for most of those here reported the radiation intensity after filtration is about 10^{-4} times that of the incident radiation. It is desirable to have the volume of air ionized large enough to furnish ionization currents

[5] R. B. Wilsey, Am. J. Roentgenology and Radium Therapy **32**, 789 (1935).

that are not troublesomely small. However, an increase in this volume augments at the same time the interelectrode capacity and the collector-to-ground capacity of the system, and the effect of both is to increase the period of the system and to produce an uncertain galvanometer zero because of induced currents resulting from random fluctuations in the potential difference between the high-potential electrode and ground.

The ionization chamber used is of the cylindrical open-air type. It consists of a thin aluminum cylinder electrode (h) spaced by hard-rubber posts from a concentric supporting brass tube 30 cm in diameter and 60 cm long, closed at the ends with aluminum. The edges of this electrode are somewhat rounded and separated several centimeters from the ends of the supporting cylinder so as to minimize field distortion. The collector electrode is a brass cylinder (c) about 1 cm in diameter and 30 cm long. Guard cylinders (f) of the same diameter extend to the earthed ends of the chamber. The chamber is covered with one-eighth inch of lead throughout, with an additional one-eighth inch thickness on the front face.

The distance from the middle of the collector electrode to the tube target is 147 cm, and from the middle of the collector to the opacity sample 74 cm.

The ionization current is measured by means of a balanced,[6] direct-current amplifier, using an F.P.-54 electrometer tube. The amplifier output is measured by means of a galvanometer having a current sensitivity of 5.7×10^{-9} ampere per millimeter and a period of 3 seconds. The over-all sensitivity of the system is 7.4×10^{-15} ampere per millimeter and the current amplification is 7.7×10^{5}. Under these conditions the stability of the galvanometer zero is satisfactory; the observed zero drift being no greater than 1 mm per hour from 30 to 60 minutes after closing the amplifier battery circuit. However, under the working conditions where the electrodes of the ionization chamber are charged two conditions combine to produce an unsteady zero. The first is a short period fluctuation of from 1 to 2 mm resulting from random bursts of ionization caused by alpha particles originating in traces of radioactive impurities [7 8] in the electrodes, and from radioactive contamination of the free air within the chamber. Because of their short period these fluctuations are readily distinguished from those resulting from variations in the X-ray input to the ionization chamber; and therefore they do not seriously affect the accuracy with which a given deflection can be read. A more serious cause of uncertainty in the galvanometer zero is the irregular displacement current produced in the ionization chamber by random fluctuations in the potential difference between the electrodes arising from variations in the emf. of the high-voltage supply. The interelectrode capacity of the chamber used is only 53 $\mu\mu$f, but a sudden variation of 0.1 volt in the potential difference produces a displacement current which registers a deflection of 30 mm at full sensitivity. Since 1,000 volts are required for saturation, it is evident that an extremely constant high-voltage supply is essential. Large B batteries in good condition are satisfactory.

[6] Lee A. DuBridge and Hart Brown, Rev. Sci. Inst. 4, 532 (1933).
[7] J. A. Bearden, Rev. Sci. Inst. 4, 271 (1933).
[8] Ziegert, Z. Phys. 46, 668 (1927).

The ionization current was measured by direct deflection. Inasmuch as ionization readings for both metallic lead and for glass are here directly compared any variation from linear amplification [9] in this system does not affect the results.

X-rays were generated by means of a thick-wall therapy X-ray tube supplied with power by a 200-kv constant-potential generator previously described.[10] The power-supply input is stabilized; variations in power input being not greater than ± 0.3 percent. The cathode of the X-ray tube was heated by storage batteries. Both tube voltage and current were continuously observed and controlled by the operator from his station near the amplifier. It is estimated that variations in X-ray input to the ionization chamber did not exceed ± 0.5 percent. When the X-ray generator is manually controlled these variations are reduced to approximately ± 0.25 percent. The potential difference across the X-ray tube was read directly by means of an accurately calibrated, high-resistance voltmeter [11] consisting of a microammeter in series with two resistance units of 100 megohms each.

IV. DESCRIPTION OF GLASSES

Commercial X-ray protective glasses now available are of two kinds:

1. Dense flint glasses whose X-ray protective qualities are practically determined by their lead content alone.
2. Barium-flint glasses whose effectiveness arises from the presence of both lead and barium.

Other constituents of both types of X-ray glasses are of comparatively low atomic number and hence do not contribute much to the protective qualities of these materials. The recent trend in X-ray glasses has been toward those of higher protection coefficient, that is, from the flint to the barium-flint glasses. Although the former are now relatively unimportant commercially as a protective product, they are here of interest as a means of understanding the newer barium-flint X-ray glasses.

This report is based on a study of 30 glasses obtained from a number of different sources. Of these, 22 are commercial X-ray glasses selected from a group of 53 as being representative of protective X-ray glasses commercially available at the present time. For the purpose of comparison, 8 standard optical glasses were included; 6 of these were obtained from the Glass Section of this Bureau.

Although lead and barium are the effective components of protective glasses, in considering the protective properties of these glasses it is convenient to consider the protection coefficient as a function of the oxides of these metals rather than of the metals themselves.

In tables 1 and 2 there are listed all flint and barium-flint X-ray glasses studied, together with such of their chemical and physical properties as are of interest in connection with this study.[12] The

[9] The ratio between output current and input current for the system used varies from a straight line by approximately one percent for deflections up to the maximum obtained. Where strictly linear amplification is essential, it is necessary to operate the electrometer tube on a fixed point of its plate current-grid potential characteristic. This is best done by the introduction of a potentiometer in the grid circuit, and the use of the system as a null instrument.

[10] L. S. Taylor, BS J. Research **2**, 771 (1929) RP56.

[11] L. S. Taylor, BS J. Research **5**, 609 (1930) RP217.

[12] We are indebted to J. I. Hoffman for checking the chemical analyses of the glasses listed; to L. W. Tilton for all refractivity measurements; and to E. L. Peffer for all density determinations.

classification of each glass is given in column 2. BC–1, BC–2, and BC–3 of table 2 are optical barium crown glasses, not used for X-ray protection, but included here for purposes of comparison. The chemical analyses given for PbO and BaO content were obtained mostly from the glass manufacturers. In several cases our measurements of the opacity to X-rays indicated that the manufacturer's analysis must be in error. In each of these a chemical analysis made by Mr. Hoffman at this Bureau confirmed our views; and for these Mr. Hoffman's analyses are recorded instead of those given by the manufacturer.

TABLE 1.—*List of flint glasses*

Glass	Classification	Number of samples of each glass	Refractive index n_D	Density	PbO	BaO	Protection coefficient (percent) for—						
							90 kv	105 kv	120 kv	135 kv	150 kv	165 kv	195 kv
					%	%							
F-1 [a]	Commercial X-rays	2	1.618	3.609	46.1	0.0	14.96	14.93	15.06	14.94	15.11	14.84	14.72
F-3 [b]	Optical flint	1	1.622	3.630	46.0	0.0	15.13	14.96	15.17	14.90	15.03	14.88	14.94
F-4 [b]	do	1	1.647	3.859	51.5	0.0	17.84	17.43	17.53	17.49	17.55	17.35	17.25
F-5 [c]	Commercial X-rays	2	1.700	4.310	60.3	0.0	22.30	22.43	22.51	22.43	22.32	22.60	22.51
F-9 [c]	do	1	1.721	4.479	65.0	0.0	23.92	24.20	23.99	24.13	23.99	-----	-----
F-12 [b]	Optical flint	1	1.775	4.932	69.8	0.0	28.42	28.66	28.77	28.66	28.62	28.52	28.50

[a] Chemical analysis made by Mr. Hoffman of NBS Chemistry Division.
[b] Batch analyses submitted by Mr. Finn of NBS Glass Section.
[c] Chemical analyses submitted by manufacturer.

TABLE 2.—*List of barium-flint and barium-crown glasses*

Glass	Classification	Number of samples of each glass	Refractive index n_D	Density	PbO	BaO	Protection coefficient (percent) for—						
							90 kv	105 kv	120 kv	135 kv	150 kv	165 kv	195 kv
					%	%							
BF-1 [a]	Optical barium flint	1	-----	3.392	6.87	29.15	-----	-----	-----	-----	-----	9.89	8.89
BF-2 [b]	do	1	1.603	3.479	23.5	14.5	15.35	14.86	14.62	13.79	13.56	12.75	11.93
BF-3 [c]	Commercial X-ray	2	1.614	3.572	44.1	<.1	14.80	14.78	14.81	14.66	14.74	14.81	14.72
BF-5 [c]	do	2	1.6949	4.323	47.1	14.35	26.43	26.56	26.31	25.76	24.65	-----	21.56
BF-7 [a]	do	2	1.6992	4.361	45.38	15.02	26.60	26.90	26.46	25.96	24.93	23.57	22.26
BF-9 [c]	do	3	1.7146	4.423	60.0	<.1	23.49	23.63	23.58	23.64	23.48	-----	23.43
BF-12 [c]	do	2	1.723	4.587	52.0	13.94	29.42	29.38	29.14	28.61	27.70	-----	-----
BF-14 [a]	do	1	-----	4.604	53.15	13.01	29.98	29.74	29.22	28.80	27.73	26.17	24.90
BF-15 [a]	do	2	1.7254	4.609	52.6	14.7	29.88	30.15	29.83	29.27	28.20	26.05	25.02
BF-17 [a]	do	1	-----	4.609	51.2	15.5	-----	29.7	-----	-----	28.0	-----	-----
BF-18 [c]	do	2	1.741	4.690	62.2	2.34	26.88	26.88	26.94	26.90	26.57	-----	-----
BF-20 [c]	do	1	1.742	4.698	61.6	2.52	27.01	27.11	27.17	27.24	26.99	26.63	26.41
BF-22 [a]	do	2	1.7396	4.712	60.9	6.5	28.43	28.62	28.64	28.54	27.91	27.54	26.81
BF-24 [a]	do	2	1.7428	4.734	62.1	5.3	28.27	28.69	28.49	28.42	27.85	27.63	27.08
BF-27 [a d]	do	1	-----	4.837	52.6	14.6	31.02	31.30	31.09	30.22	28.80	28.09	26.23
BF-28 [a e]	do	1	-----	4.856	62.0	5.3	30.50	30.29	30.27	30.19	29.60	29.29	28.25
BF-29 [a]	do	1	-----	4.906	62.0	8.0	31.37	31.30	31.30	31.01	30.14	29.83	28.44
BF-30 [a]	do	1	-----	5.055	62.0	10.0	33.38	33.39	32.97	31.67	31.69	31.16	29.25
BF-31 [a]	do	1	-----	-----	61.0	9.7	-----	32.0	-----	30.6	-----	-----	28.4
BC-1 [b]	Optical barium crown	1	1.572	3.205	0.0	31.7	14.03	12.41	11.28	10.23	9.45	8.45	7.62
BC-2 [a]	do	1	-----	3.513	0.0	38.40	-----	-----	-----	-----	-----	10.04	8.71
BC-3 [b]	do	1	1.606	3.701	0.0	42.7	23.94	20.60	17.31	14.95	13.52	12.05	10.56

[a] Chemical analyses submitted by manufacturer.
[b] Batch analyses submitted by Mr. Finn of NBS Glass Section.
[c] Chemical analyses made by Mr. Hoffman of NBS Chemistry Division.
[d] Glass BF-27 contains 5% of TiO_2.
[e] Glass BF-28 contains 2% of UO_3.

It should be noted that the commercial X-ray glasses of both the flint and barium-flint types are very similar in their chemical and physical properties to the typical optical glasses of these types. The X-ray glasses are different only in that their content of lead and barium oxide is, in general, greater.

V. PROTECTION COEFFICIENT AND QUALITY OF RADIATION

The manner in which the protection coefficient of a glass depends upon the quality of the incident X-radiation is of particular interest. If there is a marked variation in the protection coefficient of a glass as the X-ray quality is varied, the coefficient determined for any one quality may be quite adequate for calculating the glass thickness required to meet X-ray safety recommendations [13] for that particular

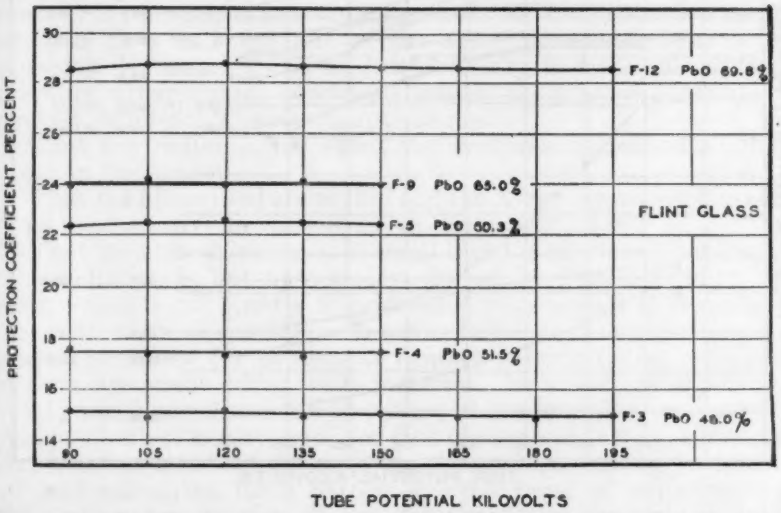

FIGURE 2.—*The variation of the protection coefficient of flint glass with* X-*ray tube potential.*

radiation but may be dangerously inadequate for a corresponding calculation for radiation of another quality. In such a case it is obviously meaningless to speak, as is often done, of the protection coefficient or lead equivalent of the glass unless the quality of radiation for which the coefficient applies is also specified.

The protection coefficient of a flint glass, which depends for its protective quality almost wholly on its lead content, is, in general, independent of the radiation quality. This is apparent from figure 2 in which the protection coefficient of the glasses listed in table 1 is plotted as a function of the excitation potential on the X-ray tube. Here the locus of the protection coefficient of any one flint glass is nearly a horizontal straight line. For most glasses of this type there appears to be a very slight, though negligible, maximum at about 105 kv, which is probably due to the light oxide components of the glass.

[13] Handb. BS HB15 (1931).

As shown in figure 3, the protection coefficient of a barium-flint glass, in contrast with that of a flint glass, is not independent of radiation quality. The protection coefficient here yields a curve with a maximum at about 105 kv irrespective of the amount of barium present. The accentuation of the maximum increases, however, with the increase of barium content, glasses containing relatively large quantities of BaO having the most marked maxima. For barium-crown glasses, such as BC–1 and BC–3, the variation of protective coefficient with radiation quality is most marked. The maxima for

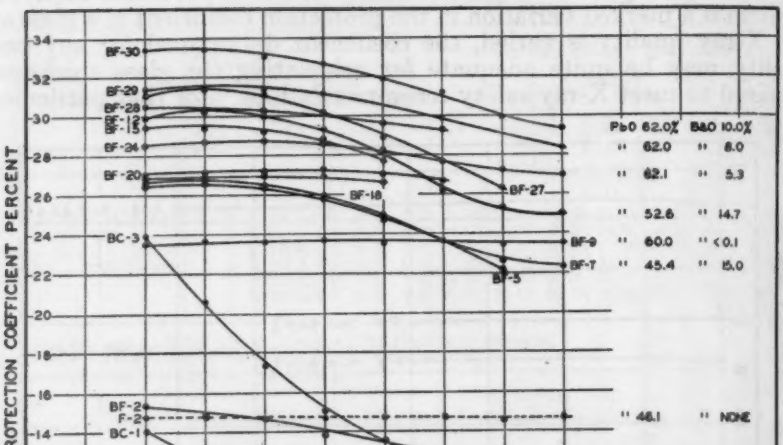

FIGURE 3.—*The variation of the protection coefficient of barium-flint and barium-crown glass with X-ray tube potential.*

these glasses are not shown since they lie below the tube-voltage ranges used.

A comparison between the protection coefficient of a flint and a barium-flint glass containing the same percentage of PbO is of interest in that effectiveness of the BaO component of the barium-flint glass then becomes apparent. In order to facilitate such a comparison, the protection coefficient curve of a flint glass, F–2, having about the same PbO content as barium-flint BF–7, has been included in figure 3. Although this is a typical case, other examples are available between glasses listed in tables 1 and 2. Comparing curves, F–2 and BF–7 reveals that the protection coefficient of a barium-flint glass is considerably greater than that of a flint glass containing the same percentage of PbO. This difference is especially marked in the vicinity of the maximum for 105-kv X-rays, but with increasing hardness of the radiation the difference in coefficients diminishes.

It is obvious that the protection coefficient of a barium-flint glass cannot be less than that of a flint glass containing the same percentage of PbO. This point is of practical interest, since it defines the lower limit of the protection coefficient of a barium-flint glass in terms of the protection coefficient of a flint glass containing the same PbO component. The protection coefficient of the latter glass does not vary appreciably with voltage and is readily determined from any one of several physical and chemical properties of the glass.

VI. PROTECTION COEFFICIENT OF GLASS FOR A NARROW SPECTRAL BAND OF RADIATION

1. FLINT GLASS

In order to understand the characteristic differences between X-ray glasses of the flint and barium-flint types described in the preceding section, it is convenient to set up equations for the protection coefficient of a glass as a function of the absorption coefficients of its component elements. To do so, it is necessary to make assumptions concerning experimental conditions which in practice cannot be rigorously fulfilled. These assumptions are:

1. That the radiation for which the coefficient is defined is homogeneous in frequency.
2. That the filters used are so thin and the X-ray beam so collimated that all incident rays traverse equal thicknesses of filter.
3. That the filter thickness is so small that the effective wave length of the radiation is not appreciably altered by filtration when the radiation used is not strictly homogeneous with respect to frequency.

The first of these conditions is never fulfilled; X-ray glasses are intended primarily for protection against heterogeneous radiation, and tests are made using such radiation. However, as is already evident from figure 2 and the discussion of the preceding section, the wave-length effect is very small for flint glasses and it may, therefore, be expected, as is indeed the case, that for such glasses the protection coefficient calculated for a narrow spectral band of radiation is a satisfactory approximation of the experimentally determined value for heterogeneous radiation. For barium-flint glasses the case is, however, quite different since there is considerable variation in protection coefficient with variation in radiation quality. Consequently the protection coefficient for barium-flint glasses calculated for a narrow spectral band is difficult to interpret and is not directly comparable with the experimental value. However, even for barium-flint glasses the equations derived for a narrow spectral band of X-rays are valuable in that they reveal the relation whereby the protection coefficient changes with variation in radiation quality.

The second assumed condition can be approximated in practice, as has here been done, by diaphragming the beam so that for all rays there is little difference in path-length through the filter.

The glass filters used were approximately one-fourth inch thick. Since filters of such thickness harden the incident heterogeneous radiation considerably, the further assumption is involved that the quality changes resulting from filtration through the corresponding thickness of metallic lead and through glass are identical.

Let a beam of a narrow spectral band of radiation of intensity I_o, be reduced to intensity I, on traversing a glass sample of thickness X_{gl}. Now let a filter of metallic lead be selected of such thickness, X_{Pb}, that it, also, will reduce the intensity of the X-ray beam from I_o to I. Then

$$I=I_0e^{-\mu_{gl}X_{gl}}=I_0e^{-\mu_{Pb}X_{Pb}}, \tag{1}$$

where μ_{gl} and μ_{Pb} are respectively the linear-absorption coefficients of the glass sample and the metallic-lead filter for the X-radiation in question. From equation 1 and the definition of the protection coefficient (C)[14], it follows that:

$$C=\frac{X_{Pb}}{X_{gl}}=\frac{\mu_{gl}}{\mu_{Pb}}=\frac{\mu_{gl}}{(\mu/\rho)_{Pb}\cdot\rho_{Pb}}, \tag{2}$$

where $(\mu/\rho)_{Pb}$ is the mass absorption coefficient for lead for the X-radiation in question, and $\rho_{Pb}=11.34$ is the density of lead. Since the mass absorption coefficient of an element is essentially independent of its physical or chemical state,[15] it is possible to express the linear absorption coefficients of the glass sample, μ_{gl}, in terms of the mass absorption coefficients of its several component elements, $(\mu/\rho)_1$, $(\mu/\rho)_2$, etc., as follows:

$$\mu_{gl}=\rho_{gl}\,[P_1(\mu/\rho)_1+P_2(\mu/\rho)_2\ \cdots\cdots\ P_n(\mu/\rho)_n], \tag{3}$$

where P_1, P_2, P_3, etc. are the ratios of the mass of each component to the total mass of the glass; $(\mu/\rho)_1$, $(\mu/\rho)_2$, etc. are the mass absorption coefficients of these components; and ρ_{gl} is the glass density. Equation 2 then becomes:

$$C=\frac{\rho_{gl}}{\rho_{Pb}}\left[P_1\frac{(\mu/\rho)_1}{(\mu/\rho)_{Pb}}+P_2\frac{(\mu/\rho)_2}{(\mu/\rho)_{Pb}}\ \cdots\cdots\ P_n\frac{(\mu/\rho)_n}{(\mu/\rho)_{Pb}}\right]. \tag{4}$$

Since lead is the most important component in all protective X-ray glasses, it is convenient to rewrite equation 4 as follows:

$$C=\frac{\rho_{gl}}{\rho_{Pb}}\cdot P_{Pb}+\frac{\rho_{gl}}{\rho_{Pb}}\left[P_2\frac{(\mu/\rho)_2}{(\mu/\rho)_{Pb}}+P_3\frac{(\mu/\rho)_3}{(\mu/\rho)_{Pb}}\ \cdots\cdots\ P_n\frac{(\mu/\rho)_n}{(\mu/\rho)_{Pb}}\right]. \tag{5}$$

By means of equation 5 it is possible to calculate the protection coefficient C of any glass for a narrow spectral beam of radiation, having given the composition and density of the glass and the mass absorption coefficient of each component element for that radiation. The total protection coefficient C is expressed as the sum of two quantities: The first of these gives the component of the total coefficient due to the metallic lead contained in the glass; the second is the component of the total coefficient due to the presence of all component elements other than lead. The first right-hand term involves no quantity which varies with the quality of the incident radiation; the second involves the mass absorption coefficient of metallic lead and of each element contained in the glass, all of which are functions of radiation quality. It is therefore to be expected that the protection coefficient of any glass is independent of radiation

[14] See footnote 4.
[15] See, for example, Int. Crit. Tables 6, 12 (1929).

quality only to the extent that the component of the total-protection coefficient due to elements other than lead is negligibly small as compared with that due to the lead content of the glass.

That the component of the total-protection coefficient due to elements other than lead is small for flint glass is evident from table 3. Here the protection coefficients of four flint glasses as calculated by means of equation 5 for wave lengths .098 and .710 A are compared with the experimentally determined values for 90 and 150 kv. The calculated coefficients given in columns 3 and 4 are lower than the experimentally determined values of columns 5 and 6. The agree-

TABLE 3.—*Protection coefficients of four typical flint glasses as calculated by equation 5 compared with experimentally determined values*

1	2	3	4	5	6	7	8
Glass	PbO	Protection coefficient (percent)				Fraction of total calculated coefficient due to components of glass other than lead for:	
		Calculated for [a]:		Observed for:			
		λ=.098 A	λ=.710 A	150 kv	90 kv	λ=.098 A	λ=.710 A
	Percent						
F-3	46.0	14.5	14.3	15.0	15.1	0.055	0.044
F-4	51.5	17.1	16.9	17.6	17.8	.046	.036
F-5	60.3	22.1	21.8	22.3	22.3	.035	.026
F-12	69.8	28.6	28.6	28.6	28.4	.012	.014

[a] The mass absorption coefficients used in these calculations were taken from data tabulated by Compton and Allison, X-rays in Theory and Practise, p. 800 (D. Van Nostrand Co. Inc., New York, 1935).

ment, however, becomes satisfactory for the denser flint glasses. It should be noted that glasses F–3 and F–4 are optical flint glasses, which are lighter than most X-ray glasses of this type. They are included here because it was desired to test the validity of equation 5 for glasses lying immediately outside the range of typical X-ray glasses. Glass F–5 is a typical X-ray flint. Glass F–12 is a very dense optical flint, heavier than any X-ray flint tested. In columns 6 and 7 of table 3 there is given for each glass the fraction of the calculated protection coefficient due to glass components other than metallic lead. For the dense flint glasses the total contribution of all elements other than lead is small, being of the order of 2 or 3 percent.

If it is therefore assumed that for heavy flint glass the effect on the coefficient of all elements other than lead is negligible, equation 5 can be simplified by dropping the second term, which gives:

$$C=\frac{\rho_{gl}}{\rho_{Pb}}P_{Pb} \tag{6}$$

Equation 6 then gives an approximation for the protection coefficient of a heavy flint glass simply in terms of the percentage of lead it contains, the glass density, and the density of lead. Since the density of lead is 11.34 and that of heavy flint glass about 4, it follows that for such glasses the protection coefficient is roughly equal numerically to one-third the percentage of lead contained. The statement is occasionally made that a flint glass containing—say 60

percent of lead—will have a protection coefficient of 60 percent; but this is not to be expected from equation 6; and that it is not true is evident from any one of the curves given in figure 2. By means of equation 5 the chief characteristics of flint glass as a protective material (as found experimentally) can be explained, namely:

1. The protection coefficient of a flint glass is practically independent of radiation quality.

2. All elements contained in a flint glass other than lead contribute little to the value of the glass as a protective material.

2. BARIUM-FLINT GLASS

It has already been noted in connection with the discussion of figure 3 that a barium-flint glass has an appreciably greater protection coefficient than a flint glass containing the same percentage of lead oxide. This is to be expected since the atomic number of barium (56) is considerably greater than that of most elements found in glass; however, the marked protective effectiveness of barium for heterogeneous radiation of about 105 kv cannot be attributed to this cause alone. It is convenient to rewrite equation 5 for a barium-flint glass as follows:

$$C=\frac{\rho_{gl}}{\rho_{Pb}}\cdot P_{Pb}+\frac{\rho_{gl}}{\rho_{Pb}}\left(P_{Ba}\cdot\frac{(\mu/\rho)_{Ba}}{(\mu/\rho)_{Pb}}\right)+\frac{\rho_{gl}}{\rho_{Pb}}\sum\frac{(\mu/\rho)_r}{(\mu/\rho)_{Pb}}, \tag{7}$$

where P_{Ba} is the fraction of the total mass of the glass which is barium-having a mass absorption coefficient $(\mu/\rho)_{Ba}$. Since the percentage of the light elements (those other than barium and lead) in an X-ray barium-flint glass is less than that in a flint glass containing the same percentage of lead, it is to be expected that the contribution toward the protection coefficient made by the lighter components is even less in a barium-flint than in a flint glass having the same percentage of lead. If we, therefore, assume the effect of the elements other than lead and barium to be negligible, equation 7 becomes

$$C=\frac{\rho_{gl}}{\rho_{Pb}}\left(P_{Pb}+P_{Ba}\cdot\frac{(\mu/\rho)_{Ba}}{(\mu/\rho)_{Pb}}\right). \tag{8}$$

From this, it is evident that the protection coefficient of a barium-flint glass must depend upon the quality of the incident radiation since the mass absorption coefficients of both lead and barium are involved, both of which are functions of wave length; moreover, the wave-length effect must vary with the percentage of barium (P_{Ba}) contained in the glass, as has already been noted in connection with the experimentally determined value. The nature of this dependence is evident from a consideration of the manner in which the mass absorption coefficient of an element varies with effective wave length of a narrow spectral beam. At the critical absorption limits of both lead and barium, there are discontinuities in their respective absorption coefficients, and since these discontinuities occur at different wave lengths, it is evident that there must be distinct discontinuities in the protection coefficient of a glass containing barium. Of particular interest are the discontinuities of these elements at their respective K absorption limits, which, for lead, occurs at 0.1405 A and for barium at 0.3307 A. As the X-ray tube voltage is increased, the K absorption limits of barium are approached from the long wave-

length side, and at this limit the mass absorption coefficient of barium is increased about sixfold. The composite protection coefficient as given by equation 8 will, therefore, be correspondingly increased. As the tube voltage is increased further, the critical absorption limit of lead is reached at which the absorption coefficient of lead is approximately doubled. For radiation of this quality, the protection coefficient will, therefore, be decreased since the mass absorption coefficient of lead occurs in the denominator of equation 8. As a result of these discontinuities the protection coefficient of a glass containing barium should have a maximum value in the interval 0.1405 A$<\lambda>$ 0.3307 A. In figure 4 the ratio of the mass absorption coefficient of barium to that of lead has been plotted as a function of wave length for a narrow spectral band of radiation.

For heterogeneous radiation, no distinct discontinuities in the protection coefficient, such as shown in figure 4, are to be expected.

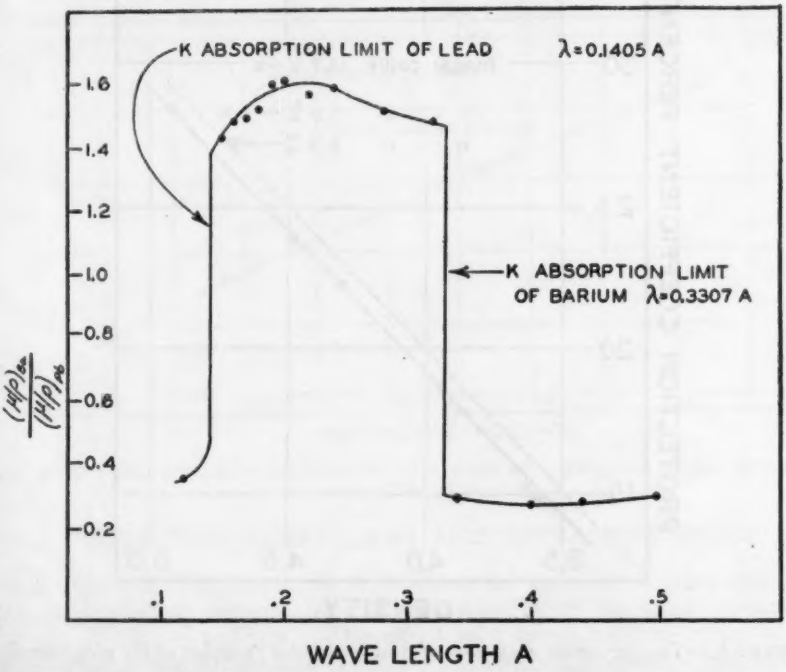

FIGURE 4.—*The ratio of the mass absorption coefficients of barium and lead as a function of the effective wave length of a narrow spectral band of* X-*radiation.*

However, since any heterogeneous beam having a minimum wave length less than 0.1405 A has some radiation lying in the above-mentioned interval, the effect of the barium component in the glass is to increase the protection coefficient. The actual increase depends upon what fraction of the total energy of the composite beam falls within the interval 0.1405 A $<\lambda>$ 0.3307 A. As the X-ray-tube voltage is increased above 105 kv less and less of the total energy of the beam falls within this interval and the protection coefficient is correspondingly decreased, as has already been noted from the experimental data. This effect is particularly noticeable in barium-crown glasses, such as BC–1 and BC–3 of figure 3.

VII. EMPIRICAL RELATIONS FOR PROTECTION COEFFICIENT OF FLINT GLASS

As already noted, the theoretical relations derived for the protection coefficient of glass are limited in their practical usefulness by the simplifying assumptions necessary for their derivation, the most formidable of which is the assumption that the X-radiation is homogeneous. Because of these limitations, empirical relations between the protection coefficient and such properties of the glass as density, refractive index, and lead-oxide and barium-oxide content are desirable. Then, when any one of these properties is known, it may be possible to predict the protection coefficient of a typical X-ray protective glass from these empirical relations without actually

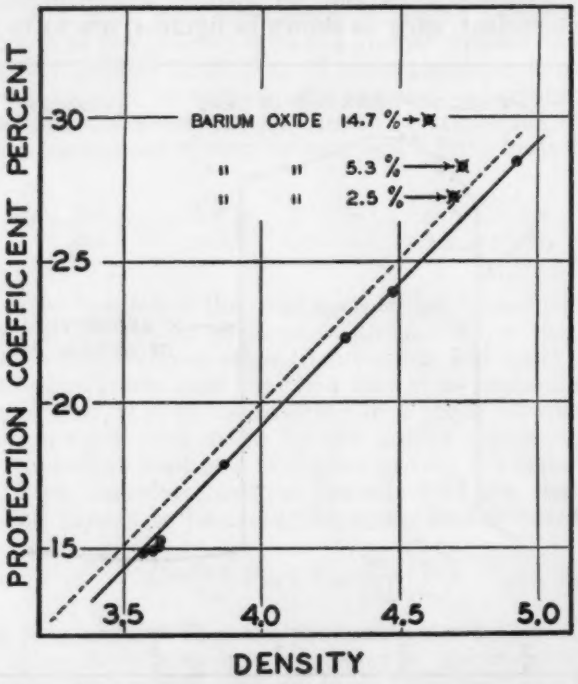

FIGURE 5.—*The protection coefficient of flint glass as a function of the glass density.*

determining the protection coefficient experimentally. The values so obtained agree with the accurately determined experimental value to within a few percent and are usually as good as the experimental value obtainable with the apparatus and equipment in the average X-ray laboratory.

It is comparatively easy to find empirical relations for a typical X-ray glass which contains only PbO as an effective component; for a barium-flint X-ray glass the problem is complicated by the presence of an additional component, BaO.

1. PROTECTION COEFFICIENT AND DENSITY

The relation between the protection coefficient and the density of a flint glass is given in figure 5 for typical X-ray glasses ranging in den-

sity from 3.61 to 4.93. Over this range, the protection coefficient is found to be a linear function of the glass density, given by the equation:

$$C=10\rho_{gl}-20.8;\ 3.61<\rho_{gl}<4.93, \tag{9}$$

where again C is the protection coefficient and ρ_{gl} the glass density. This is in substantial agreement with a similar equation by Kaye,[16] derived from a study of flint glasses ranging in density from 3.2 to 4.8.

Equation 9, based on data obtained here for 90-kv radiation, holds, within the experimental error, for radiations up to 195 kv. The values for C so obtained are about 3 percent lower than Kaye's. The effect of a small barium-oxide component may be noted from the points plotted also in figure 5 for glasses containing small quantities of barium oxide.

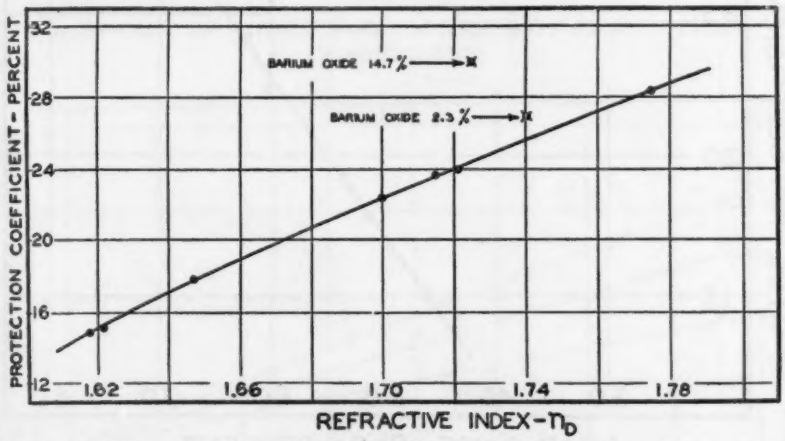

FIGURE 6.—*The protection coefficient of flint glass as a function of the refractive index of the glass.*

2. PROTECTION COEFFICIENT AND REFRACTIVE INDEX

In figure 6 the protection coefficient of each flint glass studied has been plotted against the refractive index of the glass obtained for the D line of sodium. The effect of a small barium component in increasing the protection coefficient is again apparent. Inasmuch as the refractive index of a glass is readily determined, the curve of figure 6 is a very convenient means for determining the protection coefficient of a flint glass.

3. PROTECTION COEFFICENT AND CHEMICAL COMPOSITION

Figure 2 indicates that in general the protection coefficient of a flint glass depends upon the PbO contained in the glass and increases as this component is increased. Figure 7 shows the more exact nature of this dependence, as made evident by replotting the same data with the protection coefficient as ordinate and the PbO content of the glass as abscissa. The closed circles represent experimental

[16] G. W. C. Kaye, Roentgenology, p. 89 (Paul B. Hoeber, Inc., New York, 1929).

data obtained for flint glasses listed in table 2. The open circles are points obtained by means of equation 9 from Wright's [17] collected data on the relation between the density and the PbO content of optical flint glasses. The crossed circles are for X-ray glasses containing small amounts of BaO. It appears that the protection coefficient of a flint glass is an increasing function of the percentage of lead oxide. This function is not exactly linear but for a PbO component

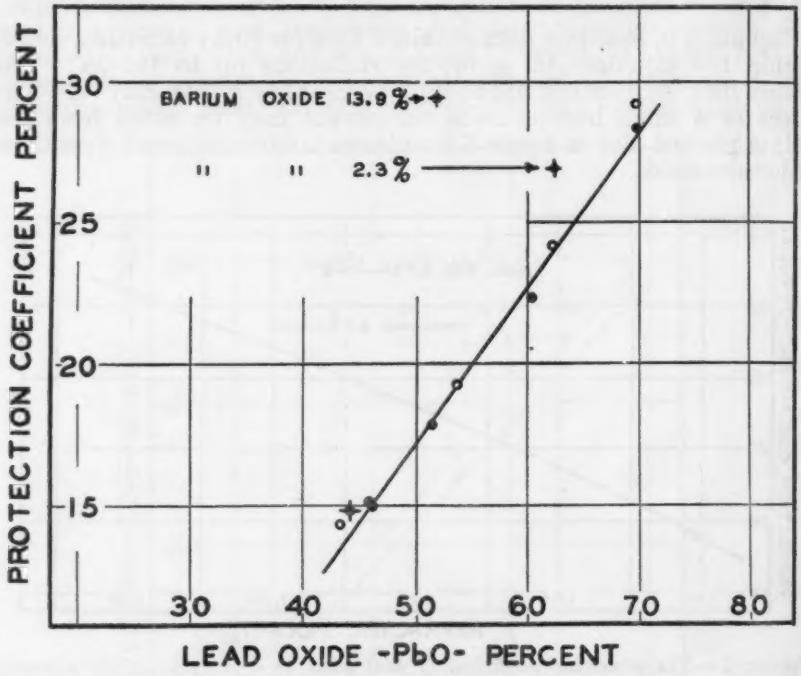

FIGURE 7.—*The protection coefficient of flint glass as a function of the percentage of lead oxide* (PbO) *contained in the glass.*

ranging from 46 to 70 percent, it can be satisfactorily approximated by the straight line equation:

$$C=0.553(P_{PbO}-19);\ 46<P_{PbO}<70, \tag{10}$$

where P_{PbO} is the percent of PbO contained in the glass. X-ray glasses commercially available fall well within the range of PbO components for which this linear approximation is satisfactory.

In table 4 the experimentally determined protection coefficients for 90- and 150-kv X-rays of all flint glasses studied are compared with the coefficient calculated by means of equation 10.

[17] The Manufacture of Optical Glass and of Optical Systems, p. 60, Ordnance Dept. Document 2037 (U. S. Government Printing Office, Washington, D. C., 1921).

TABLE 4.—*Flint glasses*

Glass	Classification	PbO	Protection coefficient (percent) for—			
			90 kv		150 kv	
			Experimental	Calculated	Experimental	Calculated
		%				
F-1	Commercial X-ray	46.1	15.0	15.0	15.1	15.0
F-3	Optical flint	46.0	15.1	14.9	15.0	14.9
F-4	do	51.5	17.8	18.0	17.6	18.0
F-5	Commercial X-ray	60.3	22.3	22.8	22.3	22.8
F-9	do	65.0	23.9	25.4	24.0	25.4
F-12	Optical flint	69.8	28.4	28.1	28.6	28.1

VIII. EMPIRICAL RELATIONS FOR BARIUM-FLINT GLASS

1. EFFECT OF ADDED BARIUM OXIDE ON PROTECTION COEFFICIENT

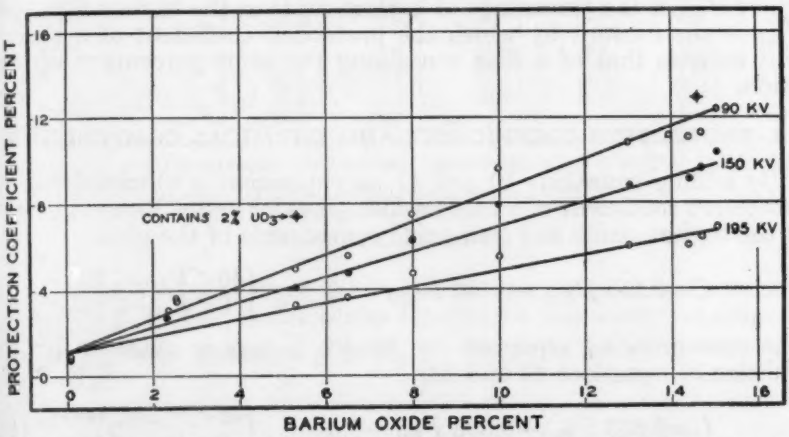

FIGURE 8.—*The component of the total protection coefficient of barium flint glass due to all elements of the glass other than lead plotted as a function of the percentage of barium oxide* (BaO) *contained in the glass.*

That there is a marked increase in the protection coefficient of an X-ray glass when BaO is added has already been noted in the discussion of figure 3. Some idea of the effectiveness of even a very small BaO component in an X-ray glass can be obtained from figure 7 in which, for 90-kv radiation, the two points with crosses are for glasses containing 2.3 and 13.9 percent of BaO in addition to their PbO component. It is apparent that for radiation of this quality, as little as 0.5 percent of BaO results in an appreciable increase in the protection coefficient of the glass. For more penetrating radiation the effect of the BaO component is less, but is still appreciable.

Further study of the relation between this increase in protection coefficient with the BaO component of the glass reveals that for radiation of a given quality, the amount by which the coefficient is increased is approximately a linear function of the BaO component

and, as is to be expected, is essentially independent of the PbO component. In figure 8 the amount by which the protection coefficient of a barium-flint glass exceeds that of a flint glass containing the same percentage of PbO, has been plotted as a function of the BaO component of the barium-flint for three different tube voltages, 90, 150, and 195 kv. The points of figure 8 show considerable scattering arising from the extent to which components other than PbO and BaO contribute appreciably to the total protection coefficient of the glass. However, for X-ray barium flints this scattering is no greater than 3 percent of the total protection coefficient of the glass. One exception is to be noted, an "experimental" X-ray glass containing 2 percent of UO_3 (uranium trioxide); in this case the heavy oxide had been included in order to test the effect of heavy oxides other than those of lead and barium. From the data plotted in figure 8, the following relations have been obtained:

$$\left.\begin{array}{l}\text{For } 90 \text{ kv: } C_{BaO}=0.727P_{BaO}+1.2 \\ \text{For } 150 \text{ kv: } C_{BaO}=0.586P_{BaO}+1.0\end{array}\right\} 0<P_{BaO}<15, \quad (11), (12)$$

where P_{BaO} is the percentage of barium oxide in the barium flint, and C_{BaO} is the amount by which the protection coefficient of a barium flint exceeds that of a flint containing the same percentage of lead oxide.

2. PROTECTION COEFFICIENT AND CHEMICAL COMPOSITION

By adding equations 10 and 11 an expression is obtained for the protection coefficient of a barium-flint glass for 90-kv X-rays in terms of the barium-oxide and lead-oxide components of the glass.

$$C=0.553\ P_{PbO}+0.727\ P_{BaO}-9.3 \qquad \begin{cases}46<P_{PbO}<70. \\ 0<P_{BaO}<15.\end{cases} \quad (13)$$

The corresponding equation for 150-kv X-rays is obtained by the addition of equations 10 and 12;

$$C=0.553\ P_{PbO}+0.586\ P_{BaO}-9.5 \qquad \begin{cases}46<P_{PbO}<70. \\ 0<P_{BaO}<15.\end{cases} \quad (14)$$

Equations 13 and 14 are based on observations of flint glasses approximately 6 mm thick. Kaye [18] has reported that for radiation of a given quality the lead equivalent of barium-sulphate plaster is not strictly proportional to the thickness of the material. He found that the departure from the linear relationship between lead equivalent and thickness increases with the X-ray voltage and is quite marked for 200-kv X-rays. Equations 13 and 14 have been tested for glasses up to 10.0 mm in thickness and have been found satisfactory. However, it should not be assumed that these equations are valid for glasses varying very much from the thickness for which they were derived.

In table 5, the experimentally determined protection coefficients for 90 and 150-kv X-rays of all barium-flint glasses studied are compared with the coefficients calculated by means of the empirical equations 13 and 14.

[18] G. W. C. Kaye, Roentgenology, p. 93 (Paul B. Hoeber, Inc., New York, 1929).

TABLE 5.—*Experimental value of protection coefficient of barium flint glasses compared with values calculated by means of equations 14 and 15*

Glass	PbO	BaO	Protection coefficient (percent) for—			
			90 kv		150 kv	
			Experimental	Calculated	Experimental	Calculated
	%	%				
BF-1 [a]	6.87	29.15	----------	15.7	----------	11.4
BF-2 [a]	23.5	14.5	15.3	14.2	13.6	12.0
BF-3 [a]	44.1	<.1	14.8	15.1	14.7	14.9
BF-5	47.1	14.35	26.4	27.2	24.6	25.0
BF-7	45.38	15.02	26.6	26.7	24.7	24.4
BF-9	60.0	<.1	23.4	24.0	23.5	23.7
BF-12	52.0	13.94	29.4	29.6	27.7	27.4
BF-14	53.15	13.01	30.0	29.6	27.7	27.5
BF-15	52.6	14.7	29.9	30.5	28.2	28.2
BF-17	51.2	15.50	29.7	30.3	28.0	27.9
BF-18	62.6	2.34	27.0	27.0	26.5	26.5
BF-20	61.6	2.52	27.0	26.6	27.0	26.0
BF-22	60.9	6.5	28.3	29.1	28.0	28.0
BF-24	62.1	5.3	28.4	28.9	28.0	28.0
BF-26	61.24	5.50	28.7	28.0	28.1	27.6
BF-27 [b]	52.6	14.6	31.0	30.4	28.8	28.1
BF-28 [c]	62.0	5.3	30.5	28.8	29.6	27.9
BF-29	62.0	8.0	31.4	30.2	30.1	29.5
BF-30	62.0	10.0	33.4	32.3	31.7	30.7
BF-31	61.0	9.7	----------	----------	30.6	29.9

[a] Equations 13 and 14 do not strictly apply here since the percentage of lead oxide (PbO) in these glasses is less than 46 percent.
[b] Glass BF-27 is an experimental X-ray glass containing 5 percent of TiO_2.
[c] Glass BF-28 is an experimental X-ray glass containing 2 percent of UO_3.

The writer acknowledges the cooperation, assistance, and advice of Lauriston S. Taylor, under whose supervision this work was done.

WASHINGTON, February 6, 1936.

U. S. DEPARTMENT OF COMMERCE NATIONAL BUREAU OF STANDARDS

RESEARCH PAPER RP871

Part of Journal of Research of the National Bureau of Standards, Volume 16, March 1936

DISTILLATION AND SEPARATION OF ARSENIC, ANTIMONY, AND TIN

By John A. Scherrer

ABSTRACT

This paper describes an apparatus and the technique for the separation, by distillation, of arsenic, antimony, and tin from one another and from elements having nonvolatile chlorides. The apparatus is made entirely of glass, for it was found that cork and rubber stoppers absorb the vapors to such an extent that significant errors may ensue.

CONTENTS

	Page
I. Introduction	253
II. Principles involved	254
III. Description of the apparatus	244
IV. Directions for using the apparatus	255
1. Preparation of the solution	255
2. Distillation of arsenic	256
3. Distillation of antimony	256
4. Distillation of tin	257
V. Determination of arsenic, antimony, and tin, and qualitative tests	257
VI. Results obtained	258
VII. Discussion of the method	259
1. Apparatus	259
2. Method	259
3. Volatility of other chlorides	259

I. INTRODUCTION

In chemical analysis it is often desirable to separate arsenic, antimony, and tin from one another and from elements having nonvolatile chlorides before determinations are attempted. This is particularly true if they occur in very small amounts, for then it is comforting to have visual evidence of their presence. Many ores and alloys contain at least two and often all three of these elements.

The separation and determination of arsenic by volatilization was first employed by Emil Fischer.[1] Various methods for the distillation of these elements from solutions containing halogen acids have been published. W. Plato[2] and W. Hartmann[3] recommend the distillation of the arsenic and antimony together, and then the tin, each distillation being made under special conditions. The arsenic is then removed from the strong acid distillate by hydrogen sulphide, and then the antimony from the partially neutralized filtrate.

K. K. Järvinen[4] recommends that arsenic be distilled by the use of a dephlegmator, leaving the antimony and tin in the residue. The three elements are then determined volumetrically.

[1] Ber. deut. chem. Ges. **13**, 1778 (1880); Liebig's Ann. **208**, 182 (1881); Z. anal. Chem. **21**, 206 (1882).
[2] Z. anorg. allgem. Chem. **65**, 26 (1910).
[3] Z. anal. Chem. **58**, 148 (1919).
[4] Z. anal. Chem. **62**, 192 (1923).

Heinrich Biltz[5] uses a combination of the above methods and distills each element separately, and then determines them by suitable methods. In the usual case distillations are made in flasks carrying cork or rubber stoppers.

In attempting to determine very small amounts of antimony in irons and steels, it was found that while arsenic, antimony, and tin could be separated sharply by distillation, the use of rubber stoppers led to significant errors. These were not only more or less attacked during distillations but also absorbed the volatilized compounds. The latter are not permanently fixed, and much of what is absorbed in one run may be given off in the next. In order to overcome these difficulties, the distilling apparatus was constructed entirely of glass. After the preliminary tests with antimony, it was decided to extend the work to the quantitiative separations of arsenic and tin as well, and to cover large as well as small amounts of all three elements.

II. PRINCIPLES INVOLVED

Arsenic trichloride boils at 130° C; antimony trichloride at 220.2° C; and stannic chloride at 114° C. Arsenic distills very readily when it is present as the trivalent chloride and the hydrochloric acid is rather concentrated. Ordinarily the temperature of the boiling solution does not exceed 112° C. There is very little danger of antimony being carried over with the arsenic, although a few tenths of a milligram may be found in the arsenic trichloride distillate if the concentration of antimony trichloride is high.

In order to bring about rapid distillation of the antimony, it is necessary to raise the temperature to about 160° C, and to add acid, drop by drop, through a tube reaching to the bottom of the distilling flask. If the hydrochloric acid is dropped on the surface of the hot solution, much of the hydrochloric acid gas escapes without coming into intimate contact with the solution of the antimony salts and the distillation is less efficient. Tin is prevented from volatilizing with the antimony at this stage by adding phosphoric acid, with which it forms a stable compound.

Finally, the stable nonvolatile compound which phosphoric acid forms with the tin salt is broken up by the addition of hydrobromic acid, and tin is distilled with a mixture of hydrobromic and hydrochloric acids at 140° C.

The temperature at which the distillations of the antimony and tin were made are those recommended by Heinrich Biltz.[6]

III. DESCRIPTION OF THE APPARATUS

In figure 1, A is a 50-ml bulb for holding the acid which is added in the course of the distillations. The tube connecting A and B, and extending into B, is made about 25 cm in length, in order to overcome the pressure of the carbon dioxide which is used to aid in carrying

[5] Z. anal. Chem. 81, 82 (1930).
[6] See footnote 5.

over the vapors from the distilling flask C. The part of this tube extending into B should have a diameter of not over 3 to 4 mm in order to prevent the acid from draining from it.

B is an arrangement for gaging the rate of flow of the acid, and is provided with a side tube for the purpose of introducing a stream of carbon dioxide.

C is a 200-ml distilling flask, the neck of which is 2.5 cm in diameter. It is provided with a side tube, a thermometer well, and a delivery tube for conveying the acids and carbon dioxide to the distilling flask. The side tube connects the apparatus to a condenser, the thermometer well is sealed to the top of the neck of the flask, and the delivery tube passes through the wall in the upper part of the neck of the flask and is connected to B. Both the thermometer well and delivery tube reach within 3 mm of the bottom of the flask. The distance between the bottom of the flask and the exit tube leading to the condenser is 17 cm.

The apparatus is clamped to a ring stand. C rests on an asbestos board (about 18 by 18 cm) having a round hole 4.5 cm in diameter.

It is desirable that all the glass should be free from the elements in question, and the suitability of the setup for the work in hand should be determined by running appropriate blanks.

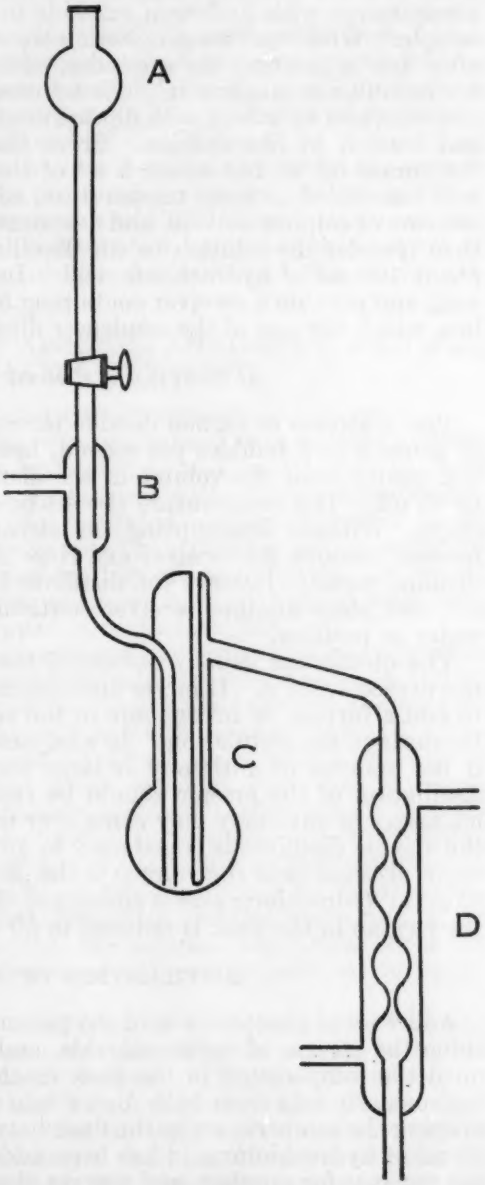

FIGURE 1.—*Distilling apparatus.*

IV. DIRECTIONS FOR USING THE APPARATUS

1. PREPARATION OF THE SOLUTION

In the usual case arsenic, antimony, and tin are first precipitated as the sulphides and then converted to sulphates by treating paper

and precipitate with nitric and sulphuric acids,[7] finally heating until copious fumes of sulphuric acid are given off. With ferrous materials, such as irons and steels, the sulphides can be obtained by direct precipitation with hydrogen sulphide in a nitric acid solution of the sample.[8] With nonferrous materials the sulphides are usually obtained after first separating the sulphides, such as copper and lead, which are insoluble in alkaline sulphide solution. With solders the precipitate obtained by attack with diluted nitric acid (1+2) can be gathered and treated in like fashion. From this point proceed as follows: Evaporate off all but about 5 ml of the sulphuric acid. When the acid has cooled to room temperature, add 30 to 50 ml of a saturated solution of sulphur dioxide, and evaporate to about 10 ml. Cool, and then transfer the solution to the distilling apparatus with the aid of about 100 ml of hydrochloric acid. Insert the thermometer in the well, and provide a receiver containing 50 to 100 ml of distilled water into which the end of the condenser dips.

2. DISTILLATION OF ARSENIC

Pass a stream of carbon dioxide through the apparatus at the rate of about 6 to 8 bubbles per second, heat the solution to boiling and boil gently until the volume in the distilling flask has been reduced to 50 ml. The temperature should be about 111 to 112° C at this stage. Without interrupting the stream of carbon dioxide or the heating, remove the receiver and rinse the end of the condenser with distilled water. Reserve the distillate for the determination of arsenic, and place another receiver containing 50 to 100 ml of distilled water in position.

The distillation usually suffices if the amount of the arsenic does not exceed 0.001 g. If larger amounts are in question, it is advisable to add a further 25 ml or more of the acid to the distilling flask and to continue the distillation. In analyses of the highest accuracy, and if the amount of antimony is large and of arsenic very small, the distillation of the arsenic should be repeated, for a few tenths of a milligram of antimony may come over with the arsenic. In this case the arsenic distillate is transferred to an empty distillation flask, and again distilled until the volume in the flask is reduced to 50 ml. Then 25 ml of hydrochloric acid is added and the distillation continued until the residue in the flask is reduced to 50 ml.

3. DISTILLATION OF ANTIMONY

Add 7 ml of phosphoric acid (85 percent) to the distilling flask, continue the stream of carbon dioxide, and increase the heat gradually until the temperature in the flask reaches 155° C. Then introduce hydrochloric acid from bulb A at a rate of 30 to 40 drops per minute, keeping the temperature in the flask between 155 and 165° C. When 75 ml of hydrochloric acid has been added, turn off the heat, change the receiver for another, and reserve the distillate for the determination of antimony. If the amount of antimony does not exceed about 0.001 g, the above amount of acid suffices. With larger amounts of

[7] Throughout this paper, whenever acids are mentioned, hydrochloric acid will mean the concentrated acid of specific gravity 1.18; hydrobromic acid, the concentrated acid of 40 percent; nitric acid, the concentrated acid of specific gravity 1.42; and sulphuric acid, the concentrated acid of specific gravity 1.84; diluted acids will be designated as follows: For example, diluted hydrochloric acid (1+99) will mean one volume of the concentrated acid of specific gravity 1.18 diluted with 99 parts of water.

[8] J. A. Scherrer, BS J. Research 8, 309 (1932) RP415.

antimony a further 25 ml or more of the acid should be added to bulb A and the distillation continued.

4. DISTILLATION OF TIN

Allow the solution in C to cool to 140° C, turn on the heat, add a mixture of three-fourths hydrochloric acid and one-fourth hydrobromic acid to bulb A. Allow it to flow into the distilling flask at a rate of 30 to 40 drops per minute as in the distillation of antimony, keeping the temperature at about 140° C. When 50 ml of the mixed acids has been added, remove the source of heat, interrupt the stream of carbon dioxide, and reserve the distillate for the determination of tin. If the amount of tin does not exceed 0.001 g, the above amount of acid is sufficient. If more is present, a further 25 ml or more of the mixed acids should be added to bulb A, and the distillation continued.

V. DETERMINATION OF ARSENIC, ANTIMONY, AND TIN, AND QUALITATIVE TESTS

The elements in the distillates were determined as follows:

Arsenic.—The cold distillate was neutralized with sodium hydroxide, made slightly acid with hydrochloric acid, and cooled to room temperature. The acid was neutralized with sodium bicarbonate, and then an excess of 20 ml of a saturated solution of sodium bicarbonate was added. The arsenic was then titrated with a standard solution of iodine, using a solution of starch as indicator. A careful blank run was made on the same amounts of reagents as were used with the sample, and the proper correction applied.

Antimony.—The distillate was neutralized with ammonium hydroxide, after which 5 ml of hydrochloric acid was added for each 100 ml of solution. Hydrogen sulphide was then passed through the solution for about 15 minutes. After standing for 30 minutes the solution was filtered and the precipitate washed 6 to 8 times with a solution of diluted sulphuric (3+97) acid which was saturated with hydrogen sulphide. The paper and precipitate were transferred to a kjeldahl flask and treated with 10 ml of sulphuric acid and 5 g of potassium or sodium sulphate. The contents of the flask were gradually heated to boiling and the boiling continued until the organic matter was completely destroyed. When cool, 250 ml of distilled water and 25 ml of hydrochloric acid were added, the solution was boiled for a few minutes, cooled to 10° C and titrated with a 0.1*N* solution of potassium permanganate.

Tin.—The distillate was transferred to an erlenmeyer flask and water added until the solution contained 25 to 30 percent of hydrochloric and hydrobromic acids (by volume). The tin was reduced by boiling with an excess of test lead for about 30 minutes. The solution was then cooled to 10° C and titrated with 0.1*N* solution of iodine using a starch solution as indicator. A stream of carbon dioxide was passed through the apparatus during the reduction, cooling, and titration.

Qualitative tests.—If the amounts of the elements are very small, it is desirable in every case to treat the distillates with hydrogen sulphide after proper neutralization in order to have visual proof that they are present. After appropriate digestion the solution is then filtered, of course, and the sulfides treated as may be desired.

VI. RESULTS OBTAINED

The procedure was first tested qualitatively by using a synthetic solution which contained 50 ml of hydrochloric acid and the maximum amounts of the elements that might be expected in 25 g of ordinary irons and steels. The amounts taken were arsenic 6 mg, antimony 3 mg, and tin 6 mg. The arsenic was distilled by adding 60 ml of hydrochloric acid in the course of 60 minutes, antimony by using 75 ml of hydrochloric acid in the course of 70 minutes, and tin by using 45 ml of hydrochloric acid and 15 ml of hydrobromic acid in the course of 45 minutes. The completeness of the distillation of each element was tested by changing the receiver, adding 25 ml more of the acid or acids, and repeating the distillation. The new distillate was treated with hydrogen sulphide after adjusting the acidity. In all cases no more of the element was obtained in the additional distillation.

TABLE 1.—*Results obtained in distillations of arsenic, antimony, and tin*

Test	Arsenic		Antimony		Tin	
	Taken	Found	Taken	Found	Taken	Found
	g	g	g	g	g	g
1	0.0100	0.0098	0.0100	0.0103	0.0100	0.0103
2	None	(a)	.0100	.0099	.0100	.0101
3	None	(a)	None	(a)	.0100	.0102
4	None	(a)	.1000	.1003	.1000	.1001
5	.1000	.1000	None	(a)	None	(a)
6	.1000	.1002	.1000	.1001	None	(a)
7	None	(a)	None	(a)	.1000	.0999
8	.1000	.0998	.1000	.0998	.1000	.1003
9	.0001	(b)	.0001	(b)	.0001	(b)
10	.0001	(b)	.1000	.0999	.1000	.1000
11	.1000	.0999	.0001	(b)	.1000	.0998
12	.1000	.0998	.1000	.0999	.0001	(b)

[a] No precipitate was obtained by treating the properly neutralized distillate with hydrogen sulphide, and digesting for several hours.
[b] Qualitative tests for the element in question were obtained.

Tests 1 to 3 in table 1 were obtained as in the preliminary qualitative test, except that 75 ml of hydrochloric acid was added for arsenic and the distillation completed in 60 minutes, 85 ml of hydrochloric acid added for antimony and completed in 50 minutes from the time that the addition of acid began, and 75 ml of a mixture of three-fourths hydrochloric and one-fourth hydrobromic acids added for tin and completed in about 45 minutes.

Tests 4 to 12 were obtained by distilling mixtures containing relatively large amounts of the three elements. The amounts of acids used and the distillates caught were somewhat in excess of the amounts specified in the procedure, in view of the amounts of the elements that were present. In the distillation of arsenic approximately 100 ml of distillate was gathered in the course of 90 minutes, in the distillation of antimony approximately 150 ml of the distillate was gathered in the course of 90 minutes from the time that the addition of the acid began, and in the case of tin, 120 ml of distillate was gathered in the course of 60 minutes.

VII. DISCUSSION OF THE METHOD

1. APPARATUS

The separate parts of the apparatus may be made with ground joints, but experience has shown that the joints may stick when used at elevated temperatures. The one-piece apparatus proved to be rugged and easily cleaned by pouring acids through A and rinsing the solutions through the condenser.

The distance from the bottom of the distilling flask to the exit tube has been found in practice to be satisfactory.

The thermometer well probably causes a slight lag in the temperature, but in view of the wide range over which the temperature may vary it is of no consequence. The well is placed in front of the exit tube so that it acts as a baffle to prevent spray from passing into the condenser.

2. METHOD

The carbon dioxide has the double purpose of aiding in carrying over the volatile compounds and to prevent bumping.

According to Heinrich Biltz,[9] when one arsenic distillation follows another the apparatus should be rinsed with hydrochloric acid between distillations, for if antimony is present it has a tendency to creep along the surface of the flask, and unless removed will finally pass over to some extent.

3. VOLATILITY OF OTHER CHLORIDES

Germanium.—100 mg of germanium as the tetrachloride was distilled under the conditions that obtain in the arsenic distillation. All of the germanium was found in the distillate.

Bismuth.—100 mg of bismuth as the trichloride was placed in the apparatus and the distillation carried out as for arsenic, antimony, and tin. No bismuth was found in any of the three distillates.

Rhenium.—When 100 mg of rhenium as the perrhenate was introduced under conditions that obtain for arsenic, antimony, and tin, no rhenium was found in the arsenic distillate, about 50 mg in the antimony distillate, about 25 mg in the tin distillate, and 25 mg in the residue.

Molybdenum.—When 100 mg of molybdenum was introduced as molybdic acid, the arsenic distillate contained no molybdenum. About 0.2 mg was found in the antimony distillate and about 0.3 mg in the tin distillate, by the thiocyanate test. When the second distillate was redistilled as for antimony, no molybdenum was found in the fraction which distilled over, the molybdenum being found in the residue. The tin distillate was concentrated in the apparatus and redistilled in the presence of the mixed acids as for tin. The fraction which passed over contained about 0.01 mg of molybdenum, the residue the rest. In very careful work a third distillation should be made.

WASHINGTON, February 3, 1936.

[9] See footnote 5.

U. S. DEPARTMENT OF COMMERCE NATIONAL BUREAU OF STANDARDS

RESEARCH PAPER RP872

Part of Journal of Research of the National Bureau of Standards, Volume 16, March 1936

NOTE ON THE EFFECT OF A COVER GLASS IN REFLECTANCE MEASUREMENTS

By Deane B. Judd and Kasson S. Gibson

ABSTRACT

It has been found from theoretical considerations that the use of a cover glass may result in an error of as much as 10 percent when two diffusing surfaces, one light and one dark, are compared for apparent reflectance. The error arises from multiple reflections between sample and cover glass, the lighter sample obtaining much more added illumination from this cause than the darker. The error depends on the angular distribution of the illuminant, the angle of view, and the diffusing characteristics of the samples as well as their reflectances.

CONTENTS

		Page
I.	Introduction	261
II.	Theory	261
III.	Experiment	264
IV.	Conclusion	264

I. INTRODUCTION

When it is necessary to measure the reflectance of a material (such as a liquid or jelly, or one composed of powder, small crystals, or chopped-up fibers) whose free surface is stable only in a horizontal position, and there is available a reflectometer which requires the surface to be other than horizontal, the use of a cover glass suggests itself. Even when the surface can be tested in a horizontal position, there are materials out of which it is difficult to form a reproducible free surface. For these materials the use of a cover glass may improve reproducibility of surface to a marked extent. This discussion deals briefly with the effect of a cover glass on reflectance measurements of such materials.

II. THEORY

The following simplified analysis applies to the comparison of two perfectly diffusing surfaces, one of reflectance, R_1, the other of reflectance, R_2. One of these may be thought of as a standard of reflectance. Without a cover glass the measured reflectance of the first relative to the second will be simply R_1/R_2. Now let both be covered with identical cover glasses of transmission T and reflectance R, and so illuminated and viewed by the reflectometer that none of the light flux may be reflected from the cover glass directly into the

photometer; that is, all light which is counted in the measurement must come from the two surfaces being compared. Let F be the flux which passes through the cover glass directly from the light source and is initially incident upon the sample. The total flux incident on the sample exceeds this initial flux because of multiple reflection between the cover glass and the sample. That is, a part, R_1, of the initial flux is diffusely reflected by the sample and strikes the cover glass which, itself, returns a fraction R, to the sample, and so on. The total incident flux, therefore, depends in addition on the reflectance R_1 of the sample, thus:

$$\begin{aligned}\text{Total flux} &= F+FR_1R+FR_1RR_1R+ \ldots \ldots \ldots \ldots \\ &= F(1+R_1R+R_1^2R^2+ \ldots \ldots \ldots). \\ &= F/(1-R_1R).\end{aligned}$$

The reflectometer measures the ratio of the flux reflected by the first surface to that reflected by the second, after both have been transmitted by the respective cover glasses; that is, it measures the ratio:

$$\frac{FR_1T/(1-R_1R)}{FR_2T/(1-R_2R)}=(1/Q)(R_1/R_2), \tag{1}$$

where Q is a correction factor equal to $(1-R_1R)/(1-R_2R)$ to be applied to the measured ratio, thus:

$$R_1/R_2=Q\times\text{measured ratio}. \tag{2}$$

This formula applies rigorously to a comparison of two perfectly diffusing surfaces regardless of the angular distribution of incident flux provided only that no light directly reflected from the source by the cover glass is counted in the measurement; that is, the distribution may be nearly completely diffused as in the Priest-Lange reflectometer, or it may be nearly unidirectional at, for example, about 45°. A similar formula should apply also to the measurement of apparent reflectances of nearly perfectly diffusing samples for these angular conditions of illumination, as in the Priest-Lange reflectometer, the Hunter reflectometer, the Appel-Hickson photometer, and as recommended by the International Commission on Illumination.

However, many real surfaces depart considerably from perfect diffusers. For such surfaces, therefore, we cannot get along with a single number, R_1, yielding the fraction of total incident light that is reflected independently of the angle of incidence. The reflected fraction of the flux incident by multiple reflection depends on the angular distribution of this flux. Also, since the angular distribution varies according to which multiple reflection is being considered, we cannot characterize the mirror reflection of the cover glass by a single number, R. The exact solution for real surfaces analogous to the simple solution for perfectly diffusing surfaces is thus seen to be very complicated and, even if complete information concerning the angular distribution of incident and reflected light were at hand for a given reflectometer and material, it is doubtful whether the exact solution would be of sufficient interest to justify the trouble of finding it. It is possible, however, to develop an argument showing that the amount of correction is reduced by an equal departure of both samples from a perfect diffuser. Formula 1 may be taken as a limiting case according to this argument.

An introduction to this argument is afforded by attempting an approximate evaluation of R for a cover glass of refractive index $n=1.5$. For perpendicular incidence, we have:

$$R=\rho\left[1+\frac{(1-\rho)^2t^2}{1-(\rho t)^2}\right],$$

where ρ is reflectance at each glass-air interface and t is transmittance, which, for a thin cover glass of good quality, may be safely taken as 1.000. For such a glass, and with index of refraction $n=1.5$, ρ is equal to 0.04 and R equals 0.077. This formula may also be used for an approximate computation of R_θ, the value of R as the angle of incidence, θ, is varied. The value of ρ_θ may readily be computed for θ between 0 and 90° from the general Fresnel formula. In the present case it will vary from 0.04 to 1.00. The approximation in the computation of R_θ by the above formula arises because (1) ρ changes in value with each multiple reflection (for any given value of θ) due to successive increase in the degree of polarization resulting from the transmission and reflection of light at a surface at other than normal incidence, (2) the angle of incidence at the second air-glass interface cannot exceed a certain critical value, much less than 90° and (3) the plate is not infinite in extent. However, neglecting these errors, we may evaluate approximately the reflectance of a glass plate for diffuse illumination as:

$$R_D=\frac{\sum_0^{\pi/2} R_\theta \sin 2\theta}{\sum_0^{\pi/2} \sin 2\theta}=0.16$$

according to the method given by McNicholas.[1]

The value of R_D thus computed is certainly too high, it may be considered as an upper limit. A lower limit for R_D is obtained by considering reflection between the sample and the first air-glass surface only; this gives about 0.10.

It is to be noted that, although for perpendicular incidence the cover glass reflects but 0.077, for grazing incidence it reflects nearly 1.00. The action of the cover glass is not only to build up the total flux incident on the sample by multiple reflection, but also to proportion it according to angle of incidence in such a way that a preponderance of the added flux is nearly at grazing incidence. If the sample, itself, by departure from a perfect diffuser also favors this distribution of reflected flux, it is evident that much of the light added to the sample by multiple reflection will not be counted in the measurement of the relative reflectance but will be lost by passage both through the edges of the cover glass and through the small gap between cover and sample. We may take, therefore, formula 1, which applies to perfect diffusers, also as a limiting case for the comparison of actual samples of identical imperfectly diffusing types; that is, two samples of similar diffusing characteristics will show a cover-glass effect similar to that represented by formula 1 but smaller. If the samples being compared are not identical in diffusing characteristics,

[1] H. J. McNicholas, *Absolute methods in reflectometry*, BS J. Research 1, 29 (1928) RP3. See equation 18, p. 50.

the direction of the cover-glass effect may, however, reverse; that is, it may be expected that a highly diffusing sample may obtain more effective illumination by multiple reflection than a light glossy sample.

III. EXPERIMENT

The approximate validity of these considerations has been checked in the following way. Two paper samples were compared on the Priest-Lange reflectometer [2] with and without a cover glass. The first sample was a gray paper diffusely reflecting about 0.42 and cut from the cover of a reprint from the JOSA of 1920. The second sample was mimeograph paper diffusely reflecting about 0.75.

According to formula 1 the ratio measured with the cover glass should be:

$$\frac{R_1}{R_2}\cdot\frac{1-0.75R}{1-0.42R},$$

where R is less than 0.16 and greater than 0.10; that is, the measured ratio should lie between $0.943(R_1/R_2)$ and $0.966\ (R_1/R_2)$. The actual experimental results were:

Observer	R_1/R_2	Ratio with cover glass
KSG	0.556	$0.533=0.958\ (R_1/R_2)$
DBJ	.559	$.533=.954\ (R_1/R_2)$

The agreement is seen to be good and it supports the assumption that these samples do not deviate from perfect diffusers enough to invalidate the analysis.

IV. CONCLUSION

For diffusing surfaces the use of a cover glass may result in an error of as much as 10 percent of the reflectance. A cover glass should, therefore, be avoided wherever possible because it may give results not comparable to those obtained without it. The effect of the cover glass cannot be easily calculated because it depends on the diffusing characteristics of the two samples being compared as well as on their reflectances. In such practical cases as the use of abaca fibers (manila fibers) or sisal fibers, relative to porcelain or magnesium oxide, the analysis may be in serious error. Experiment alone can tell what the magnitude and sign of the effect may be.

WASHINGTON, January 31, 1936.

[2] I. G. Priest, *The Priest-Lange reflectometer applied to nearly white porcelain enamels*, J. Research NBS 15, 529 (1935) RP847.

U. S. DEPARTMENT OF COMMERCE NATIONAL BUREAU OF STANDARDS

RESEARCH PAPER RP873

Part of Journal of Research of the National Bureau of Standards, Volume 16, March 1936

SOME TESTS OF STEEL COLUMNS INCASED IN CONCRETE

By Ambrose H. Stang, Herbert L. Whittemore, and Douglas E. Parsons

ABSTRACT

In cooperation with the Bridge Department of the Port of New York Authority, the National Bureau of Standards tested four carbon-steel columns incased in reinforced concrete to determine their strength and stiffness. The steel columns were duplicates of columns TC1 and TC2 reported in Bureau Research Paper RP831.

The temperatures in the columns were measured during the aging of the concrete. The readings of telemeters attached to the steel members indicated that no appreciable stress in the steel members was caused by the aging of the concrete. When the columns were loaded, the telemeter stresses were always less than the quasi-stress obtained by dividing the load by the cross-sectional area of the steel members. The concrete, therefore, carried a portion of the load.

At the column yield strength, the load on the incased columns was 51 percent greater than the load on the unincased columns. At the final maximum load the load on the incased columns was 42 percent greater than the load on the unincased columns.

The greatest stress in the reinforcement rods was 10 kips/in^2. [1]

The lateral deflection was very small until the load on the column approached the maximum. At or about the maximum load, the columns having a length of 24 feet deflected about 6 inches, and large pieces of concrete fell from the columns.

CONTENTS

	Page
I. Introduction	266
II. The specimens and the method of testing	266
1. The columns	266
(a) Description	266
(b) Reinforcement	267
(c) Concrete	267
(d) Placing the concrete	267
(e) Measurements made during the aging of the concrete	269
(f) Testing procedure	269
(1) Compressometers	269
(2) Telemeters	270
(3) Lateral deflection	270
(4) Strain in the reinforcement	270
(5) Loading	270
2. Coupons	270
(a) General	270
(b) Extensometer	270
(c) Yield strength	271
(d) Testing machine	271
(e) Speed of the movable platen	271
III. Results for the auxiliary tests	271
1. Coupons	271
(a) Tensile tests	271
(b) Chemical composition	272
2. Concrete	273
3. Reinforcement	273

[1] 1 kip=1,000 lb.

Page
IV. Results for the columns 274
1. Stress in the steel members caused by aging of the concrete 274
2. Temperature during aging of the concrete 274
3. Quasi-stress 275
4. Telemeter stress 275
5. Strain in the concrete 277
(a) Average strain 277
(b) Repeated loading 278
6. Stress in reinforcement 280
7. Lateral deflection 281
8. Maximum load 282
(a) Final loading 282
(b) Description of the failure 284
(c) Strength 285
V. Conclusions 286
1. Stress in the steel members 286
2. Average strain 286
3. Stress in reinforcement 287
4. Lateral deflection 287
5. Failure 287
6. Strength 287

I. INTRODUCTION

At the request of the Bridge Department of the Port of New York Authority, the National Bureau of Standards, cooperated in an investigation of the strength and behavior, under load, of four steel columns incased in reinforced concrete. The results are directly comparable with those for columns given in National Bureau of Standards Research Paper RP831, Tests of Steel Tower Columns for the George Washington Bridge,[1] because the steel portions of the incased columns were duplicates of the carbon-steel columns TC1 and TC2 in the previous investigation.

The incasement of steel columns in reinforced concrete has been used to increase their strength and stiffness, and to protect them from corrosion. This investigation was undertaken to determine the increase in strength and stiffness.

II. THE SPECIMENS AND THE METHOD OF TESTING

1. THE COLUMNS

(a) DESCRIPTION

The nominal dimensions of the columns are given in table 1.

TABLE 1.—*The nominal dimensions of the columns*

Symbol	Number of specimens	Kind of steel	Cross-sectional area of steel	Length	Remarks
			in.²	ft	
IC1, IC2	2	Carbon	* 159	24	Loaded on steel only.
IC3, IC4	2	Carbon	* 159	24	Loaded on both steel and concrete.

* The concrete incasement was 37.5 in. square, with corners slightly beveled. The cross-sectional area of the concrete was 1,245 in².

[1] J. Research NBS 15, 317 (1935) RP831.

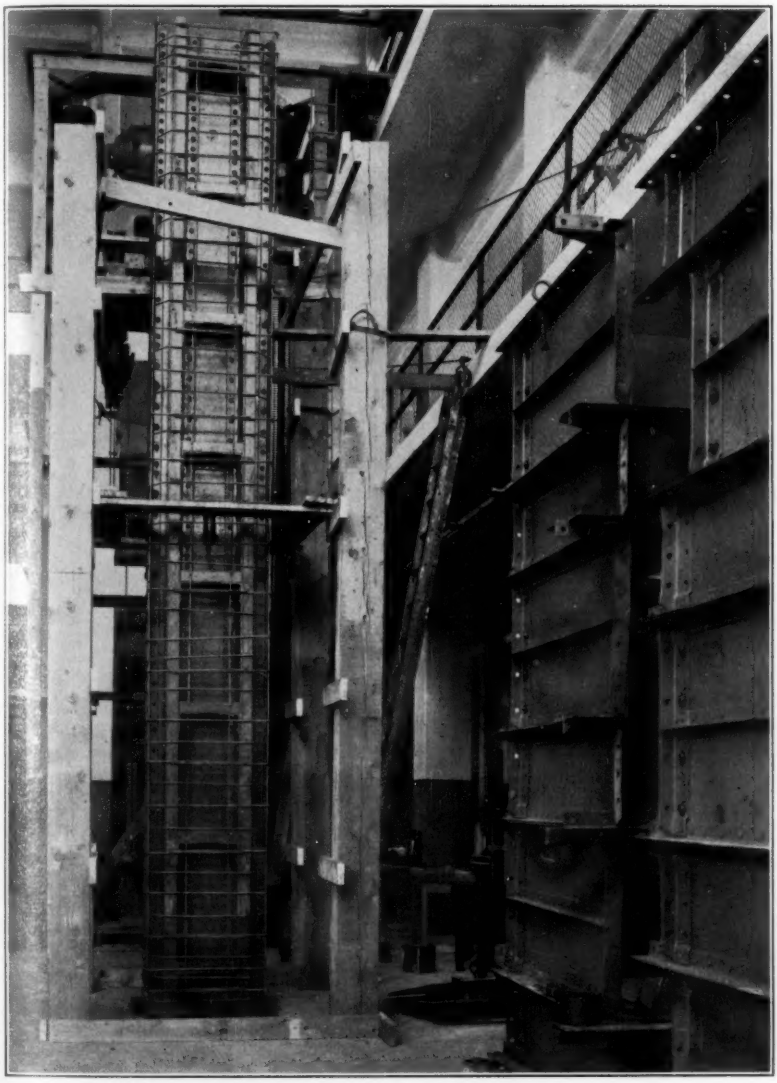

FIGURE 1.—*Column* IC3 *with the reinforcement in place.*

Note the telemeters covered with rubber pads. The steel forms are shown in the right foreground.

UNIV. OF MICH.

There were 4 columns fabricated by riveting from carbon steel. They were of the same size and shape as the steel columns, TC1 and TC2 of Research Paper RP831. The columns were designated IC, followed by the numerals 1, 2, etc., for the individual columns.

The longitudinal pieces of each column, that is, the longitudinal plates and angles, were cut as shown in the cutting diagram in figure 1 of RP831. Each longitudinal piece of the column was match-marked to correspond with a coupon cut from the same plate or angle, and its location in the column was recorded.

(b) REINFORCEMENT

The reinforcing rods were plain bars (0.5 in. diameter) of structural-steel grade rolled from new billets. Tensile and bending tests were made in accordance with ASTM Standard Specifications for Billet-Steel Concrete Reinforcement Bars, A15–14.[2]

A column with the reinforcement in place is shown in figure 1, and the layout of the reinforcement is shown in figure 2. The tie rods, A and B, were bent to shape, lapped 1 ft 8 in. at the ends and seized with wire. There was a splice in every fourth rod on each side of the column.

(c) CONCRETE

The materials for the concrete were purchased locally. All of the cement for the columns was delivered before beginning construction. The cement complied with the requirements of ASTM Standard Specification and Tests for Portland Cement, C 9–26.[3]

The aggregate consisted of Potomac River sand and gravel such as is used locally in building construction. The aggregates were delivered as needed, and although they were obtained from the same source, the gradings of the sand and the gravel were not the same in all deliveries.

The proportions of the ingredients of the concrete were controlled to maintain a constant water-cement ratio and approximately a constant slump. On account of the differences in the gradings of the sand and gravel the proportions of cement to aggregates ranged from 1 : 2.1 : 3.6 to 1 : 2.24 : 3.92 by separate volumes of the cement and of the dry, compacted sand and gravel, respectively. The total water content of each batch of concrete, including the moisture in the aggregate, was 7.1 gal per sack of cement, plus an allowance for the absorption of the aggregate equal to 1 percent of the dry weight of the aggregate. The slump of the concrete was usually between 3 and 5 in. when tested in accordance with the ASTM Tentative Method of Test for Consistency of Portland Cement Concrete, D 138–26 T.[4]

Twelve concrete cylinders, 6 in. in diameter and 12 in. long, were made from the concrete for each of the four columns. They were placed in the damp storage rooms in the concrete laboratory when they were 24 hours old and remained there until they were removed for testing.

(d) PLACING THE CONCRETE

After the reinforcement was placed, the steel forms shown at the right in figure 1 were placed around the column and bolted together. The sections were from 13.5 to 24 in. high, and each section was filled before the next section was attached to it.

[2] Stand. Am. Soc. Testing Materials (I) p. 132 (1927).
[3] Stand. Am. Soc. Testing Materials (II) p. 23 (1927).
[4] Proc. Am. Soc. Testing Materials (I) **21**, 874 (1926).

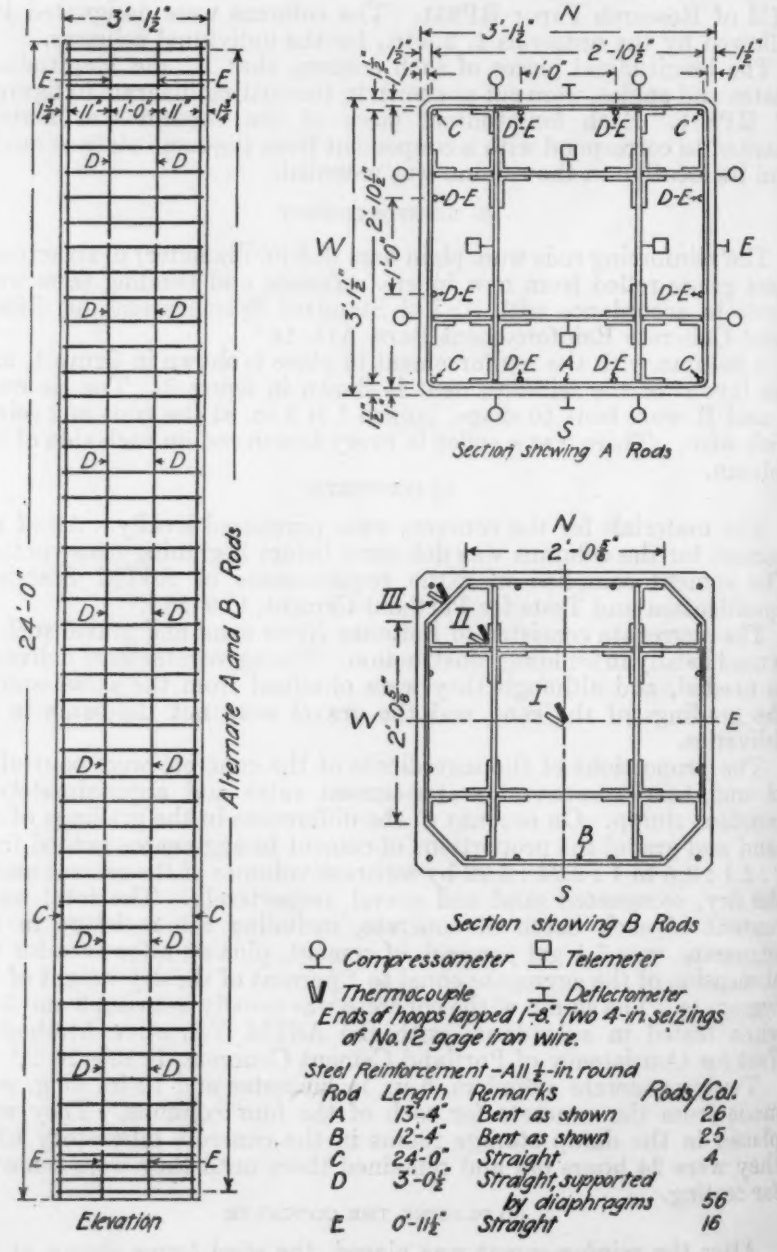

FIGURE 2.—*Steel reinforcement for the columns.*

Shows location of compressometers, telemeters, and thermocouples.

FIGURE 3.—*An incased column and one being incased.*

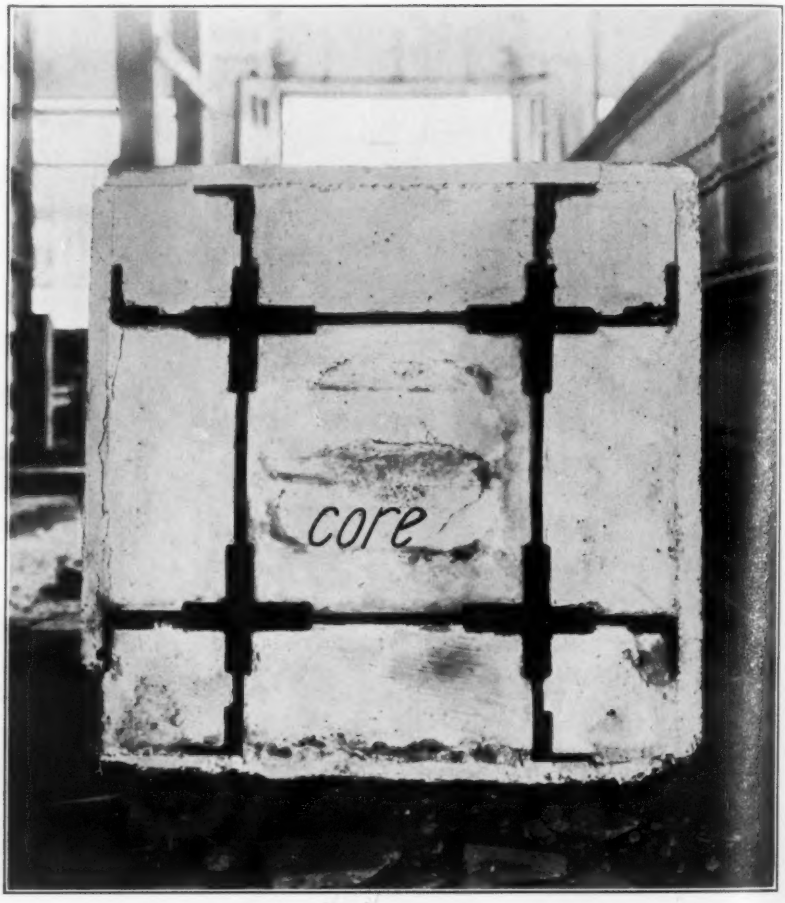

FIGURE 4.—*Lower end of incased column* IC2 *after test.*

The concrete was mixed for 2 minutes in a batch mixer. It was carefully rodded into place to produce a dense concrete free from honeycombing. A light air hammer was also applied to the forms to assist in compacting the concrete. The concrete for the core was deposited through a pipe, the lower end of which was never more than 2 ft above the concrete in the core. The concrete inside and outside the steel column was maintained at as nearly the same level as possible. An incased column and one being incased are shown in figure 3.

For columns IC3 and IC4 the concrete was flush with the ends of the steel column. For the columns IC1 and IC2 the ends of the steel column projected 0.5 in. from the ends of the concrete. Wood fillers were used temporarily at the lower end of the column and the forms filled to 0.5 in. below the upper end of the steel column.

The forms remained on the columns for at least 48 hours after the concrete was placed. The columns were tested at ages from 71 to 74 days. The lower end of column IC2 after test is shown in figure 4.

(e) MEASUREMENTS MADE DURING THE AGING OF THE CONCRETE

Telemeters having a gage length of 8 in. were placed on vertical gage lines at midheight of each column at the four locations shown in figure 2. For column IC1 only, there were four additional telemeters. They were placed in the east and west locations shown in figure 2, two at 2 ft, 6 in. from the lower end and two at the same distance from the upper end. The telemeters were attached to the steel plates before the reinforcement was placed. They were protected by heavy brass castings attached to the column by screws. There was a gasket between the casting and the column. Pads of soft rubber were placed over the castings and secured by wires. A waterproof cable was connected to each telemeter and led out through a hole in the steel form. The readings of the telemeters were recorded during the aging of the concrete.

Nine copper-constantan thermocouples were placed in the concrete at the locations shown in figure 2, three at midheight, and three at 4 ft from each end of the column. It is believed that the error in the temperature determined from the thermocouple readings did not exceed 1° F.

After column IC3 had been incased the room temperature and the readings of the thermocouples and of the telemeters were recorded every half hour for 2 days. Thereafter they were recorded daily (except on holidays) until the column was tested. For the other three columns the readings were recorded daily.

(f) TESTING PROCEDURE

All the columns were tested as flat-end columns by the use of the equipment and methods described in RP831. Columns IC1 and IC2 loaded on the steel only were tested in the same way as columns TC1 and TC2. For the columns IC3 and IC4 loaded on both steel and concrete the method of testing was similar, except that a thin coat of plaster of paris was used between the ends of the column and the bearing plates. An incased column in the testing machine is shown in figure 5.

(1) *Compressometers.*—The compressometers used for the tower columns (gage length 20 ft) were used to measure the shortening of

the concrete under load. The locations of the eight compressometers are shown in figure 2.

(2) *Telemeters.*—The locations of the telemeters are described under section II, 1, (e), page 679.

(3) *Lateral deflection.*—The lateral deflection of the column was measured by the use of the taut wire and mirror-scale deflectometer. The distance between the supports for the wire was 20 ft, and the middle of the wire was at midheight of the column. The locations of the three deflectometers are shown in figure 2. One division on the scale was 0.1 in. and readings were estimated to 0.1 of a division.

(4) *Strain in the reinforcement.*—The strain in the four horizontal reinforcing rods nearest midheight of the column was measured manually by the use of a Berry strain gage having an 8-in. gage length. There was one gage line on each rod, each on a different side of the column.

(5) *Loading.*—The columns were loaded repeatedly as follows:

Loading number	Minimum	Maximum
	kips	kips
1	0	7, 314
2 to 20, incl	5, 565	7, 314
21	0	7, 314
22 to 25, incl	5, 565	7, 314
26	0	Failure

For the twenty-sixth loading the load was increased by increments, and the compressometers and the lateral deflections were read for each increment of load. This procedure was continued until the deflection of the column brought it into contact with some of the compressometers. The compressometers were then removed, and the pump of the testing machine operated at a constant speed. Load readings were taken at intervals of 1 minute until the load had reached a maximum and then decreased. The telemeter reading at midheight of column IC3 showed that the stress in the steel was 18 kips/in.^{2} for a load of 5,565 kips and 30 kips/in.^{2} for a load of 7,314 kips.

2. COUPONS

(a) GENERAL

The coupons for the steel portion of the incased columns were taken and tested in tension as described in RP831. The axis of each coupon was parallel to the direction of rolling (axis) of the plate or angle.

The coupons were standard ASTM tensile specimens for plates, shapes, and flats.[5] These coupons had a gage length of 8 in., a width of 1.5 in., and the thickness was that of the material as rolled.

(b) EXTENSOMETER

The strains in some coupons were measured by the use of a Ewing extensometer having a gage length of 8 in. One division on the scale of this instrument corresponded to a strain of 0.000 025 in the coupon. The readings were estimated to 0.1 division.

[5] Figure 1, Stand. Am. Soc. Testing Materials (I) p. 68 (1933).

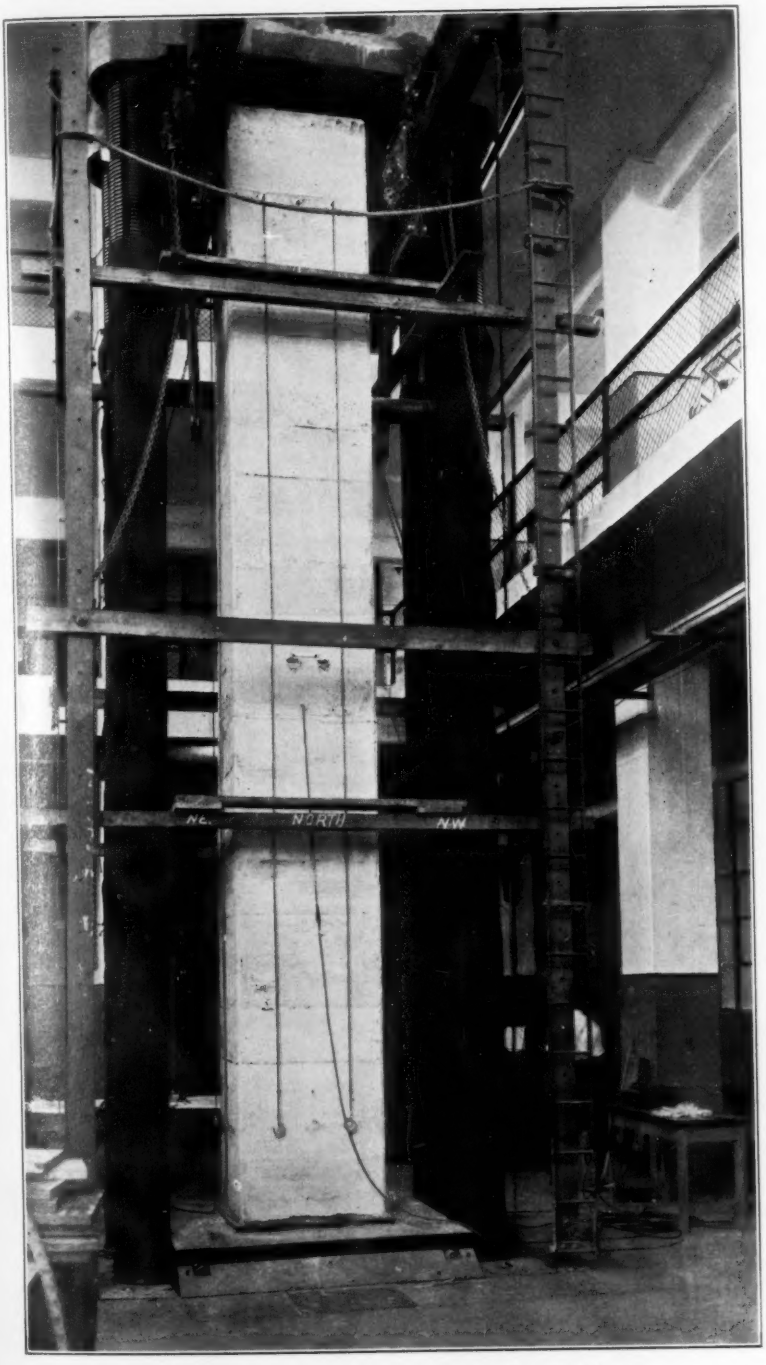

FIGURE 5.—*Column* IC4 *in the testing machine.*

(c) YIELD STRENGTH

For the coupons on which the extensometer was used the yield strength was taken as the stress for which the strain was 0.002 greater than the strain computed from the stress and Young's modulus of elasticity. The values obtained in this way agreed closely with those obtained by the drop of the beam of the testing machine. For the coupons on which the extensometer was not used the yield strength was determined by the drop-of-beam method.

(d) TESTING MACHINE

The coupons were tested in a screw-power, beam-and-poise machine having a capacity of 100 kips.

(e) SPEED OF THE MOVABLE PLATEN

For the coupons on which a Ewing extensometer was used the speed of the movable platen of the testing machine was 0.04 in./min until the stress was about three-quarters of the yield strength. For higher stresses the speed was 0.01 in./min. After the extensometer was removed the speed was 0.4 in./min until the coupon ruptured.

For the coupons on which the extensometer was not used, the speed was 0.04 in./min until the drop of the beam was observed. For higher stresses the speed was 0.4 in./min.

III. RESULTS FOR THE AUXILIARY TESTS

1. COUPONS

(a) TENSILE TESTS

The results for the tensile tests of the coupons are given in table 2. The properties of the material are average values for the longitudinal members of the same size and shape. The values of the yield strength are drop-of-beam values. Each weighted average was obtained by weighting the value for a coupon in the ratio of the cross-sectional area of the main member which it represented to the total cross-sectional area of the column.

TABLE 2.—*Results for the tensile tests of coupons*

COLUMN IC1 CARBON STEEL

Shape	Nominal size	Number of coupons	Yield strength, average	Tensile strength, average	Elongation in 8 inches, average	Reduction of area, average
	in.		kips/in.²	kips/in.²	%	%
2 plates	34⅜ by ⅝	2	32.9	61.0	30.8	53.5
2 plates	17 by ⅝	2	32.1	55.2	30.6	59.6
4 plates	7⅝ by ⅝	4	31.2	55.2	32.9	60.6
4 angles	4 by 4 by 9/16	4	32.4	56.0	32.6	58.3
8 angles	4 by 3 by ½	8	33.6	59.6	28.0	53.3
12 angles	3 by 3 by ½	12	38.6	63.2	28.5	53.7
Weighted average			33.8	59.2	30.3	55.7

TABLE 2.—*Results for the tensile tests of coupons*—Continued

COLUMN IC2 CARBON STEEL

Shape	Nominal size	Number of coupons	Yield strength, average	Tensile strength, average	Elongation in 8 inches, average	Reduction of area, average
	in.		kips/in.²	kips/in.²	%	%
2 plates	34⅜ by 5/16	2	32.9	60.1	30.0	54.1
2 plates	17 by 5/16	2	32.9	54.7	32.8	65.0
4 plates	7⅝ by 5/16	4	31.6	55.2	31.1	60.7
4 angles	4 by 4 by 9/16	4	32.4	55.9	32.9	56.9
8 angles	4 by 3 by ½	8	33.4	58.3	28.8	56.6
12 angles	3 by 3 by ½	12	38.6	63.5	28.2	51.9
Weighted average			34.0	58.8	30.2	56.6

COLUMN IC3 CARBON STEEL

2 plates	34⅜ by 5/16	2	33.1	59.6	31.1	54.9
2 plates	17 by 5/16	2	33.2	55.6	30.0	55.3
4 plates	7⅝ by 5/16	4	30.8	55.7	33.2	60.8
4 angles	4 by 4 by 9/16	4	33.4	57.3	30.7	57.1
8 angles	4 by 3 by ½	8	32.9	58.4	28.1	55.3
12 angles	3 by 3 by ½	12	38.8	63.7	29.0	53.6
Weighted average			34.0	59.0	30.2	55.7

COLUMN IC4 CARBON STEEL

2 plates	34⅜ by 5/16	2	33.0	60.6	29.0	55.8
2 plates	17 by 5/16	2	34.4	56.6	32.6	59.4
4 plates	7⅝ by 5/16	4	32.2	56.4	33.2	61.0
4 angles	4 by 4 by 9/16	4	32.9	57.2	32.2	56.2
8 angles	4 by 3 by ½	8	33.0	58.3	27.6	54.0
12 angles	3 by 3 by ½	12	39.2	63.4	28.3	52.3
Weighted average			34.4	59.4	30.0	55.9

A typical Ewing stress-strain graph for this carbon steel is shown in Figure 9 of RP831.

The speed of the movable head was much lower than is customarily used when determining the yield strength. If the yield strength is determined by the drop of the beam, the value is dependent on the speed—the higher the speed, the higher the yield strength.[6] For these coupons the rate at which the stress was increased is more nearly the rate for the columns than the rate customarily used for coupons.

(b) CHEMICAL COMPOSITION

Chemical analyses were made by the Chemistry Division of the Bureau of samples from coupons having the highest and the lowest tensile strength for each thickness and each shape. The results are given in table 3.

[6] Proc. Am. Soc. Testing Materials (I) 28, 105 (1928).

TABLE 3.—*Chemical composition of the steels*

Description of samples			Chemical composition				
Thickness	Shape	Tensile strength	Carbon	Manganese	Phosphorus	Sulphur	Silicon
in.		kips/in.²	%	%	%	%	%
½	Angle	55.1	0.18	0.56	0.015	0.033	0.03
½	do	66.9	.24	.55	.018	.037	.03
9/16	do	53.3	.14	.46	.012	.031	.02
9/16	do	61.0	.18	.53	.026	.048	.04
⅝	Plate	53.0	.14	.33	.009	.023	.11
⅝	do	61.6	.19	.46	.019	.022	.11

2. CONCRETE

The cylinders (6 in. in diameter by 12 in. in length) of the concrete for each of the columns were separated into four groups of three cylinders each. One group was tested at each of the following ages: 7 days, 28 days, 2 months, and 6 months. The results are given in table 4. The columns were tested at an age of about 70 days. At that time the strength of the concrete was very nearly the same as the strength of the cylinders at an age of 2 months.

TABLE 4.—*Strength of concrete cylinders*

[Cylinders 6 in. in diameter by 12 in. long]

Column	Number of cylinders tested for each age	Average compressive strength at age of—			
		7 days	28 days	2 months	6 months
		kips/in.²	kips/in.²	kips/in.²	kips/in.²
IC1	3	1.55	2.52	2.89	3.80
IC2	3	1.47	2.04	2.81	2.83
IC3	3	1.77	3.18	3.23	3.47
IC4	3	1.83	2.73	2.91	3.28
Average compressive strength for the four columns		1.66	2.62	2.96	3.35

3. REINFORCEMENT

The carbon and phosphorus content and the tensile properties of the reinforcing bars are given in table 5.

TABLE 5.—*Carbon and phosphorus content and tensile properties of the reinforcing bars*

[Plain bars, 0.5 in. diameter]

Specimen	From reinforcement [1]	Chemical content		Tensile properties			
		Carbon	Phosphorus	Young's modulus of elasticity	Yield strength	Tensile strength	Elongation in 8 inches
		%	%	kips/in.²	kips/in.²	kips/in.²	%
A1	A	0.13	0.108	29,200	51.6	73.4	23.1
A2	A			29,800	50.2	70.6	23.7
B1	B	.11	.110	29,700	45.6	65.3	24.2
B2	B			29,400	47.3	67.9	24.0
C1	C			30,000	47.1	66.0	24.8
C2	C			30,000	45.5	63.0	21.3
C3	C			28,700	40.3	55.7	28.2
C4	C			29,600	44.2	63.0	26.0

[1] The reinforcement is shown in figure 2.

IV. RESULTS FOR THE COLUMNS

1. STRESS IN THE STEEL MEMBERS CAUSED BY AGING OF THE CONCRETE

The telemeters attached to the steel members of the incased columns were read during the aging of the concrete (about 70 days) to determine the stresses in the members. With one exception, these readings did not differ from the initial readings before the columns were incased by more than 1 division of the scale on the milliammeter, indicating that the stress did not exceed 3.75 kips/in^2. The last reading on column IC1 exceeded the initial reading by 1.3 divisions, indicating a stress of about 4.88 kips/in^2. Some of the readings of the telemeters indicated tensile and some compressive stresses, and consequently the readings do not show that aging of the concrete caused appreciable stresses in the steel members.

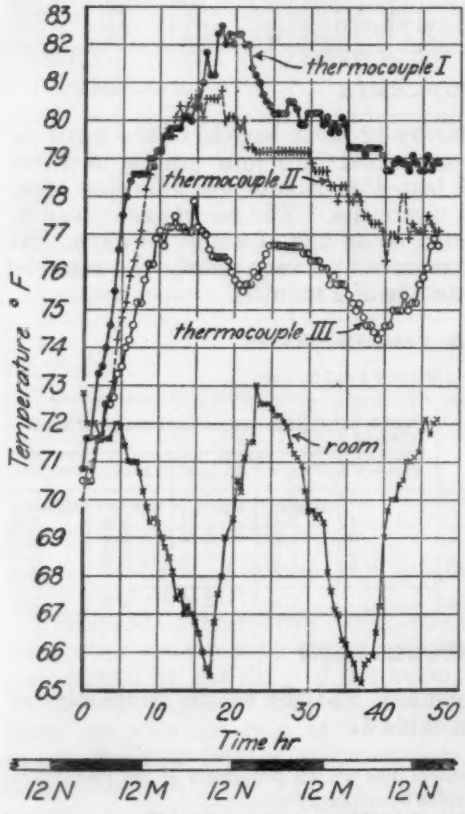

FIGURE 6.—*Temperatures at midheight of column* IC3 *for 2 days after the column was incased in concrete.*

Figure 2 shows the locations of the thermocouples.

2. TEMPERATURE DURING AGING OF THE CONCRETE

The temperatures at midheight of column IC3 for 2 days after the column was incased in concrete are shown in figure 6. During this period the temperatures in the concrete were greater than the room temperature. The temperatures in the concrete were a maximum between 14 and 18 hours after the column was incased. The temperatures were greatest at the axis of the column (thermocouple I). After the temperature at the axis reached a maximum, it decreased continuously with variations which did not exceed 1° F. The temperature at thermocouple III, nearest the sides of the column increased and decreased appreciably with the changes in the room temperature, but there was a time lag of from 2 to 5 hours.

The temperatures at the axis at midheight of colum IC2 from the time the column was incased until it was tested are shown in figure 7.

The temperature-time graphs for the other columns were similar to figure 7. After about 5 days the temperature of the concrete increased and decreased noticeably with changes in the room temperature, and after about 10 days the increase and decrease became marked, but there was a time lag of from 1 to 5 days. The temperature of the concrete became about equal to the room temperature after 45 days. The temperature-time graphs for the concrete near the top and the bottom of the columns were similar to figure 7, except that there was less difference between the temperature of the concrete and the room temperature.

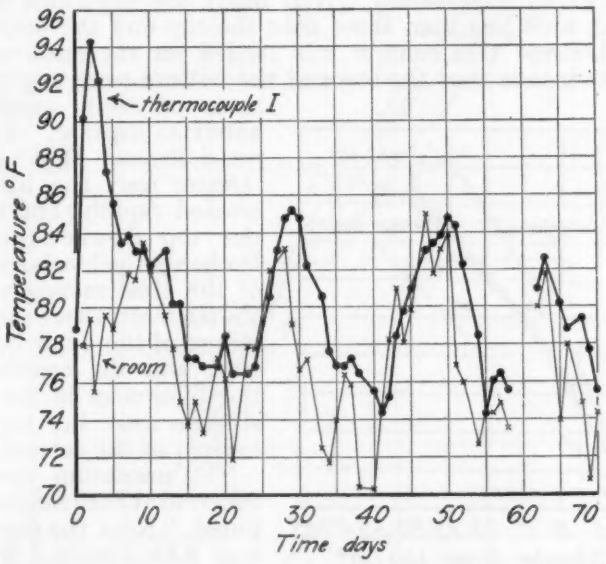

FIGURE 7.—*Temperatures in the axis (thermocouple* I) *at midheight of column* IC2 *from the time the column was incased until it was tested.*

Figure 2 shows the locations of the thermocouples. Usually the temperatures were recorded at 9:30 a. m.

3. QUASI-STRESS

For these columns it is convenient to consider as a quasi-stress in the steel members, the stress obtained by dividing the load on the column by the transverse sectional area of the steel members.

4. TELEMETER STRESS

For column IC1 (loaded on steel only) there were telemeters near the top, the bottom, and at midheight. The strains obtained from the telemeter readings were averaged for the telemeters at each height. The average telemeter stress was computed from the average telemeter strain and the average Young's modulus of elasticity (29,100 kips/in ^{2}) for the coupons. The telemeter stresses for

column IC1 are shown in figure 8. The dashed line a–b shows what the relation would be between the telemeter stress and the quasi-stress if the steel members carried all of the load and none of it were carried by the concrete. The telemeter stress was always less than the quasi-stress, indicating that the concrete carried a portion of the load. Let the length of the abscissa for any point on line a–b represent the total load on the column, as, for example, c–d. Then at midheight the portion of the load carried by the steel members is represented by the line c–e and that carried by the concrete by line e–d. As the load increased, the steel members carried a greater proportion of the load.

For a given quasi-stress (given load) the telemeter stresses at midheight were less than those near the top and the bottom of the column because this column was loaded on the steel only. The telemeter stresses near the top and the bottom were very nearly the same up to a quasi-stress of about 35 kips/in^2. For greater quasi-stresses the telemeter stresses near the bottom increased rapidly, but those near the top decreased rapidly. Probably the local deformations of the steel members to which the telemeters were attached and failure of the bond between the steel and the concrete caused the differences in the telemeter stresses near the top and the bottom of the column.

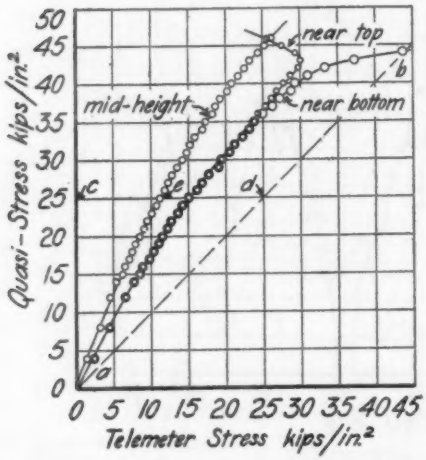

FIGURE 8.—*Average telemeter stresses for incased column* IC1 *loaded on steel only.*

The dashed line a–b shows what the relation would be between the telemeter stress and the quasi-stress, if the steel members carried all of the load.

The maximum stress in the concrete at each height was computed. Near the top this stress was 2.62 kips/in.^{2} when the quasi-stress was 46 kips/in^2. At midheight it was 2.56 kips/in.^{2} when the quasi-stress was 46 kips/in^2. Near the bottom it was 1.40 kips/in.^{2} when the quasi-stress was 36 kips/in^2.

The average telemeter stresses at midheight for each of the columns are shown in figure 9. The dashed line a–b shows what the relation would be between the telemeter stress and the quasi-stress if the steel members carried all of the load and none of it were carried by the concrete.

There was not much difference between the telemeter stresses for the columns loaded on steel only and those loaded on both steel and concrete. No explanation was found for the fact that the telemeter stresses at midheight for the columns loaded on both the steel and concrete were somewhat greater than those for the columns loaded on the steel only. For a quasi-stress of 20 kips/in.^{2}, about the design load, the telemeter stress was between 8 and 10 kips/in.^{2}; therefore at this load about one-half the load was carried by the steel members and one-half by the concrete.

5. STRAIN IN THE CONCRETE

(a) AVERAGE STRAIN

The average strains for the first loading computed from the readings of the compressometers attached to the concrete are shown in figure 10. The values for the unincased tower columns TC1 and TC2 are also shown. The strain in the incased columns was much

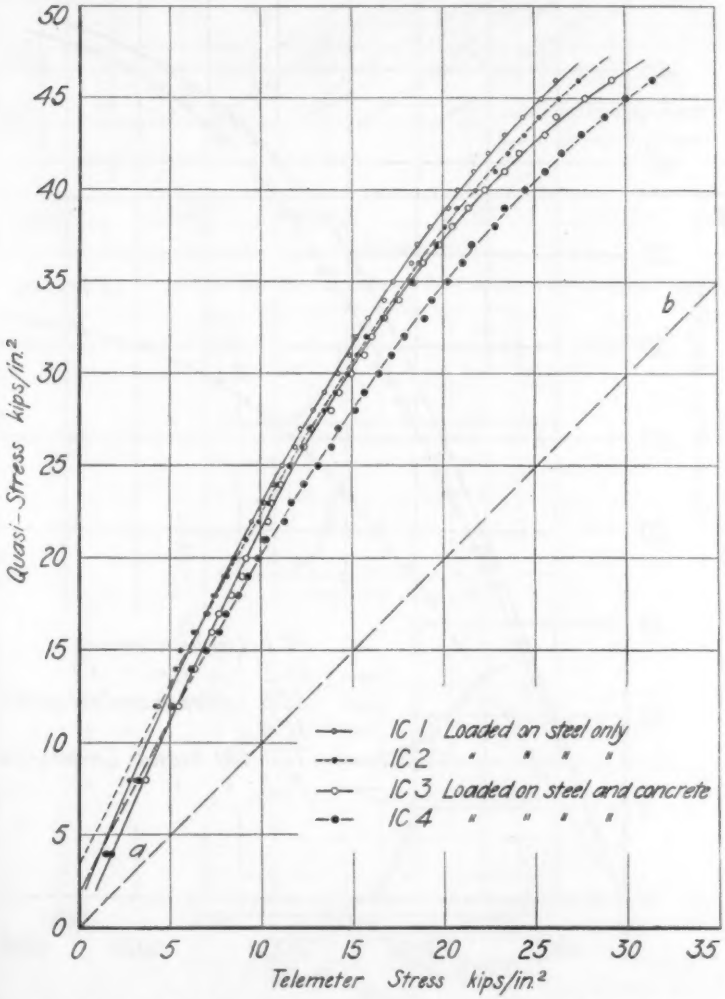

FIGURE 9.—*Average telemeter stresses at midheight for each of the columns.*

The dashed line a–b shows what the relation would be between the telemeter stress and the quasi-stress, if the steel members carried all of the load.

less than the strain in the unincased columns. For a stress of 20 kips/in.² in the unincased columns, about the design load, the strain was 0.0007. At this strain in the incased columns the quasi-stress was about 30 kips/in². Therefore, for the same shortening (strain) the load on the incased columns was about 50 percent greater than the load on the unincased columns.

(b) REPEATED LOADING

The average strains for column IC1 under repeated loading are shown in figure 11. For each application of load the strain increased. The increase was smaller and smaller as the loading number increased. The graphs for the other incased columns were similar to figure 11.

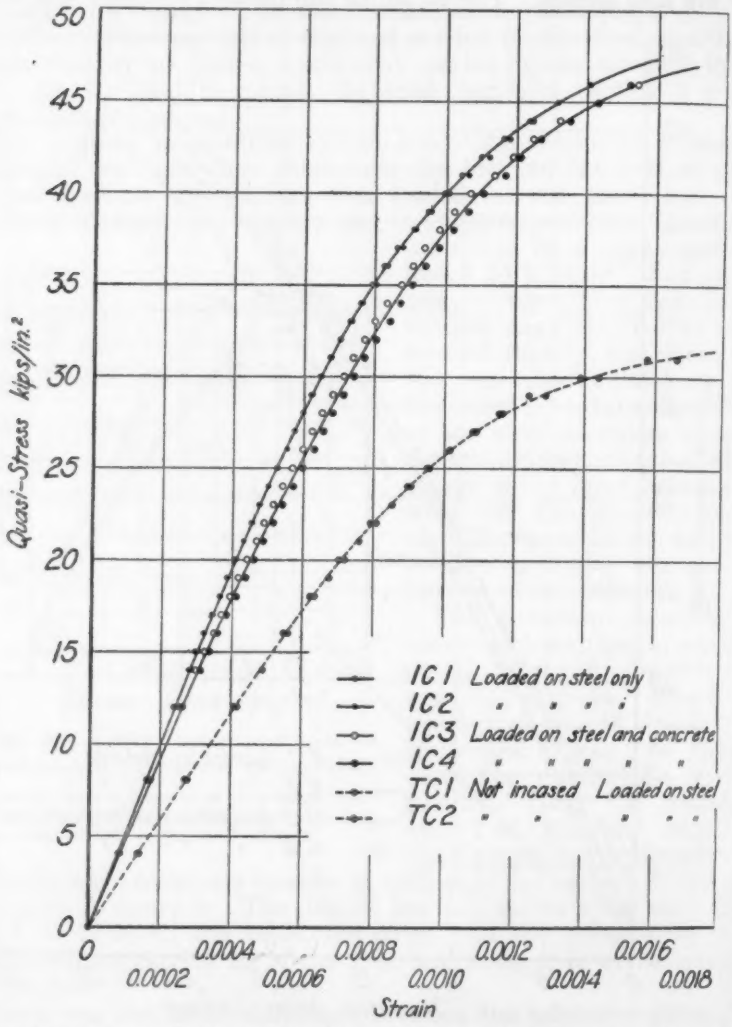

FIGURE 10.—*Average strains for the first loading computed from the readings of the compressometers attached to the concrete.*

The values for the unincased columns are also shown.

The average strain at each application of the loads given in section II, 1, (f), (5) for each of the incased columns is shown in figure 12. The strains in the columns loaded on the steel only were less than those for the columns loaded on both the steel and the concrete. The stress-strain graphs for the first and the twenty-sixth application of load for each of the incased columns are shown in figure 13. The

permanent set after the twenty-fifth application of load was less in the columns loaded on the steel only than that for the columns loaded on both the steel and concrete.

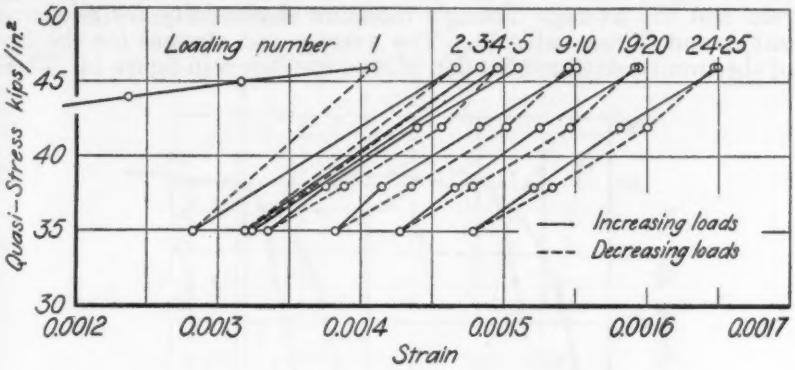

FIGURE 11.—*Average strains for column* IC1 *under repeated loading.*

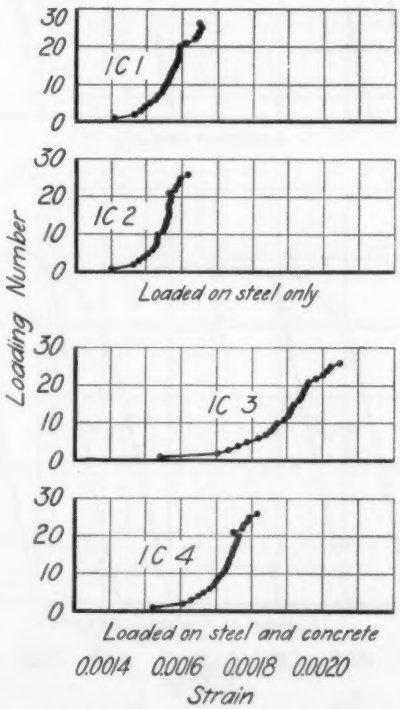

FIGURE 12.—*Average strain for each application of load for each of the columns.*

The results for these steel columns incased in concrete indicate that the steel and the concrete did not act as a unit when loads were applied repeatedly. It appears probable that this was due to the large proportion of steel and the insufficient bond between the steel and the concrete. Whether the behavior of these columns after many years under fluctuating loads can be predicted from the results of these tests is questionable.

6. STRESS IN REINFORCEMENT

The strains in the A and B tie rods near midheight of each column were averaged. The average stress was computed from the average strain and the average Young's modulus of elasticity for reinforcement A and B (see table 5). The average rod stresses for the first and the twenty-sixth application of load are shown in figure 14. There

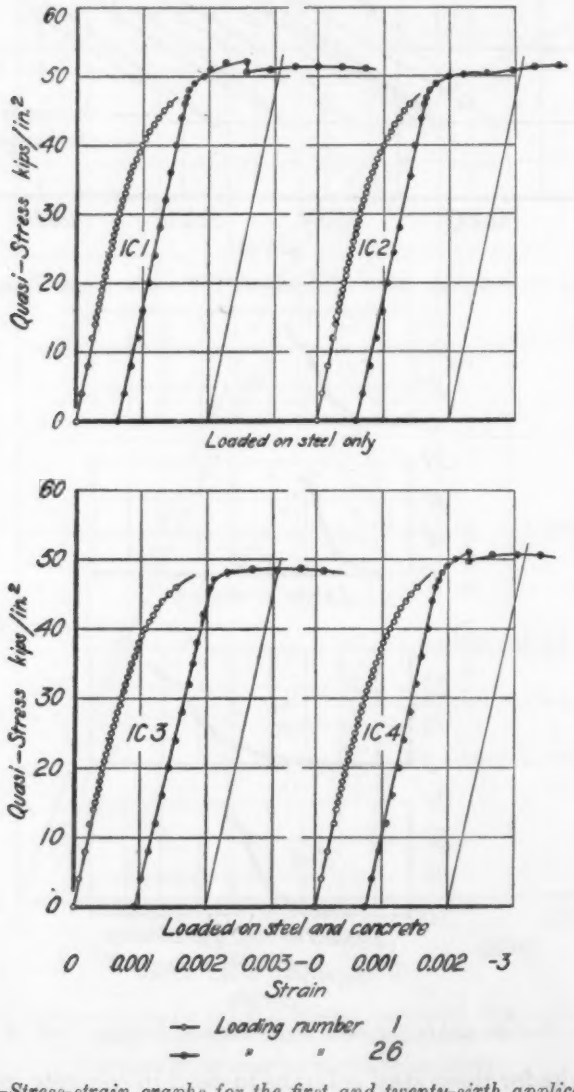

FIGURE 13.—*Stress-strain graphs for the first and twenty-sixth application of load for each of the columns.*

were considerable differences in the strains for the individual gage lines for a given load. Probably more consistent average strains would have been obtained if readings had been taken on more of the rods.

The stress in the rods increased with an increase in the quasi-stress in the column. Although the stress in the rods under the first application of load was less than one-fourth the proportional limit of the steel, the stress in the rods did not decrease to zero when the load on the column was decreased to zero.

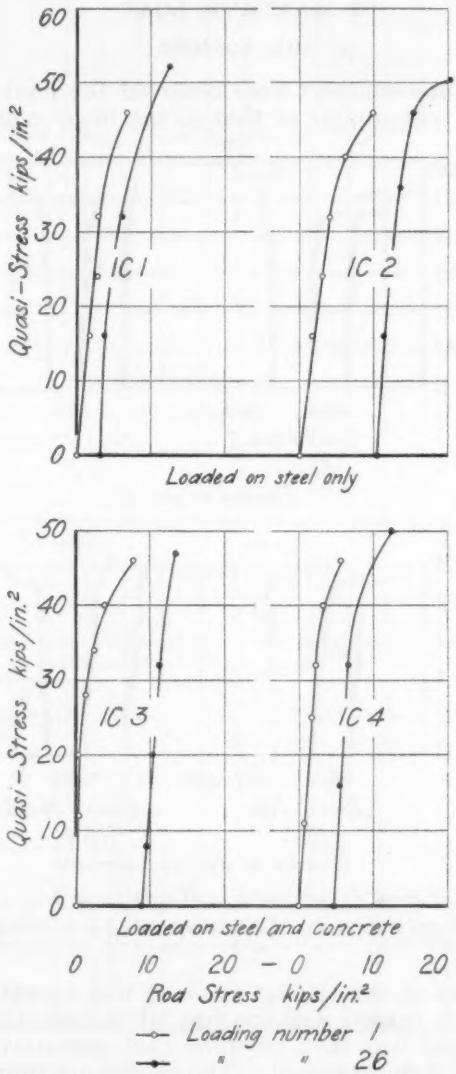

FIGURE 14.—*Average rod stresses at midheight for the first and twenty-sixth application of load for each of the columns.*

7. LATERAL DEFLECTION

The lateral deflections at midheight of each column are shown in figure 15. For quasi-stresses greater than 46 kips/in.^{2} the deflections are the values for the twenty-sixth application of load. For lower

quasi-stresses they are the values for the first application of load. The deflections were very small until the load on the column approached the maximum. For each of the columns except column IC2 there was an appreciable increase in the lateral deflection as the number of loadings increased.

8. MAXIMUM LOAD

(a) FINAL LOADING

After the compressometers were removed the final loading of the incased columns was similar to that of the tower columns TC1 and

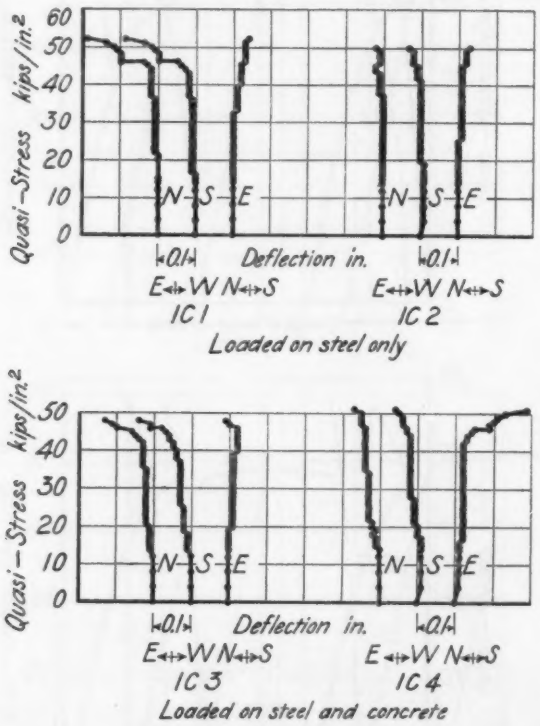

FIGURE 15.—*Lateral deflections at midheight for each of the columns.*

For quasi-stresses greater than 46 kips/in.² the deflections are the values for the twenty-sixth application of load. For lower quasi-stresses they are the values for the first application of load.

TC2. The pump of the testing machine was operated continously at a speed which caused a shortening of the column of about 0.1 in./min. The load was then recorded each minute until it reached a maximum and then decreased. The results are shown in figure 16. The maximum load on column IC1 was applied before the compressometers were removed. Pumping for more than an hour did not induce a greater load. For column IC4 pumping was stopped about 3 minutes after the maximum load was recorded. The lateral deflection at midheight was about 6 inches. Large pieces of concrete were falling from the column and it was considered inadvisable to carry the test further. The graphs for each column show several

more or less pronounced maxima. Each of the columns showed either "pick-up" or "hang-on."[7]

When cracks suddenly appeared in the concrete or large pieces of concrete fell from the column there was an appreciable decrease in

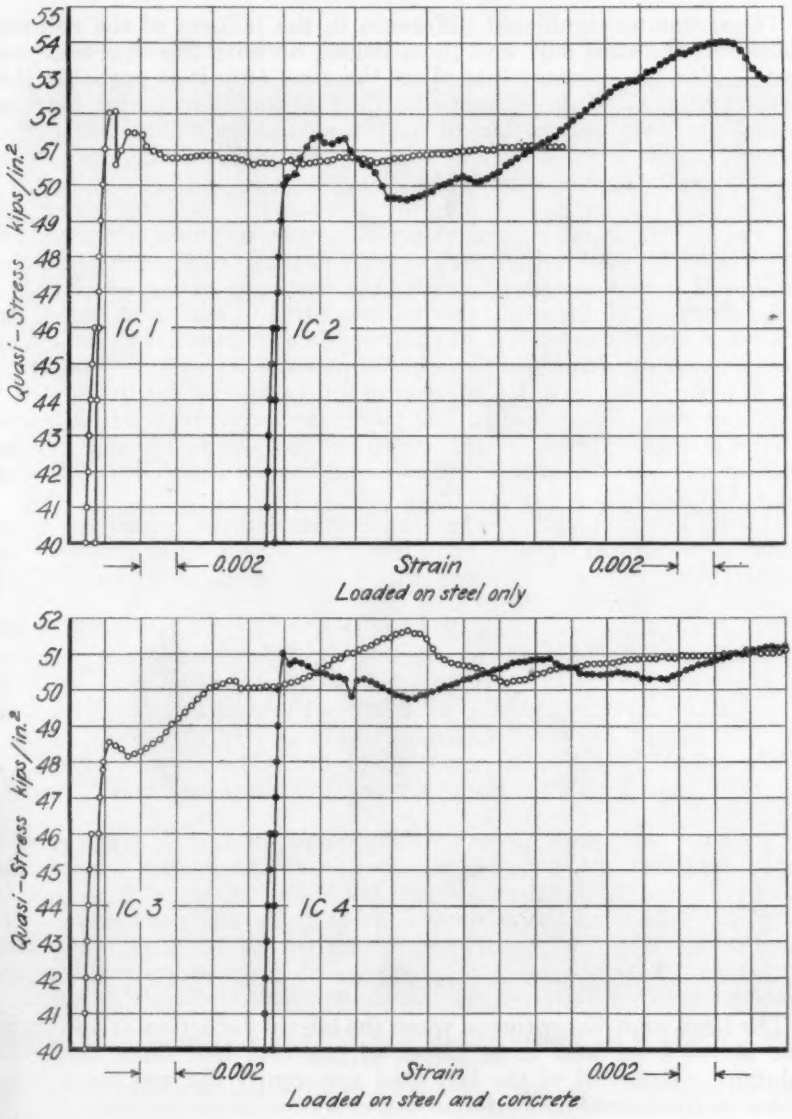

FIGURE 16.—*Final loading for each of the columns.*

the load. It is probable, therefore, that the properties of the concrete had a much greater effect upon the graphs shown in figure 16 than the properties of the steel members. The slenderness ratio of

[7] J. Research NBS **15**, 317 (1935) RP831; BS Tech. Pap. **21**, 59 (1926) T328.

the incased columns was less than that of the tower columns. The incased columns were therefore more likely to show pick-up or hang-on than the unincased columns.

(b) DESCRIPTION OF THE FAILURE

There was no significant difference in the failures of the columns loaded on the steel only and those loaded on both the steel and concrete. For the columns loaded on the steel only it is probable that the concrete came into contact with the platens of the testing machine during the first application of load (quasi-stress 46 kips/in ^{2}). For subsequent loadings, therefore, there was no essential difference in the way in which the load was applied.

The first cracks in the concrete appeared in the sides near the bottom and the top of the column. They were approximately vertical and where the steel angles were nearest the side of the column. For column IC4 they appeared during the first application of load at a quasi-stress of 17 kips/in.^{2}, and on the other columns at somewhat greater loads. The bottom of column IC1 is shown in figure 17 after the first application of load to a quasi-stress of 46 kips/in ^{2}. The cracks did not increase in width appreciably under subsequent loads.

Under repeated loading horizontal cracks appeared near the A and B rods about midheight. The width of these cracks increased as the loading number increased until horizontal strips of concrete fell from the column, as shown in figure 18.

During the final loading when the load exceeded the previous maximum of 46 kips/in.^{2} the C rods (see fig. 2) near the corners of the column bent outward between the A rods, causing spalling of the concrete as shown in figure 18.

None of the B rods (see fig. 2) fractured. They restrained the steel angles nearest the sides of the column, which buckled locally between these rods as shown in figure 19. Some of the concrete was removed after the column was tested so as to expose the steel members and show the buckling of the steel angles.

The lateral deflection after test of column IC2 is shown in figure 18, and of column IC4, after the concrete on one face had been removed, in figure 20.

As shown in figures 19 and 20 the length of a buckle in the steel angles was only a few inches, whereas in the unincased columns the length of a buckle was the distance between diaphragms.

In some cases, as the column shortened, the concrete between the diaphragms was forced outward, as shown in figure 21. The ends of the short D rods (see fig. 2) came into contact and were bent outward as the column shortened.

The tests were discontinued when the lateral deflection at midheight was about 6 in. and large pieces of concrete had fallen from the columns. Removal of the last load apparently did not cause a decrease in the lateral deflection.

For future tests of columns incased in concrete which are to be loaded on the steel only the steel members should extend beyond the concrete so far that they will not come into contact with the platens of the testing machine at the maximum load.

FIGURE 17.—*Bottom of column* IC1 *after the first application of load to a quasi-stress of* 46 kips/in^2.

The cracks are where the steel is nearest the side of the column. These cracks appeared on all four sides of the column, both near the bottom and near the top. They were the first cracks to appear.

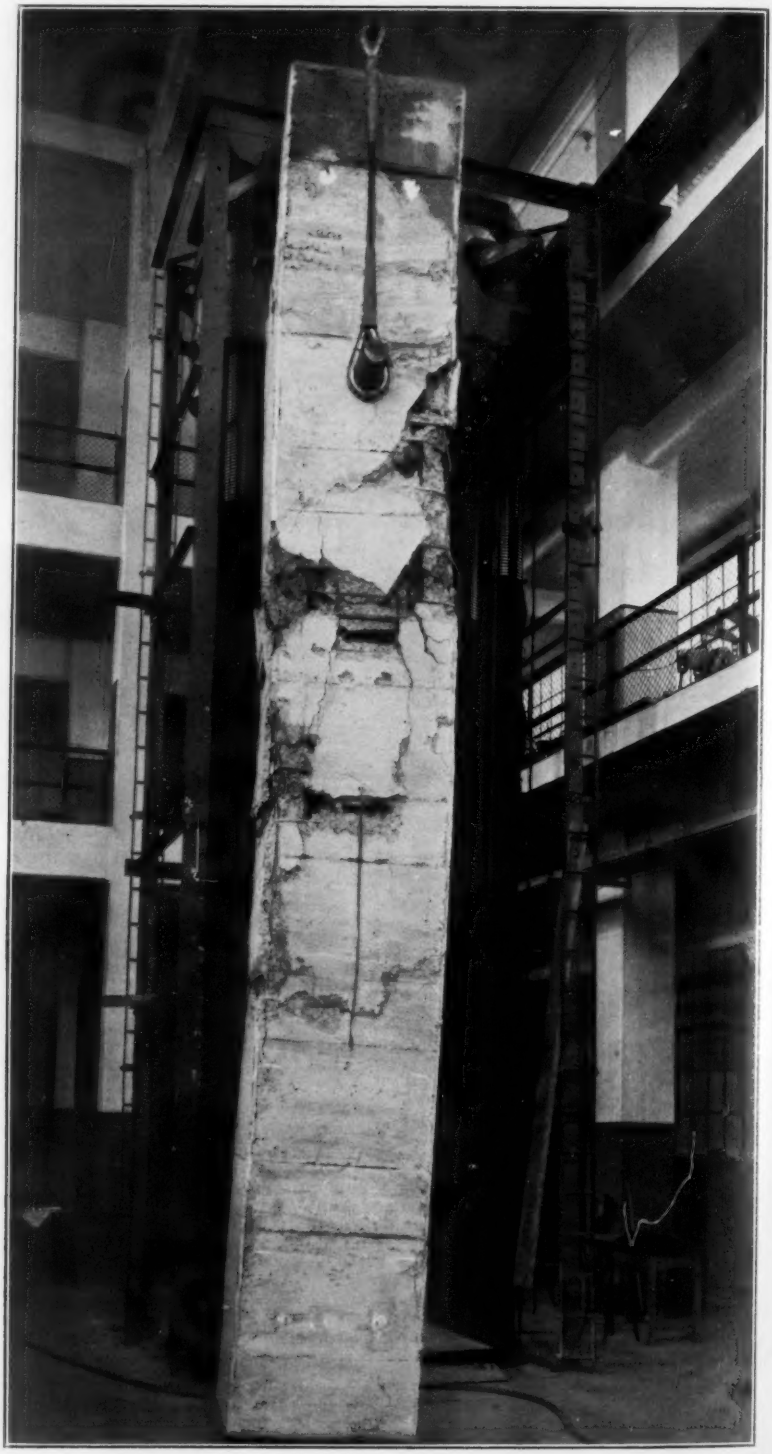

FIGURE 18.—*Column* IC2 *after test.*

About midheight horizontal strips of concrete have fallen from the column and the rods C near the corners of the column have bent outward causing spalling of the concrete.

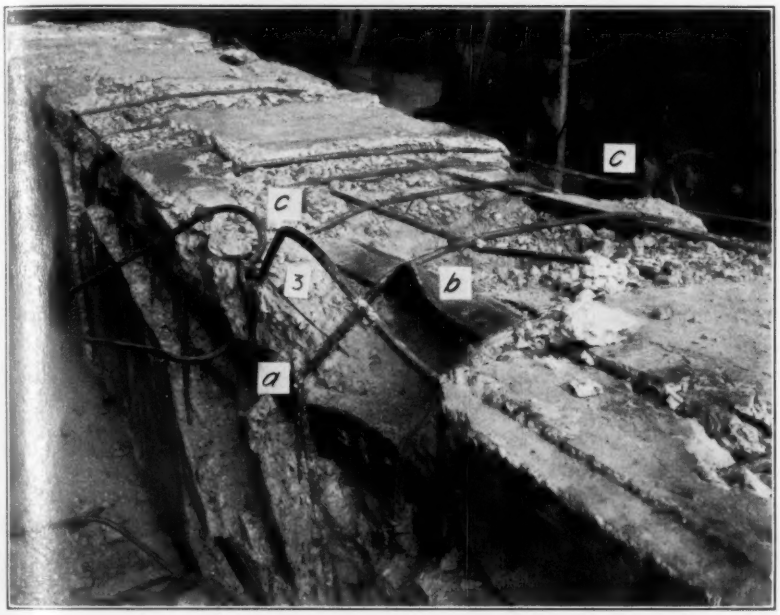

FIGURE 19.—*Column* IC3 *after test.*

Some of the concrete was removed to expose the steel members. (*a*) One A rod was fractured at the corner. (*b*) None of the B rods fractured. The steel angles nearest the sides of the column buckled locally between the B rods. (*c*) The C rod near the corner of the column bent outward between the A rods.

FIGURE 20.—*Incased column* IC4 *after test.*

The concrete on one side has been removed. The steel angles in the incased columns did not buckle between the diaphragms as they did in the unincased tower columns.

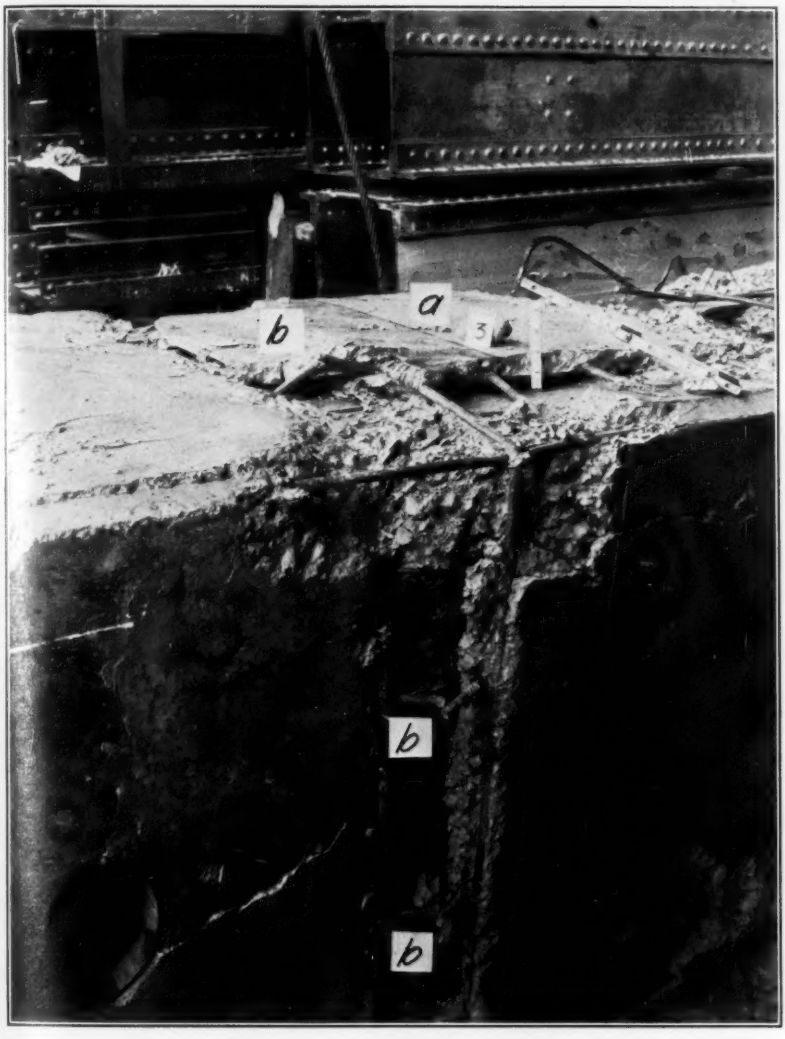

FIGURE 21.—*Column* IC3 *after test.*

As the column shortened (*a*) the concrete between the diaphragms was forced outward; (*b*) the ends of the short D rods came into contact and were bent outward.

(c) STRENGTH

The column strengths given in BS Technologic Paper T328 were the values of the first maximum stress. It was stated that "the practically definite first maximum stress, occurring before any appreciable lateral deflection of the column, and fairly reproducible when the column material and test conditions are reproduced, should furnish a good measure of the strength of the column in practical use. This justifies the practice followed in this report of recording the first maximum stress observed in a column test as the 'column strength' under the given test conditions. However, as was previously pointed out, this would not be justified in case no maximum were observed before the column was badly deformed."

With regard to the procedure that should be followed when no maximum is observed before the column is badly deformed, it was stated that "the best criterion could only be determined by a series of tests on columns in this range, in which the stress deformation curves were carefully determined."

In tensile tests of steel which do not show a definite yield point, it has become customary to define a yield strength in terms of the stress necessary to produce a definite strain (usually 0.002) in the coupon in excess of the computed elastic strain. It seemed probable that a similar definition of a column yield strength would be satisfactory for columns for which no definite first maximum load is observed, and for this reason the column yield strengths were computed on this basis.

The strengths of the incased columns are given in table 6. Although the column yield strengths and the maximum loads for the columns

TABLE 6.—*Strength of the columns*

Column	Loaded on	Cross-sectional area		Column yield strength	Final maximum load	Final maximum quasi-stress
		Steel	Concrete			
		in.²	in.²	kips/in.²	kips	kips/in.²
IC1	Steel only	159	1,245	51.2	8,278	52.0
IC2	do	159	1,245	51.0	8,587	54.0
IC3	Steel and concrete	159	1,245	48.6	8,211	51.6
IC4	do	159	1,245	50.7	8,179	51.4
Average				50.4	8,314	52.29

loaded on the steel only were somewhat greater than those for the columns loaded on both the steel and concrete, probably the difference is not significant because differences in the strength of the concrete may have had more effect on the strengths of the columns than the differences in the way in which the load was applied. The strengths of the four columns, therefore, were averaged. A comparison of the average strengths of the incased and of the unincased tower columns follows:

Average of the final maximum loads for the incased columns.. 8,314 kips.
Average of the final maximum loads for the unincased columns. 5,853 kips.
Increase in the average of the final maximum loads due to the concrete ..... 2,461 kips (42%).

Total area of concrete	1,245 in².
Strength of the concrete based on total area	1.98 kips/in².
Concrete area within A rods	1,190 in².
Strength of the concrete based on this area	2.07 kips/in².
Concrete area within B rods	1,140 in².
Strength of the concrete based on this area	2.16 kips/in².
Strength of concrete cylinders at age of 2 months	2.96 kips/in².

The strength of the concrete in the incased columns may be computed by dividing the increase in the strength of the incased columns due to the concrete by the total cross-sectional area of the concrete. The concrete outside the rods spalled before the maximum loads were applied. The strength of the concrete was, therefore, also computed by dividing by the area within the rods. These strengths are given above. The computed strength of the concrete in the incased columns is about two-thirds the strength of the concrete cylinders.

This difference in strength may have been due, at least in part, to the differences in the temperature and the humidity during aging.

V. CONCLUSIONS

1. STRESS IN THE STEEL MEMBERS

The stresses in the steel members were obtained from the readings of telemeters attached to the steel members and were designated "telemeter stresses." The telemeter stress was always less than the quasi-stress, indicating that the concrete carried a portion of the load. The quasi-stress was obtained by dividing the load on the column by the cross-sectional area of the steel members. As the load increased, the steel members carried a greater proportion of the load.

The telemeter stresses at midheight were less than those near the top and the bottom of the column for the columns loaded on the steel only. For quasi-stresses greater than about 35 kips/in². the telemeter stresses increased rapidly. The maximum stress in the concrete near the top was 2.62 kips/in². when the quasi-stress was 46 kips/in². At midheight it was 2.56 kips/in². when the quasi-stress was 46 kips/in²., and near the bottom it was 1.40 kips/in². when the quasi-stress was 36 kips/in².

There was not much difference between the telemeter stresses for the columns loaded on steel only and those loaded on both the steel and concrete.

2. AVERAGE STRAIN

For an average strain of 0.0007 under the first loading the quasi-stress was 30 kips/in². for the incased columns, and 20 kips/in². for the unincased columns, indicating that for the same shortening (strain) the load was about 50 percent greater on the incased columns than on the unincased columns.

For each application of load on the incased columns the strain increased, but the increase was smaller and smaller as the loading number increased.

The strains in the incased columns loaded on the steel only were less than those loaded on both the steel and concrete.

3. STRESS IN REINFORCEMENT

The stress in the reinforcing tie rods increased with an increase in the quasi-stress in the column. The greatest stress was about 10 kips/in^2.

4. LATERAL DEFLECTION

The lateral deflection of the incased columns was very small until the load on the column approached the maximum. There was an appreciable increase as the number of loadings increased.

5. FAILURE

At or about the maximum load the incased columns having a length of 24 ft. deflected about 6 in., and large pieces of concrete fell from the column. Each column showed either pick-up or hang-on.

There was no significant difference in the failures of the columns loaded on the steel only and those loaded on both the steel and concrete.

6. STRENGTH

At the column yield strength the load on the incased columns was 51 percent greater than the load on the unincased columns. At the final maximum load the load on the incased columns was 42 percent greater than the load on the unincased columns.

The program and testing procedure were prepared by O. H. Ammann, chief engineer, L. S. Moisseiff, consulting engineer, and R. S. Johnston, research engineer, of the Port of New York Authority, and by L. J. Briggs, L. B. Tuckerman, and H. L. Whittemore, of the National Bureau of Standards. The following members of the staff of the Port of New York Authority assisted in making the tests and obtaining the data: A. H. Baker, F. J. Hinners, S. K. Hoppen, B. A. Lefeve, L. D. Mork, R. B. Morris, and G. A. Woods.

The chemical compositions of the steels were determined by the Chemistry Division of the Bureau.

The mix of the concrete was supervised by C. W. Ross of the Masonry Construction Section of the Bureau. He also placed the thermocouples for measuring the temperature in the columns.

WASHINGTON, November 1, 1935.

○